17th Workshop of the

FCPPN/L

France-China Particle Physics Network and Laboratory

Lyon, France • 29 June – 3 July 2026

Highlights on recent ATLAS results

Haijun Yang (for the ATLAS Collaboration)

上海交通大學 SHANGHAI JIAO TONG UNIVERSITY | 李政道研究所 Tsung-Dao Lee Institute

The 17th Workshop of the FCPPN/L at Lyon, France
June 29 – July 3, 2026

Outline

- Introduction
- Higgs, Di-Higgs, Tri-Higgs
- VBS Diboson, Triboson
- Top quark and heavy flavor
- Beyond SM Searches
- Heavy Ion & Proton-Oxygen
- Summary and Outlook

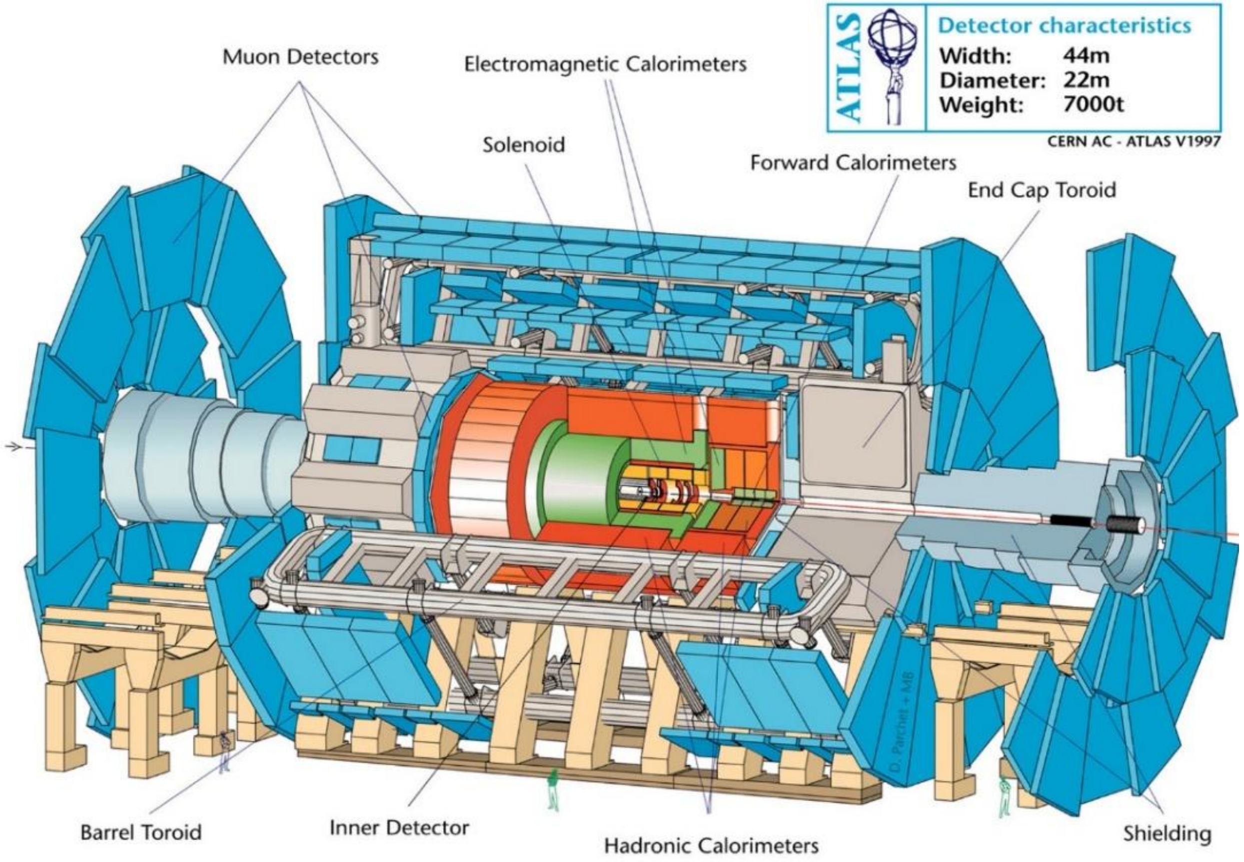

Data-taking highlights

- More than **500 fb^{-1}** pp collisions data recorded by ATLAS detector
- **Run3: 2022-2026 @ 13.6 TeV, 332 fb^{-1} recorded, pile-up <μ> ~ 60**
- ATLAS recording 95% of delivered data, 94% is good for physics
- Low-μ (1.3 fb^{-1}), p-O(7.84nb^{-1}), O-O(8.16nb^{-1}), Ne-Ne (1.05nb^{-1})

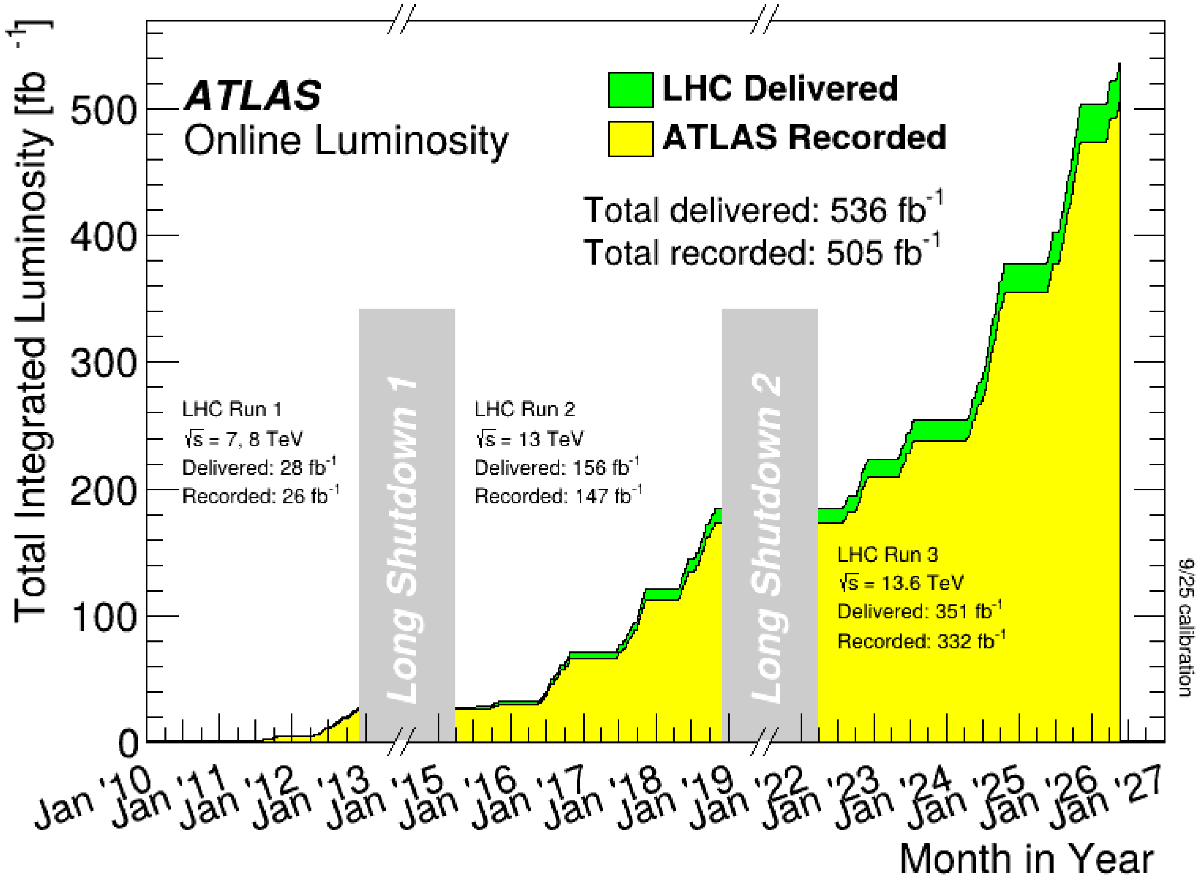

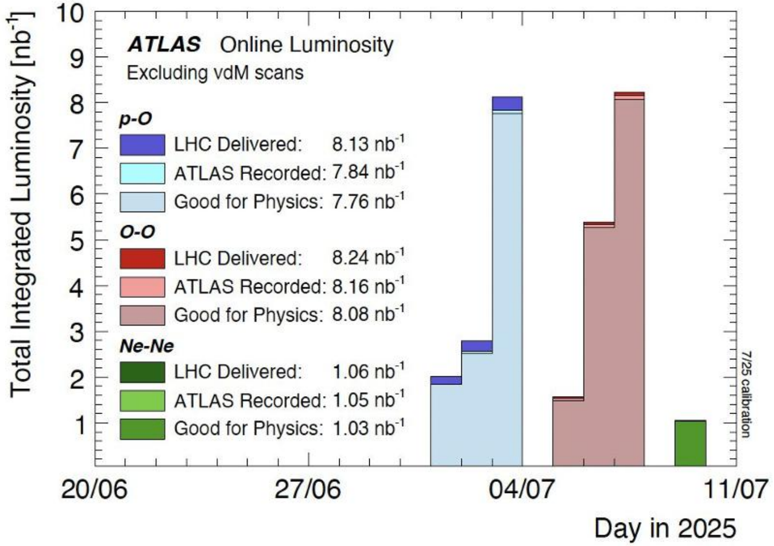

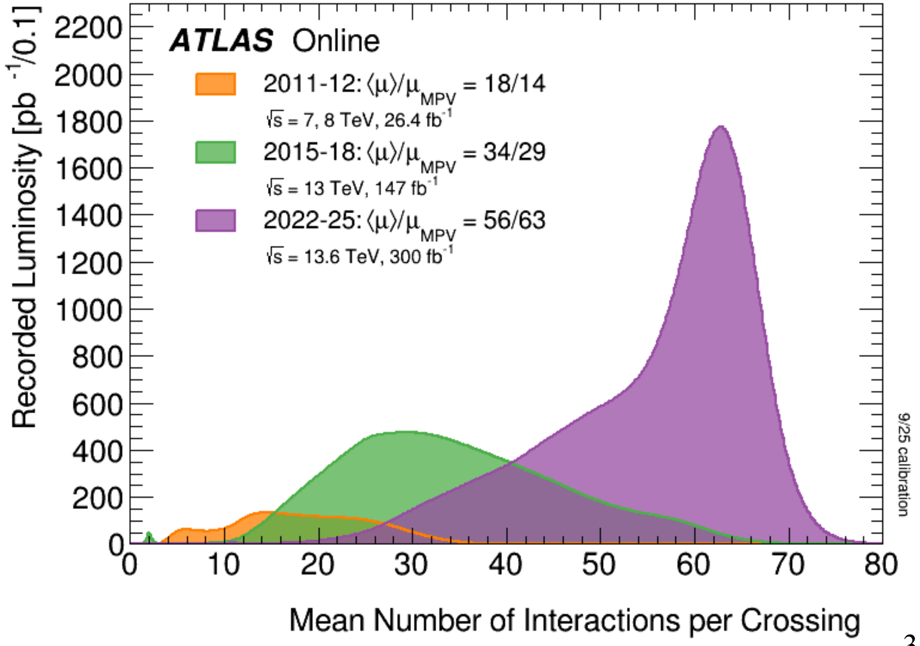

SM Cross section Measurements

- **pp cross section measurements agree with SM predictions: 100mb ~ 0.1 fb**

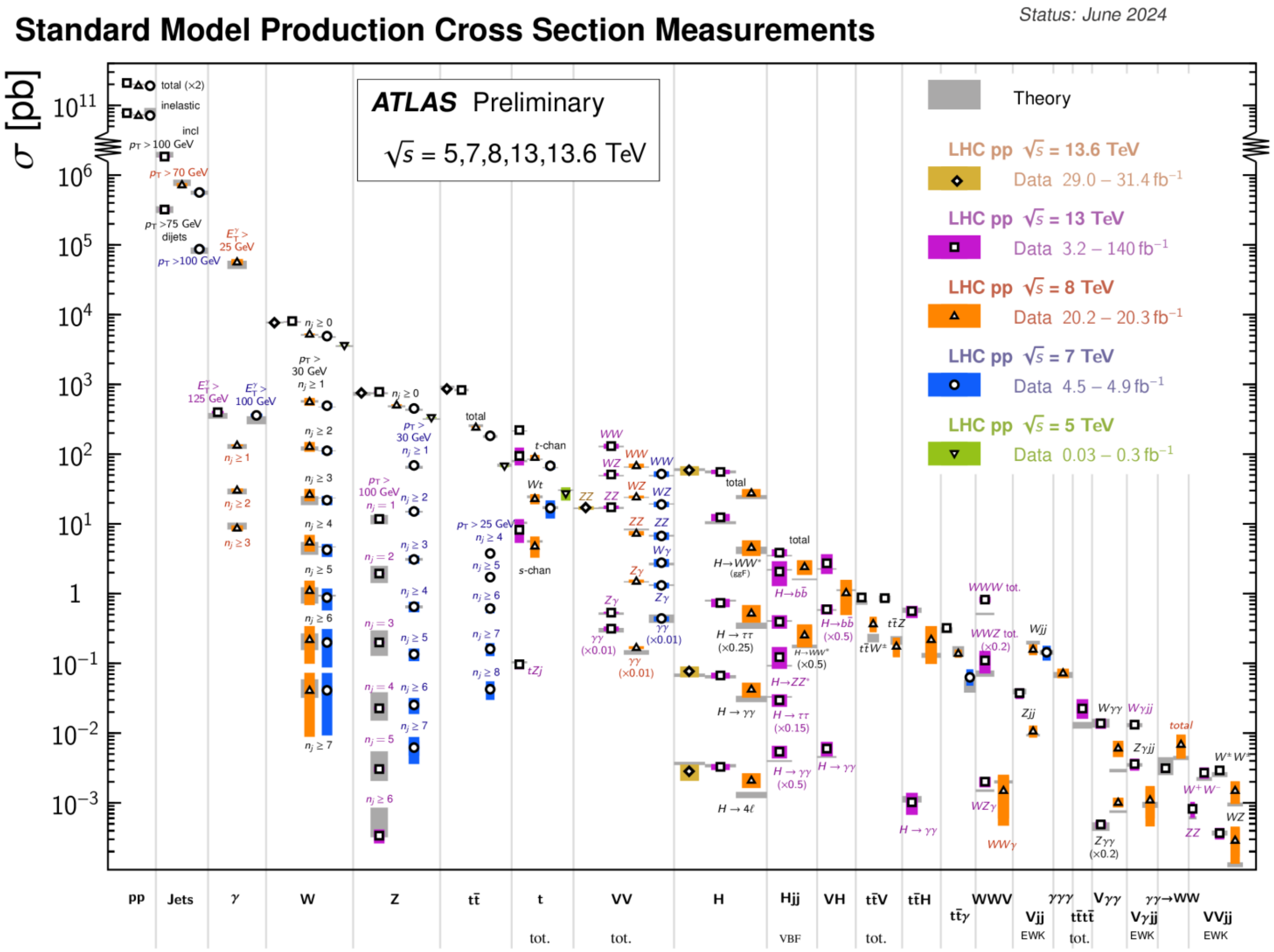

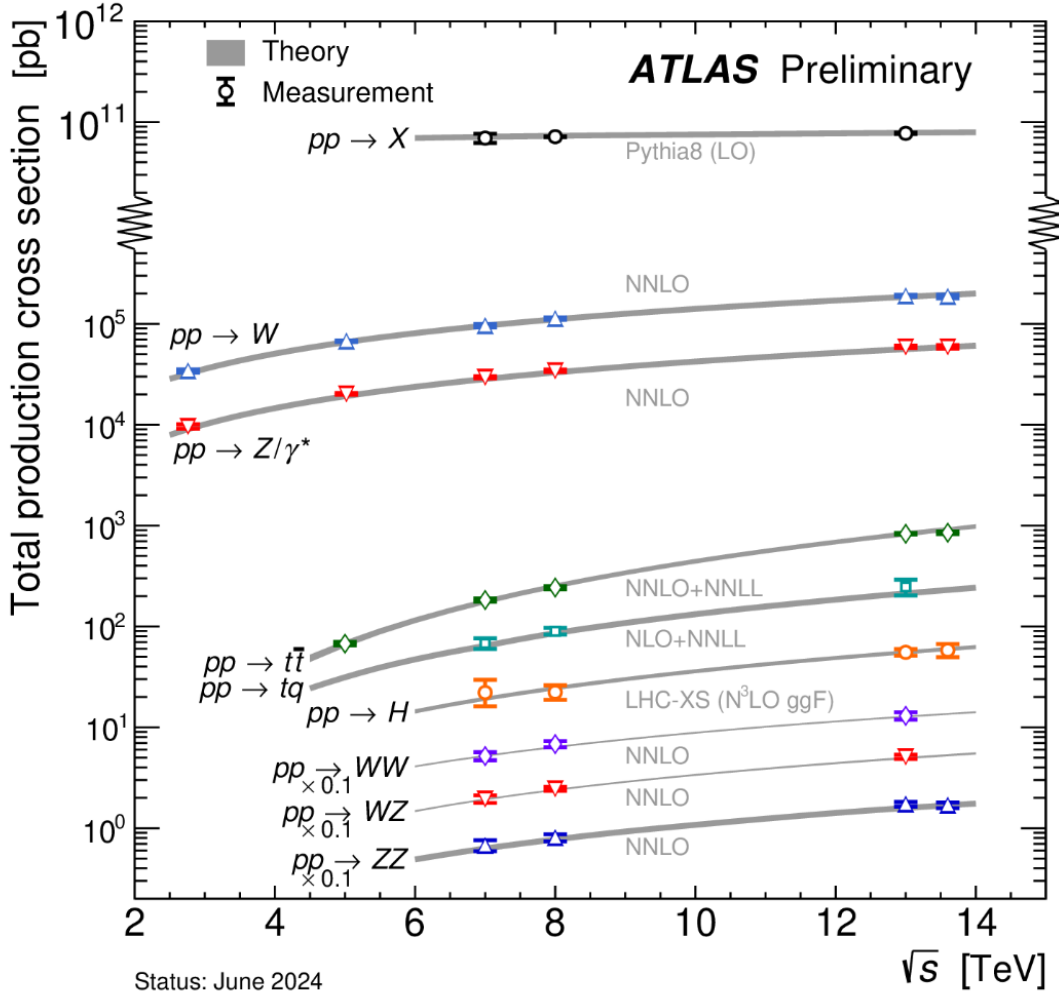

Higgs Properties

- Higgs productions at LHC: ggF, VBF, VH, ttH
- Higgs decays: bb, cc, gg, ττ, μμ (Yukawa coupling)
  WW, ZZ, γγ, Zγ (Gauge coupling)

Higgs Production

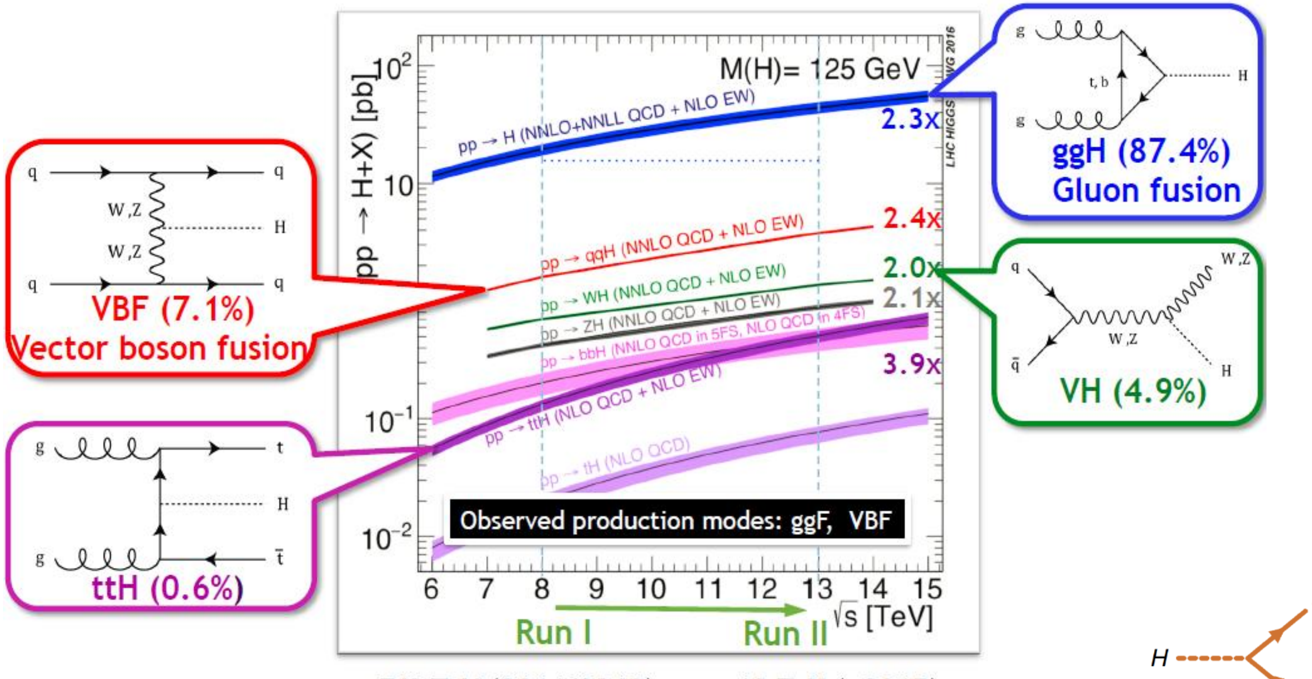

7/8 TeV (2011/2012) 13 TeV (>2015)

Higgs Decays

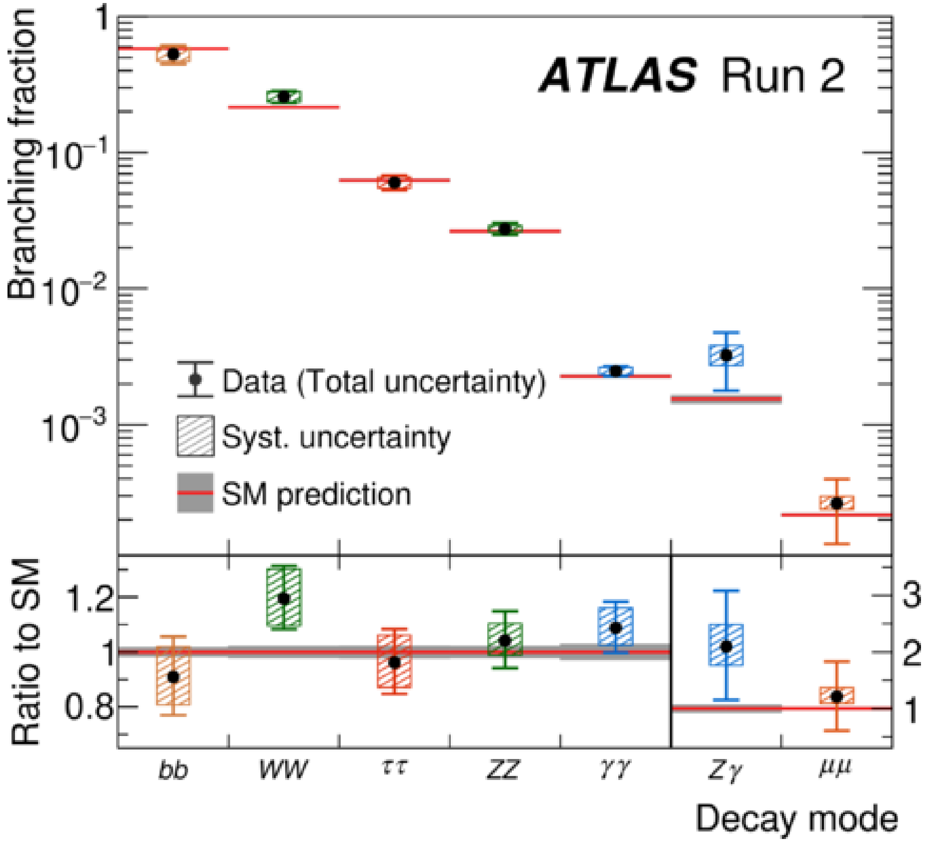

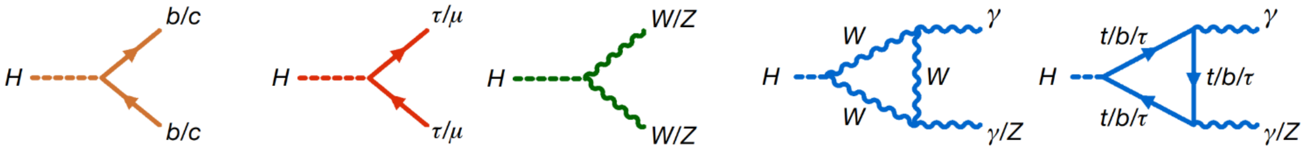

Nature 607, 52 (2022)

Higgs Couplings and Width

- **Higgs couplings agree well with SM**

ATLAS: ATLAS-CONF-2025-006, CMS: arXiv:2602.18611

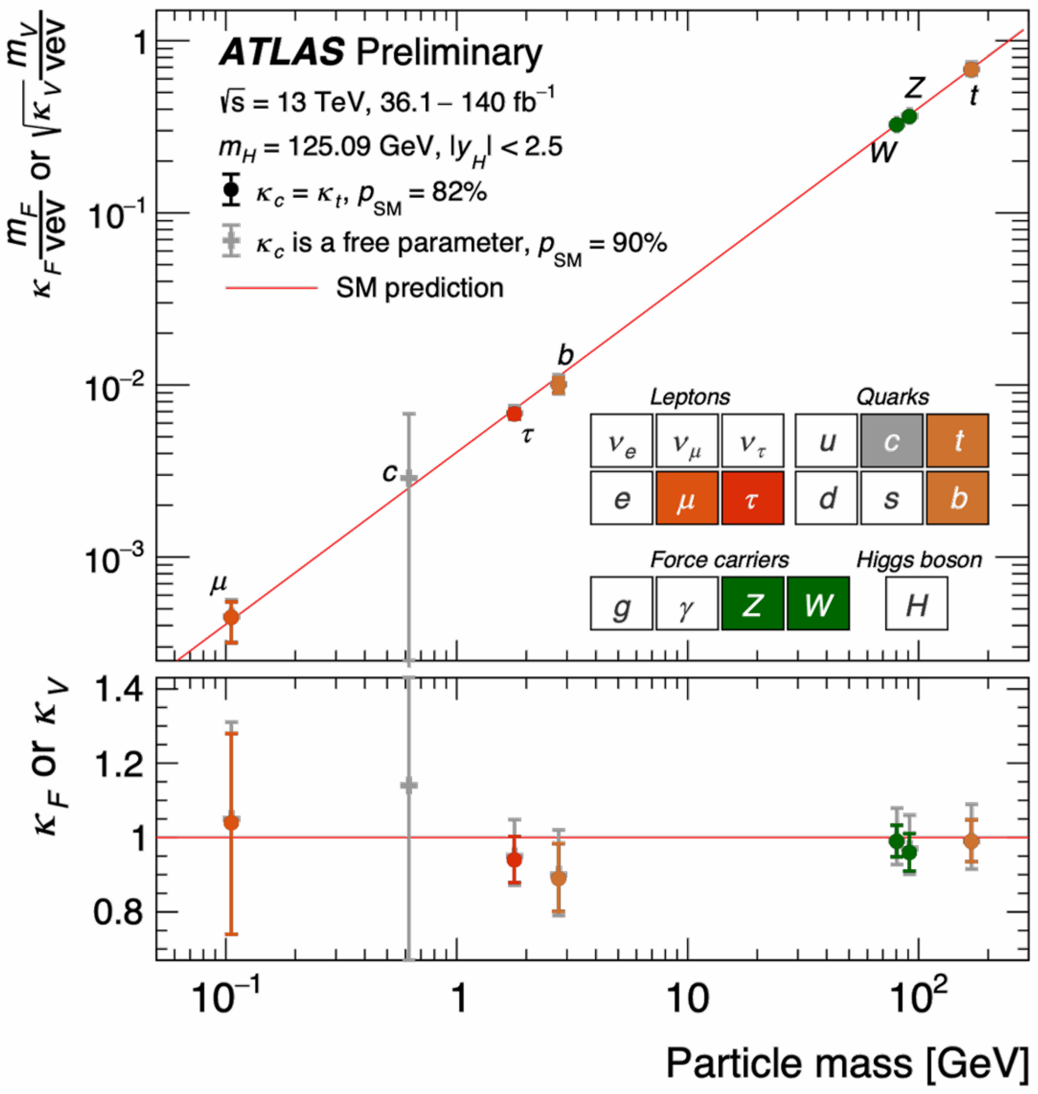

- **Higgs off-shell H→ZZ→4l, 2l2ν:**
- **Observed significance of 3.7σ (2.4σ exp.)**

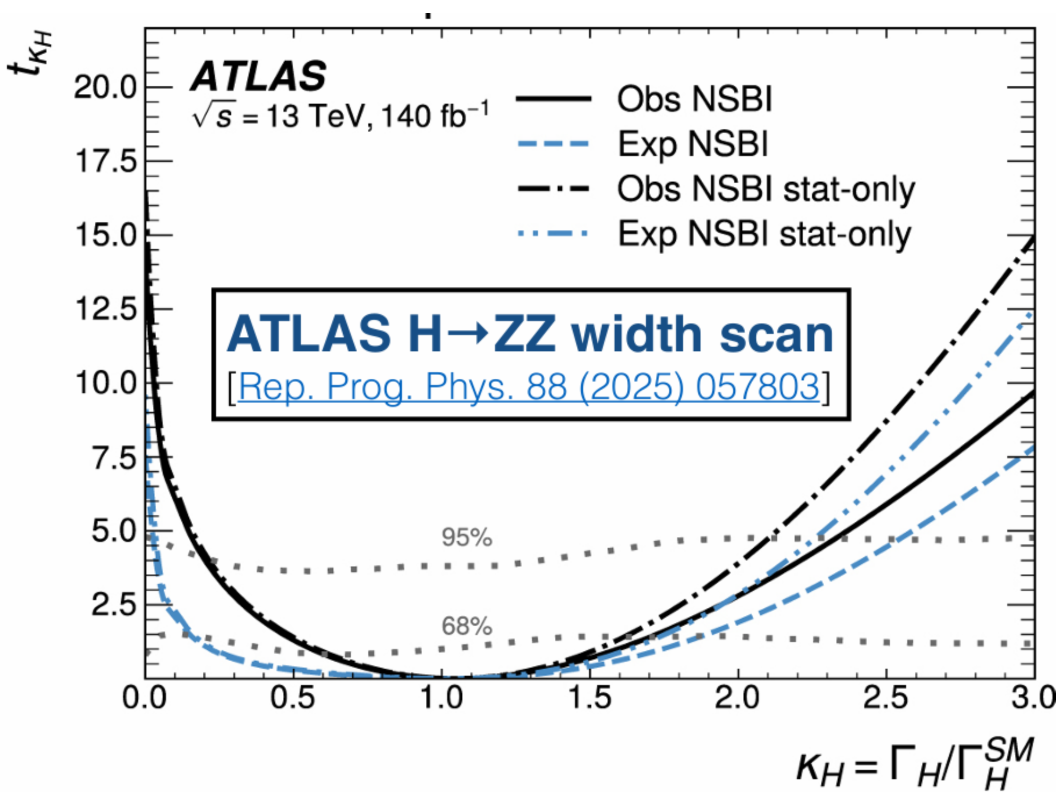

ATLAS H→ZZ width scan

[Rep. Prog. Phys. 88 (2025) 057803]

$$\kappa_H = 1.05^{+0.65}_{-0.46} \quad \left(1.00^{+0.86}_{-0.84}\right),$$

$$\Gamma_H = 4.3^{+2.7}_{-1.9} \quad \left(4.1^{+3.5}_{-3.4}\right) \text{ MeV}.$$

Higgs Cross Section

- Total Higgs cross sections at different CME are consistent with SM values (13.6 TeV, $\sigma^{\text{SM}}_{\text{total}} = 59.9 \pm 3.0\ \text{pb}$).

$$\sigma_{\text{total}} = 59.3 \pm 4.8(\text{stat.}) \pm 3.1(\text{sys.})\ \text{pb}$$

$$\sigma_{\text{fid}} \equiv \sigma \cdot \mathcal{B}(H \to ZZ^* \to 4\ell) =$$
$$3.65 \pm 0.30(\text{stat.})\ {}^{+0.18}_{-0.16}(\text{sys.})\ \text{fb} = 3.65^{+0.35}_{-0.33}\ \text{fb}$$

$$\mu = 0.99 \pm 0.08(\text{stat.}) \pm 0.10(\text{sys.}) = 0.99 \pm 0.13$$

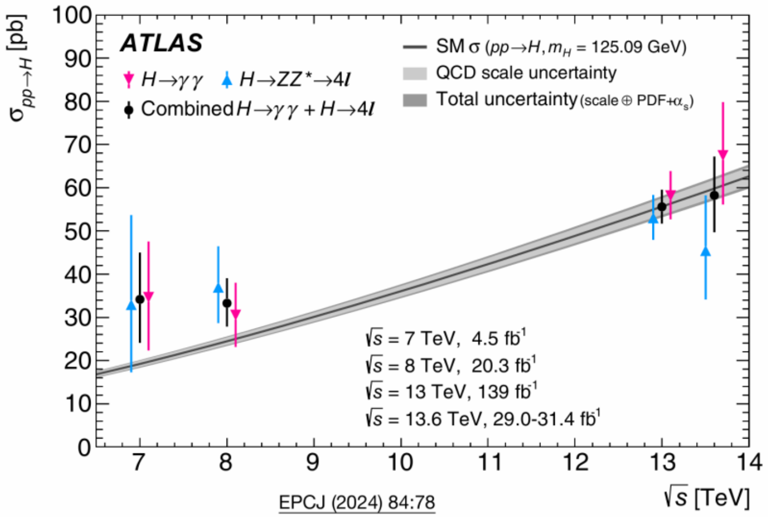

EPCJ (2024) 84:78

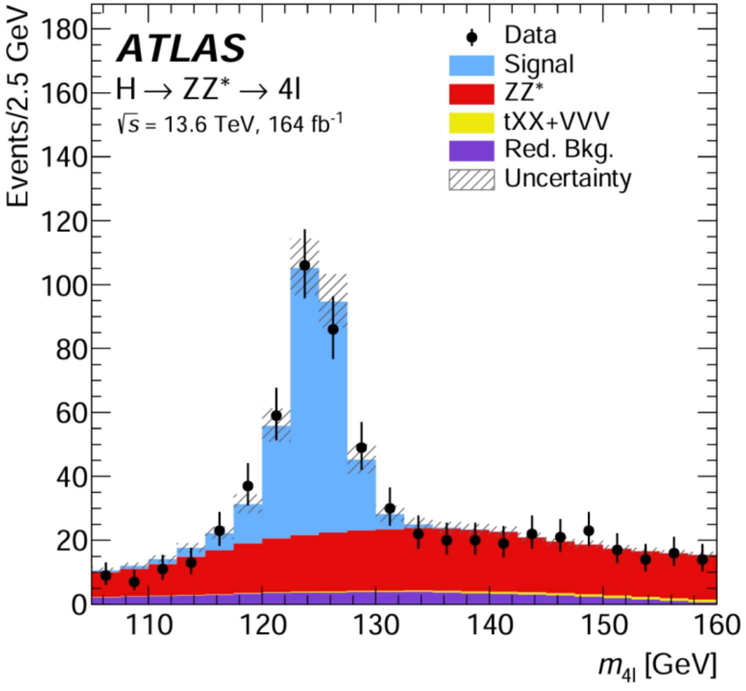

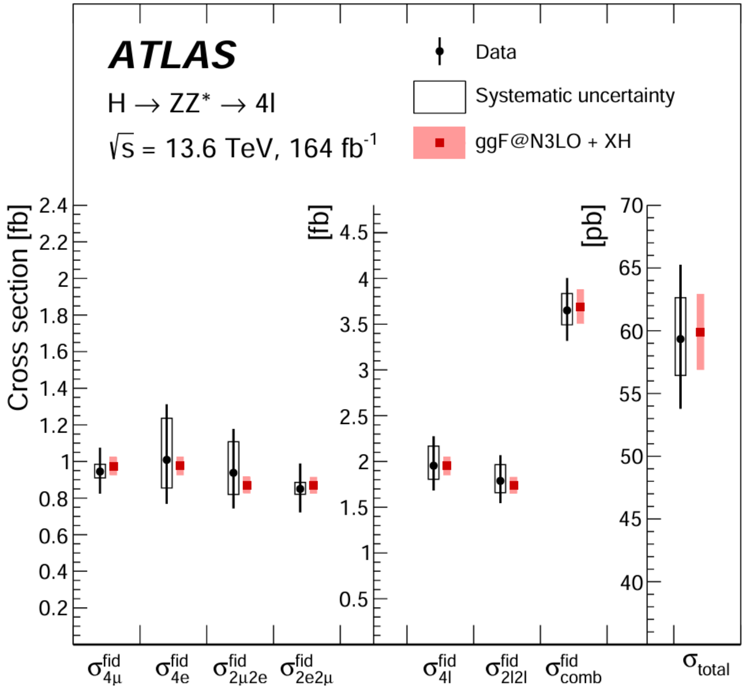

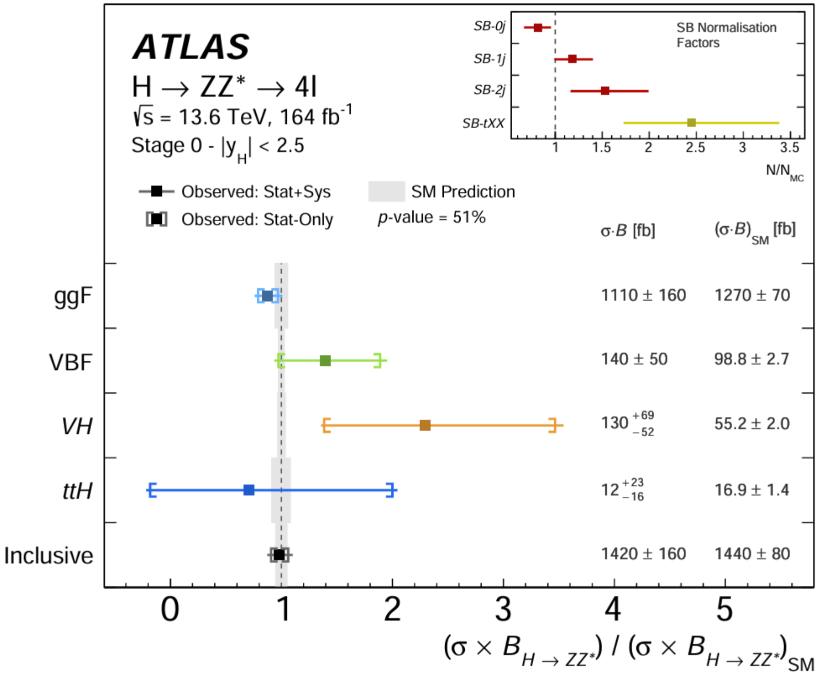

arXiv:2605.19016

H→bb, cc in VH and VBF Production

- Simultaneous search for H→bb and cc in VBF production using Run2 and Run3 data

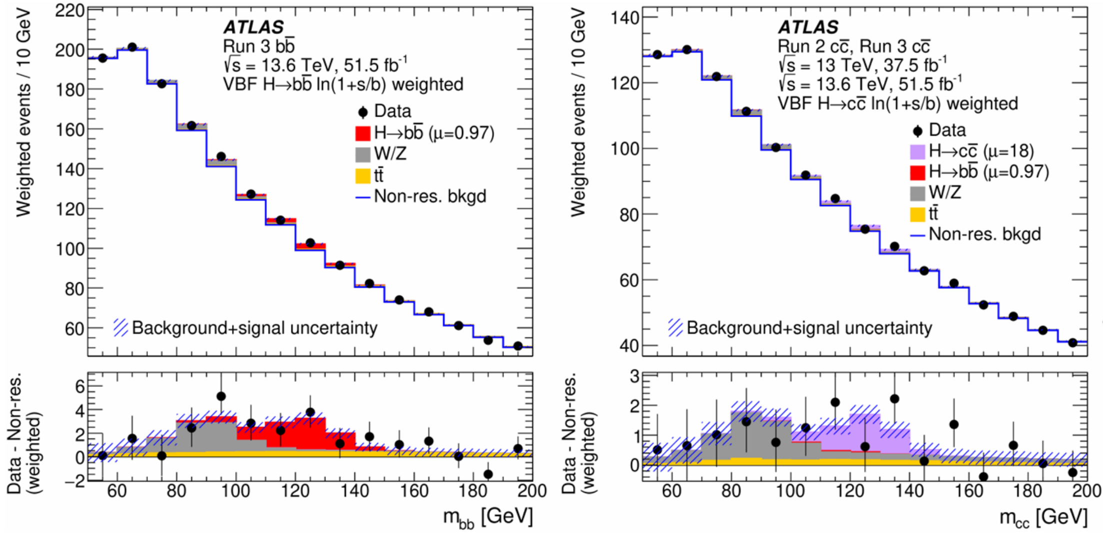

- **VBF H(bb) w/ Run3**
  - $\mu_{bb} =$ $0.97 \pm 0.45(\text{stat})^{+0.35}_{-0.22}$ (syst)
  - Significance:
    - obs (exp) = 2.0 (2.1) σ
- **VBF H(cc) w/ Run2+Run3**
  - $\mu_{cc} = 18 \pm 12$ (stat) $\pm$ 7(syst)
  - Upper limit @ 95% CL:
    - obs (exp) = 41 (28) x SM

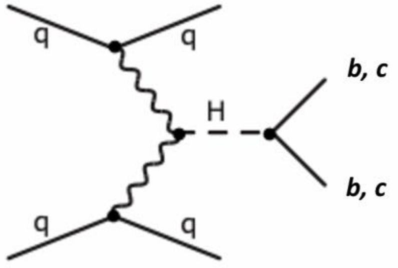

PLB 877 (2026) 140279
JHEP 04 (2025) 075
arXiv:2511.21911
arXiv:2509.14005

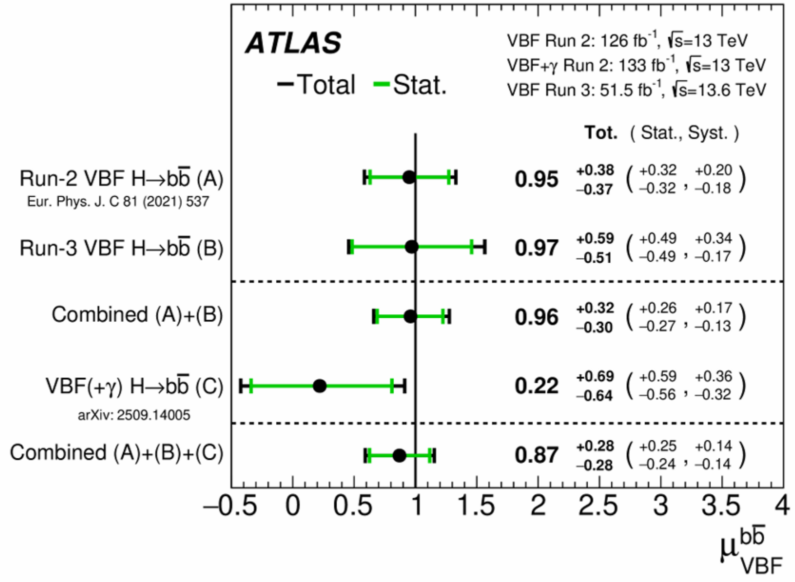

Significance:

- Obs (exp) = 3.2 (3.6) σ
  - => Evidence of VBF H(bb) !

- **Combined** $\mu_{cc} = 3.3^{+5.2}_{-5.0}$
- 95% CL Upper limit on μ_{cc} :
  - obs (exp) = 12.7 (9.8) x SM

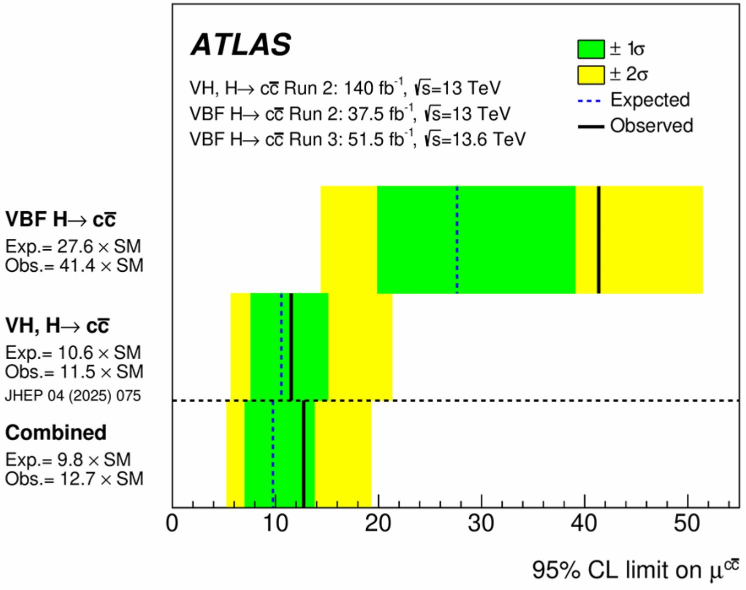

Evidence of boosted Higgs→bb,ττ at high-pT

■High-pT Higgs is sensitive to BSM loop effects, via ggF coupling modifications.

Inclusive H→bb:

- Transformer-based boosted H→bb tagger
- Improved jet mass and pT resolution via transformer-based regression model
- Z→bb signal used to calibrate the ML
- X10 in significance compared to Run2

Evidence for H→bb with $p_T(H)>450$ GeV at 3.8σ (2.5σ exp.)

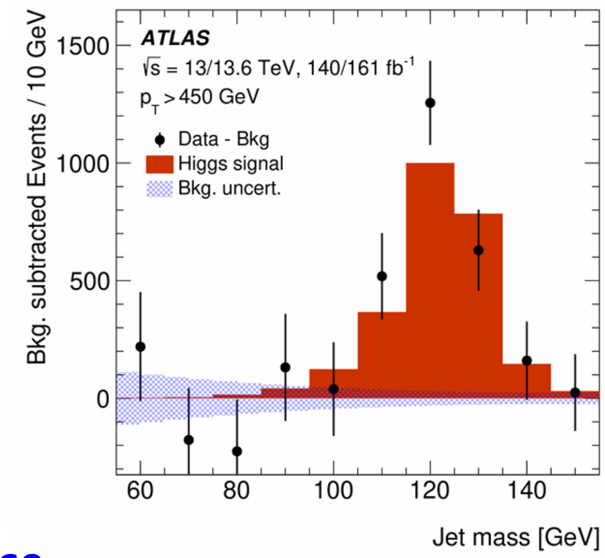

arXiv:2603.19369

Inclusive H→ττ:

- First ATLAS high-pT H→ττ analysis
- Dedicated boosted 2-τ reconstruction
- Transformer-based boosted H→ττ tagger
- BDT for better S/B, used as fit variable

Evidence for H→ττ with $p_T(H)>300$ GeV at 3.8σ (3.3σ exp.)

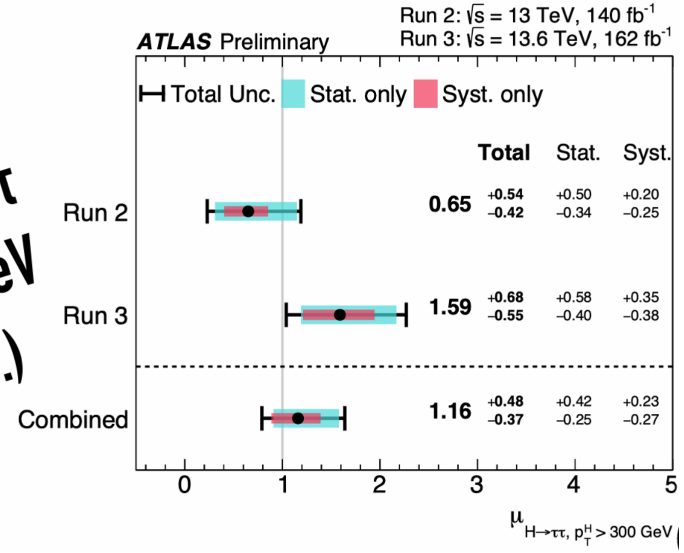

Evidence of $H \to \mu\mu$ Rare Decay

- $H \to \mu\mu$, direct probe of Higgs yukawa coupling to the 2nd generation fermions
- Challenge: Low BR ~ 0.022%, $S/B \sim 10^{-3}$
- Partial Run3 (165/fb): $\mu=1.6\pm0.6$, 2.8σ (1.8σ exp.)
- **Run2+Run3 (305/fb): $\mu=1.4\pm0.4$, 3.4σ (2.5σ exp.)**

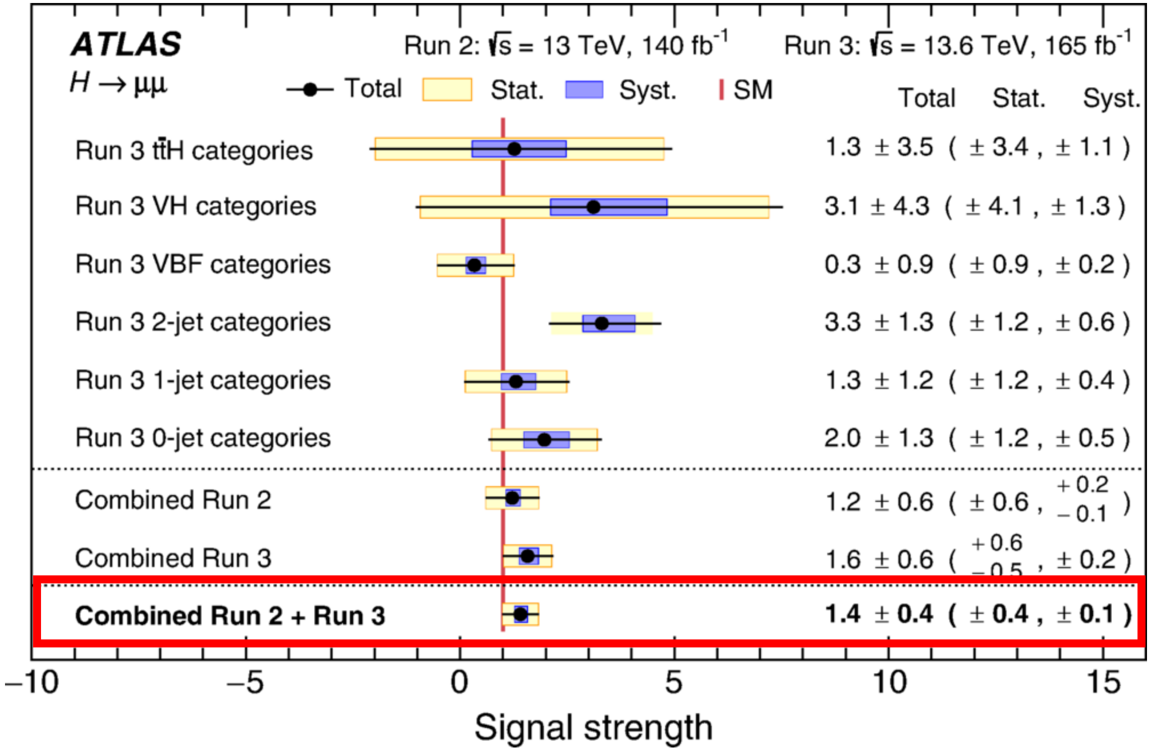

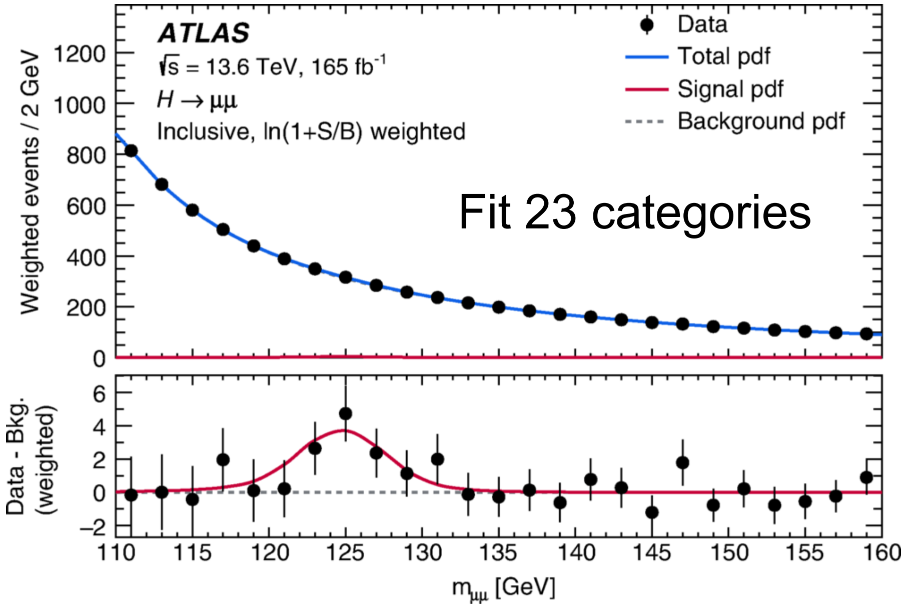

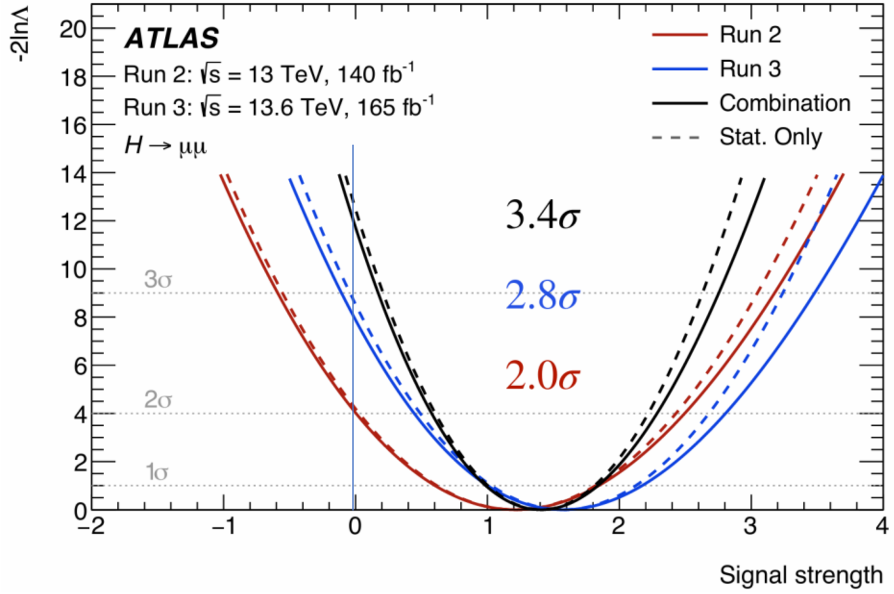

PRL135 (2025) 231802

Evidence of H → Zγ Rare Decay

- H→$Z\gamma$ is a loop-induced process, sensitive to probe BSM particles entering loop diagram
- Challenge: Low BR ~ 0.15%, Z→ll (6.7%), S/B ~ 10^{-3}
- Run2 ATLAS+CMS: **μ=2.2±0.7, 3.4σ (1.6σ exp.)**
- Run2 +Run3 (305/fb): **μ=1.3±0.6, 2.5σ (1.9σ exp.)**

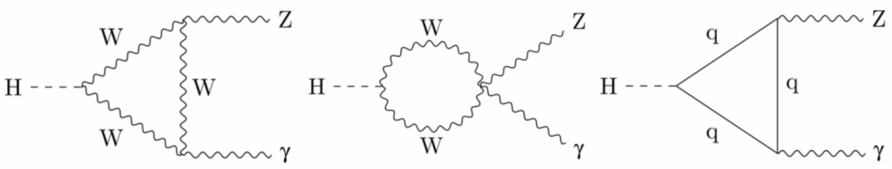

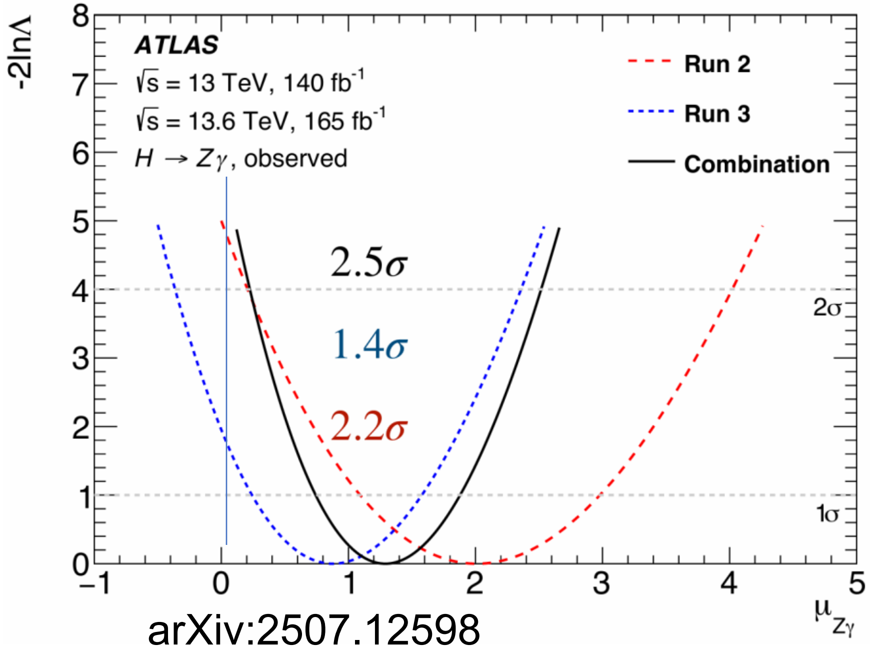

arXiv:2507.12598

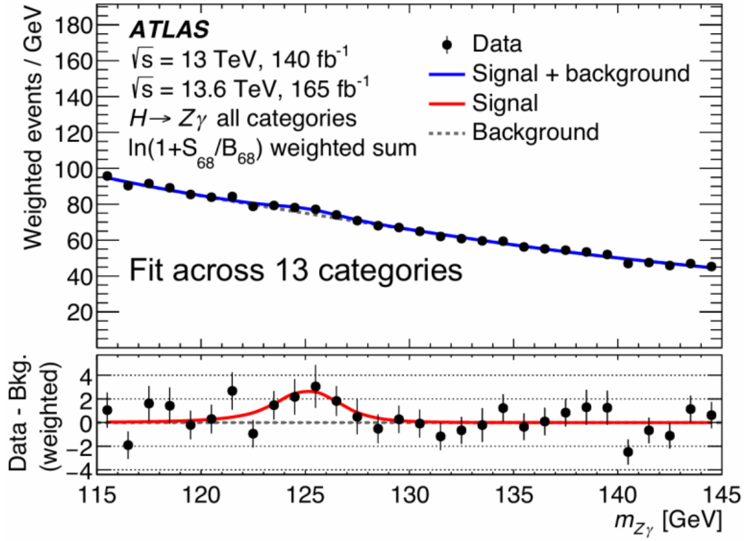

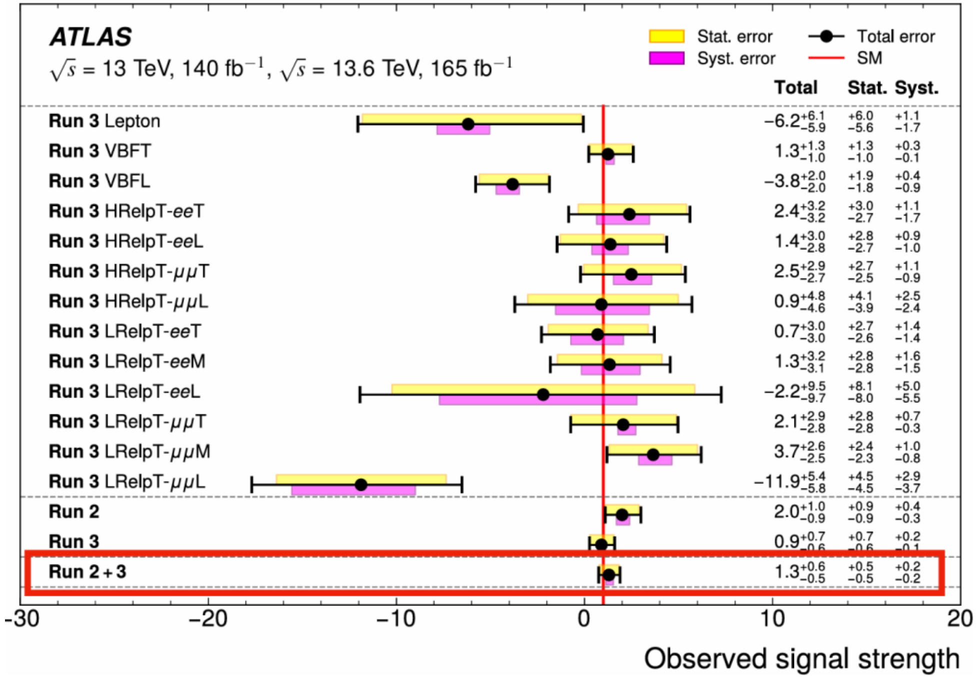

Higgs CP Violation

- CP violation (CPV) is crucial to understand matter-antimatter asymmetry in the universe, but the amount of CPV in SM (quark sector) is too small.
- Higgs boson has opened a window to search for CPV beyond the SM

CP violation in Higgs-Vector boson coupling

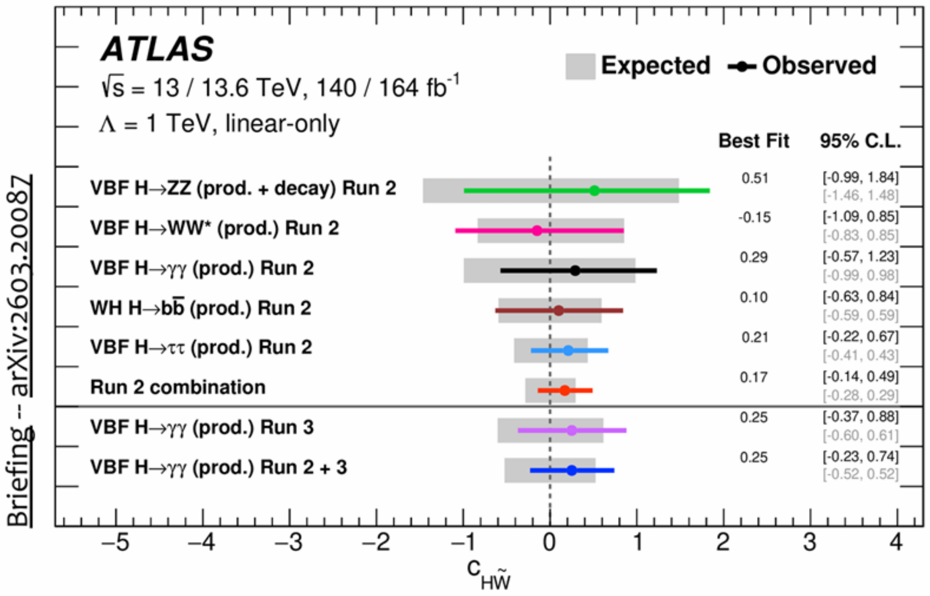

One of CP-violating SMEFT Wilson coefficients: measured consistent with zero

CP violation in H-t coupling (via ttH or tH production)

- New measurement of H-t Yukawa coupling in H → γγ using **Run 2+Run 3 (2022-2024) data**
- **Excluded |α|>38° at 95% CL,** best direct constraint to date
- **Excluded α=90° at 5.8σ,** first > 5σ rejection for purely CP-odd Higgs-fermion Yukawa coupling

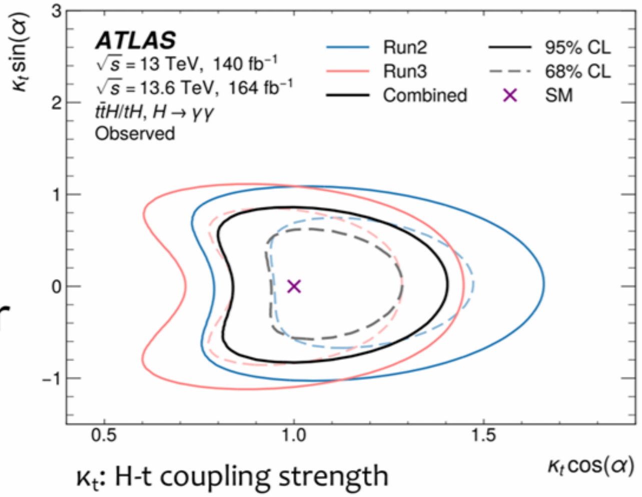

κ_t: H-t coupling strength

α: fraction of CP-odd component, α_{SM}=0

ATL-CONF-2026-002

Di-Higgs Search

- The shape of the Higgs potential is still unknown
- Di-Higgs is a key process to measure Higgs self-interaction
- Challenges: very low σ ~ 32.8fb, complicated final states

$$V(H) = \boxed{-\frac{1}{2}m_H H^2} \boxed{-\lambda_3 v H^3 - \lambda_4 H^4}$$

Higgs mass term

Higgs self-interaction term

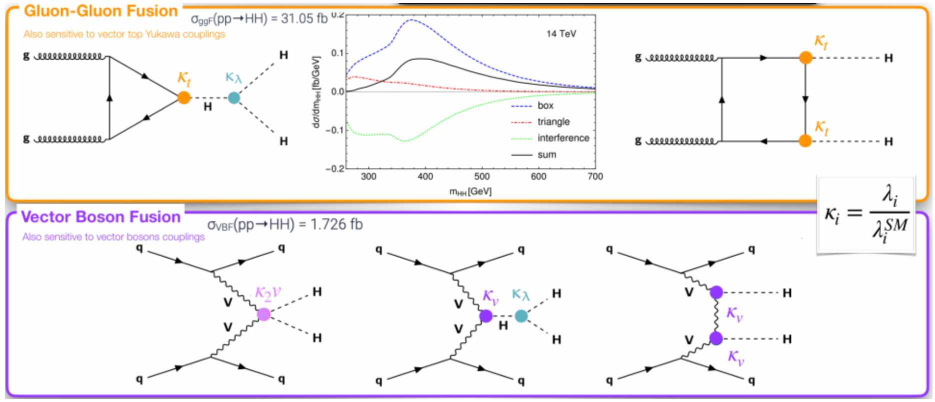

$$\kappa_i = \frac{\lambda_i}{\lambda_i^{SM}}$$

HH combination
Phys.Rev.Lett. 133 (2024) 101801

H+HH combination
Phys.Lett. B 843 (2023) 127745

$b\bar{b}b\bar{b}$
$b\bar{b}\tau^+\tau^-$
$b\bar{b}\gamma\gamma$

$b\bar{b}ll + E_T^{miss}$
- $b\bar{b}VV^*$ $(V = W, Z)$
- $b\bar{b}\tau^+\tau^-$

Multilepton
- $b\bar{b}ZZ^*$
- VV^*VV^* $(V = W, Z)$
- $VV^*\tau^+\tau^-$
- $\gamma\gamma VV^*$
- $\gamma\gamma\tau^+\tau^-$

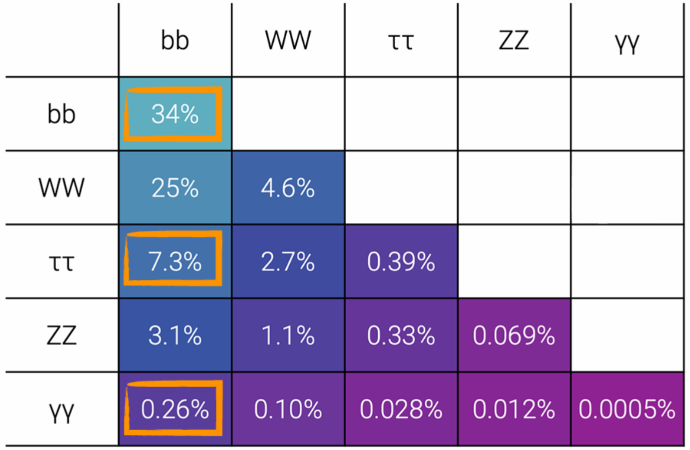

	bb	WW	ττ	ZZ	γγ
bb	34%				
WW	25%	4.6%			
ττ	7.3%	2.7%	0.39%		
ZZ	3.1%	1.1%	0.33%	0.069%	
γγ	0.26%	0.10%	0.028%	0.012%	0.0005%

▭ "Silver bullet" channels

All combinations are based on full Run 2 luminosity, most decay channels

HH combination
Phys.Rev.Lett. 133 (2024) 101801

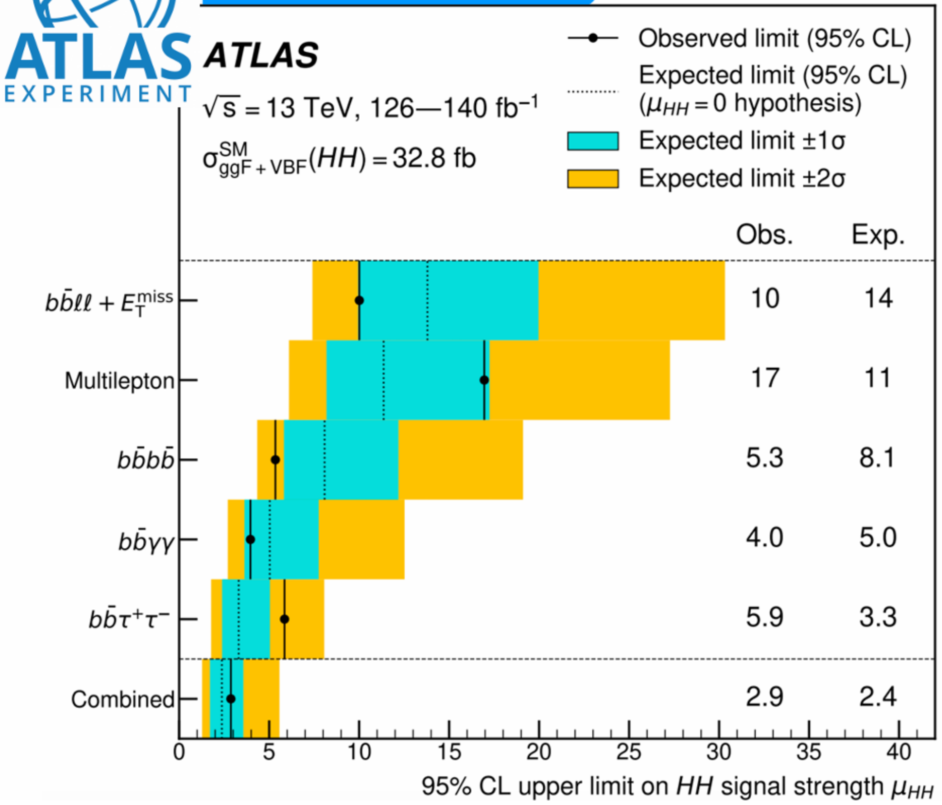

	Obs.	Exp.
$b\bar{b}\ell\ell + E_T^{miss}$	10	14
Multilepton	17	11
$b\bar{b}b\bar{b}$	5.3	8.1
$b\bar{b}\gamma\gamma$	4.0	5.0
$b\bar{b}\tau^+\tau^-$	5.9	3.3
Combined	2.9	2.4

H+HH Combination

- Single Higgs processes can be used to constraint κ_λ through NLO effects.

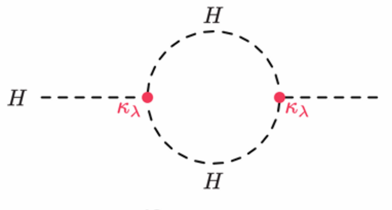

self-energy correction

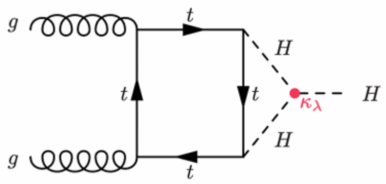

ggF

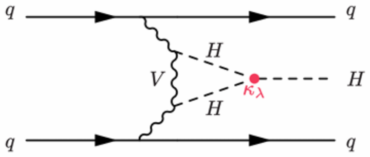

ttH

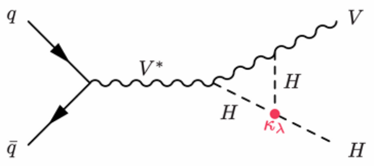

VBF

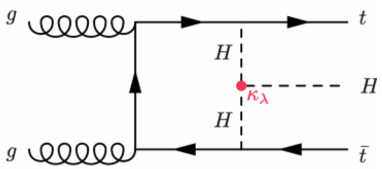

VH

- H+HH: combination of 7 single Higgs and 3 double Higgs channels

H+HH combination

Phys.Lett. B 843 (2023) 127745

$HH \to b\bar{b}\gamma\gamma$	139
$HH \to b\bar{b}\tau^+\tau^-$	139
$HH \to b\bar{b}b\bar{b}$	126
$H \to \gamma\gamma$	139
$H \to ZZ^* \to 4\ell$	139
$H \to \tau^+\tau^-$	139
$H \to WW^* \to e\nu\mu\nu$ (ggF,VBF)	139
$H \to b\bar{b}$ (VH)	139
$H \to b\bar{b}$ (VBF)	126
$H \to b\bar{b}$ $(t\bar{t}H)$	139

$-0.4 < \kappa_\lambda < 6.3$ $(-1.9 < \kappa_\lambda < 7.6)$

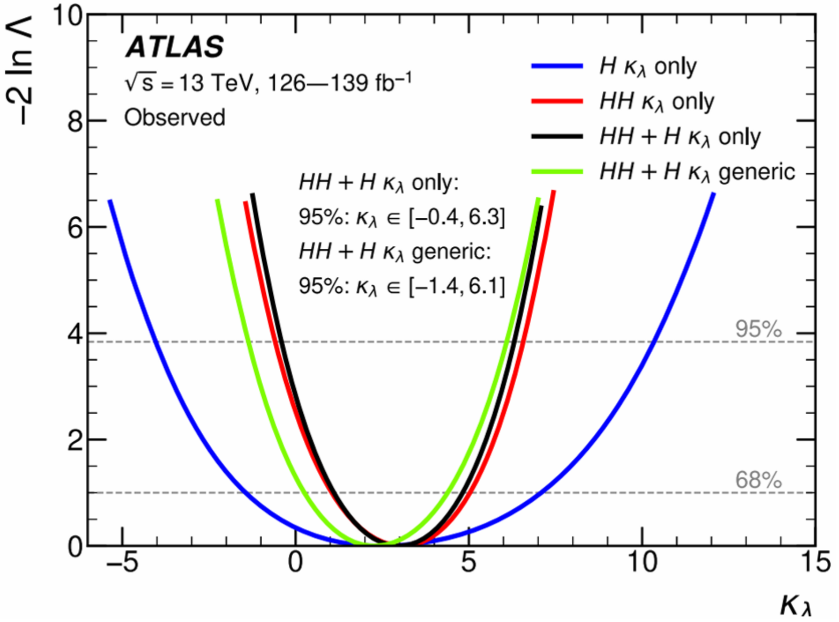

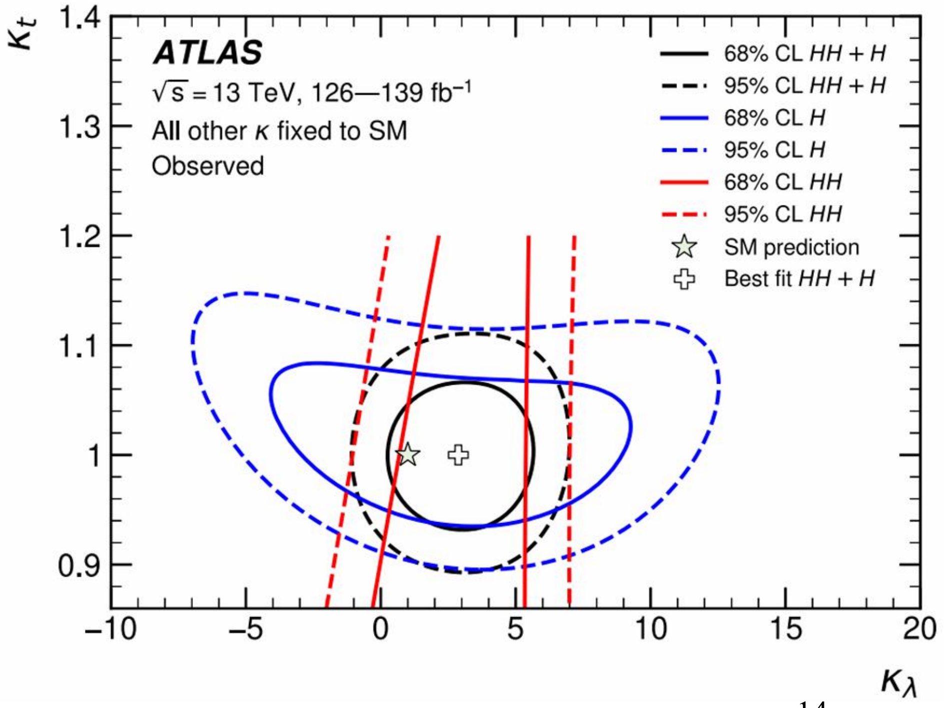

HH ATLAS and CMS Combination

- The best combined fit of HH signal strength at Run2
- **The observed (expected) local significance: 1.1σ (1.3σ)**

$$\hat{\mu}_{\mathrm{HH}} = 0.8^{+0.9}_{-0.7} = 0.8^{+0.7}_{-0.6}(\mathrm{stat.})^{+0.4}_{-0.2}(\mathrm{theory})^{+0.3}_{-0.3}(\mathrm{exp.})$$

$$\hat{\mu}^{\mathrm{exp}}_{\mathrm{HH}} = 1.0^{+0.9}_{-0.8} = 1.0^{+0.7}_{-0.6}(\mathrm{stat.})^{+0.5}_{-0.3}(\mathrm{theory})^{+0.3}_{-0.3}(\mathrm{exp.})$$

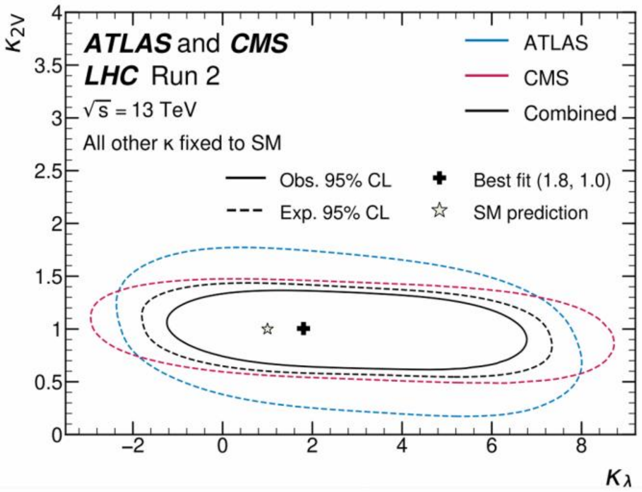

Best fit κ_λ = **1.8**, κ_{2V} = **1.0** —> Compatible with the SM prediction

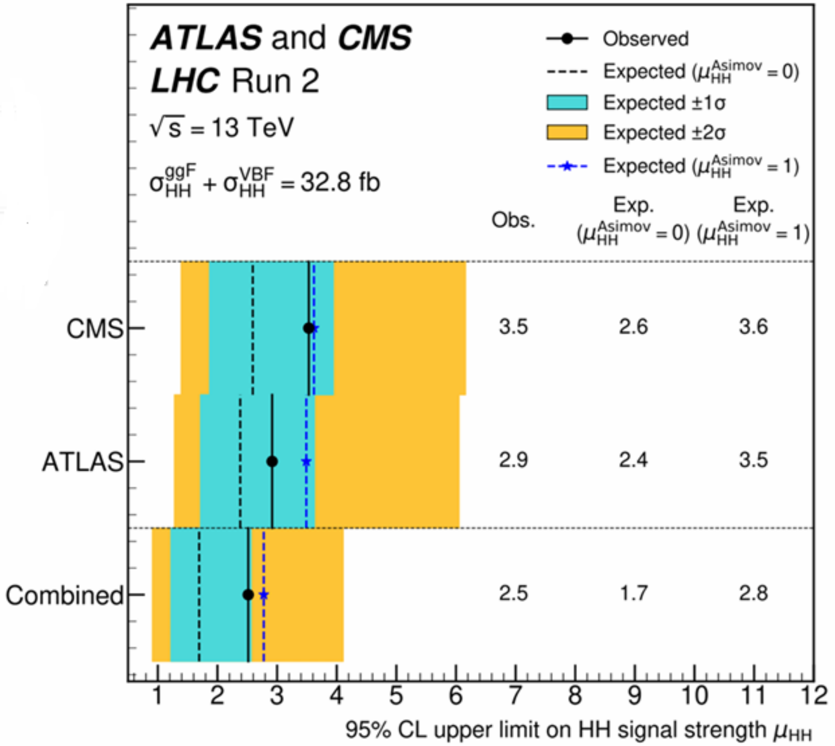

	Obs.	Exp. ($\mu_{\mathrm{HH}}^{\mathrm{Asimov}} = 0$)	Exp. ($\mu_{\mathrm{HH}}^{\mathrm{Asimov}} = 1$)
CMS	3.5	2.6	3.6
ATLAS	2.9	2.4	3.5
Combined	2.5	1.7	2.8

-HH combination-

CERN-EP-2026-011

-0.71 $< \kappa_\lambda <$ **6.1** $(-1.3 < \kappa_\lambda < 6.7)$

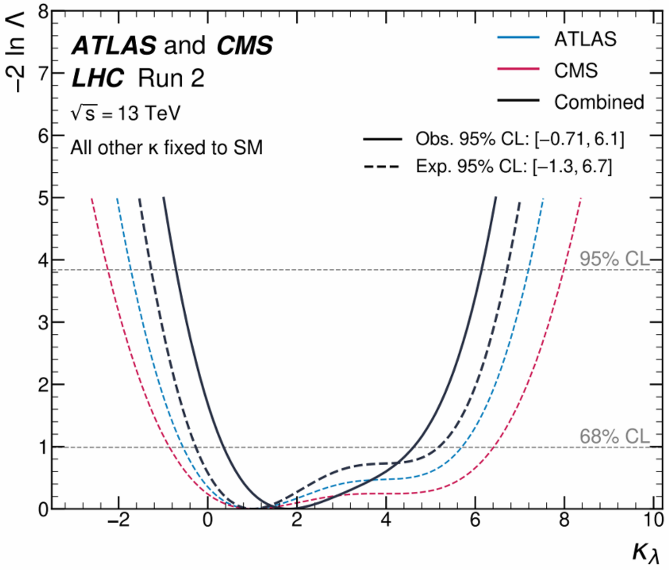

0.73 $< \kappa_{2V} <$ **1.3** $(0.66 < \kappa_{2V} < 1.4)$

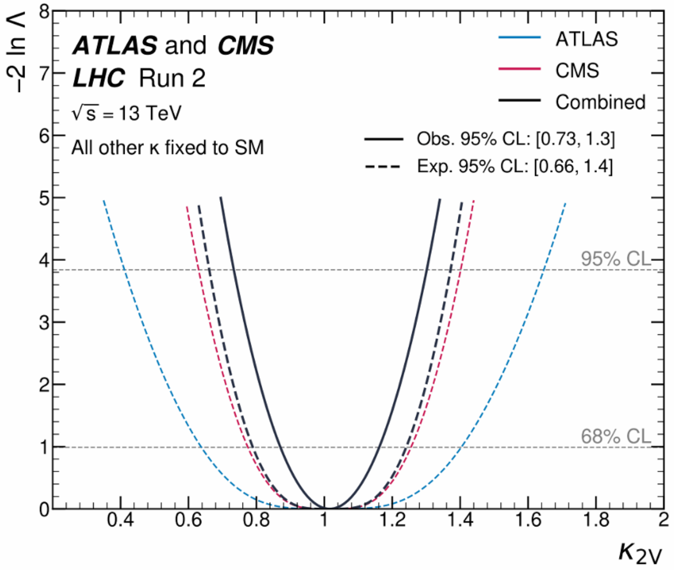

HHH → bbbbbb Search

- **The 1st search of tri-Higgs** by the LHC, X→SH→HHH (TRSM)
- Deep Neural Network (DNN) classifiers for better S/B separation
- Data-driven method to estimate major multijet background, extrapolate DNN distribution from 4b and 5b control regions.
- Set limits on trilinear (λ_3) and quartic (λ_4) Higgs self-coupling.
- **An upper limit of 59 fb is set at 95% CL.**

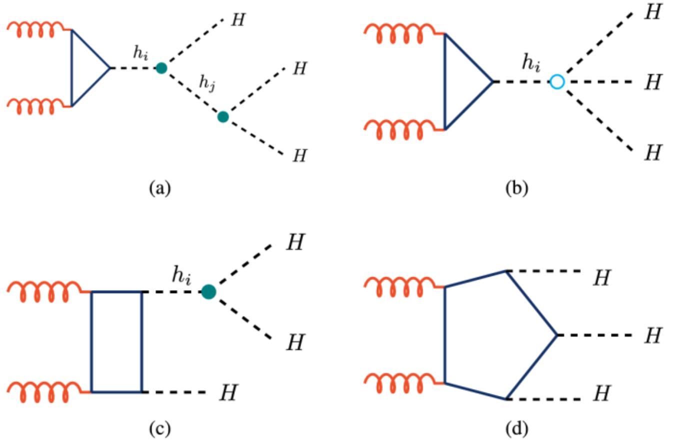

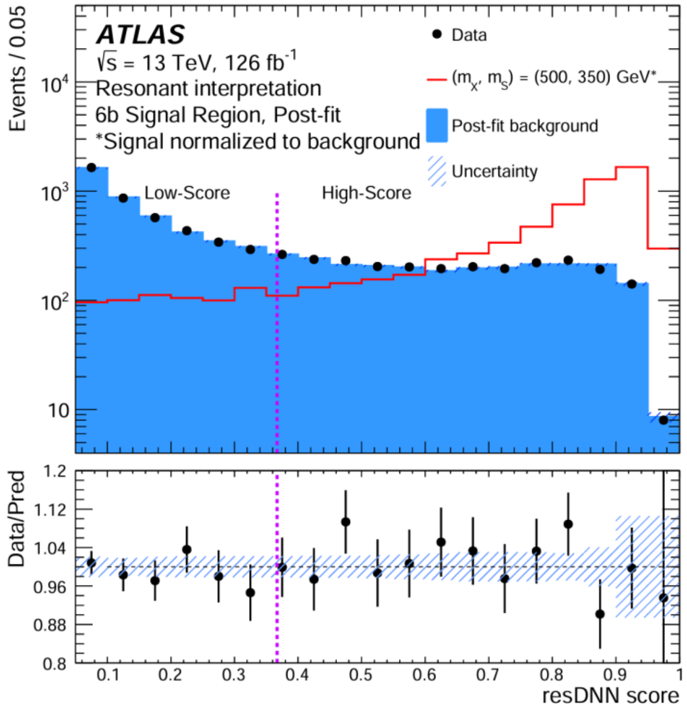

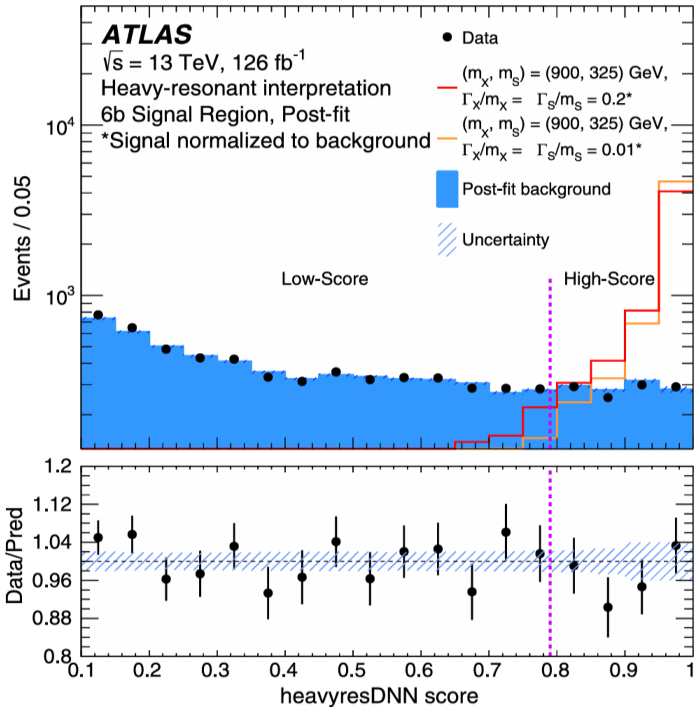

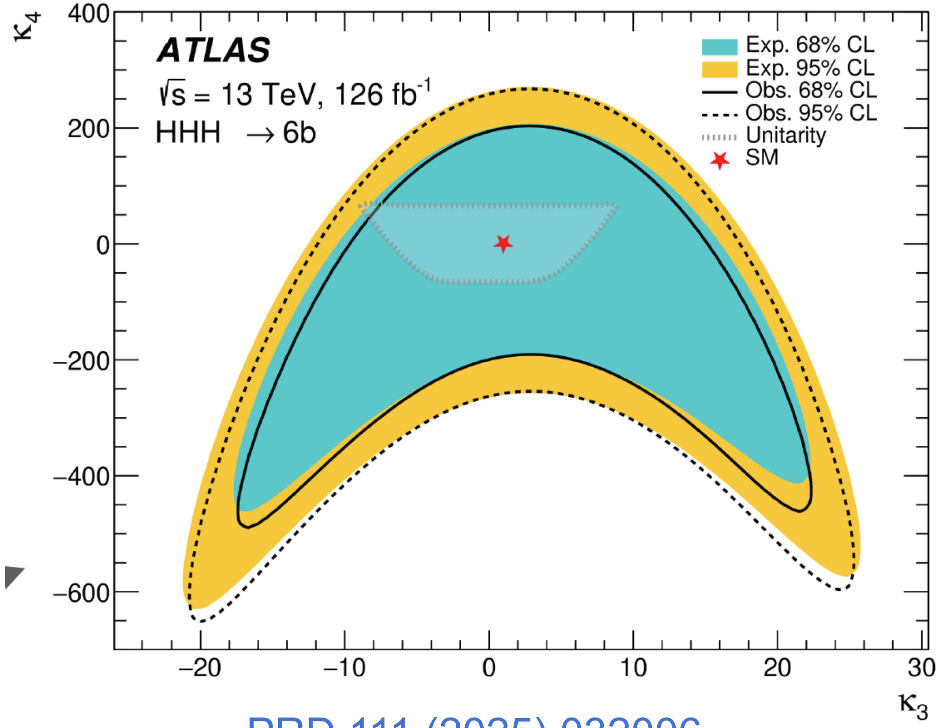

PRD 111 (2025) 032006

https://atlas.cern/Updates/Briefing/First-Tri-Higgs-Search

Longitudinal Polarized VBS

Importance of $W_L^\pm W_L^\pm \rightarrow W_L^\pm W_L^\pm$

- Higgs Goldstone bosons result in longitudinal polarized vector bosons:

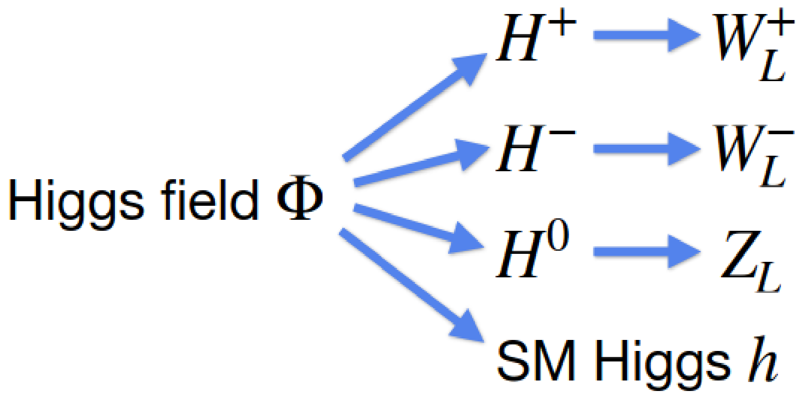

Higgs field Φ

$H^+ \longrightarrow W_L^+$

$H^- \longrightarrow W_L^-$

$H^0 \longrightarrow Z_L$

SM Higgs h

- Longitudinal $W_L^\pm W_L^\pm \rightarrow W_L^\pm W_L^\pm$ would **violate unitarity if Higgs coupling deviates from SM prediction**

➡ $W_L^\pm W_L^\pm \rightarrow W_L^\pm W_L^\pm$ is a **unique opportunity to probe electroweak symmetry-breaking**

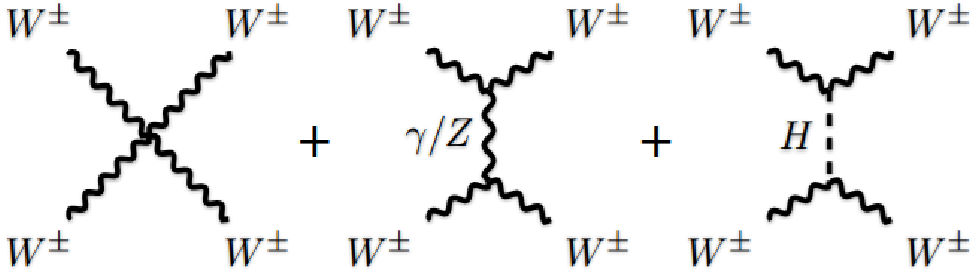

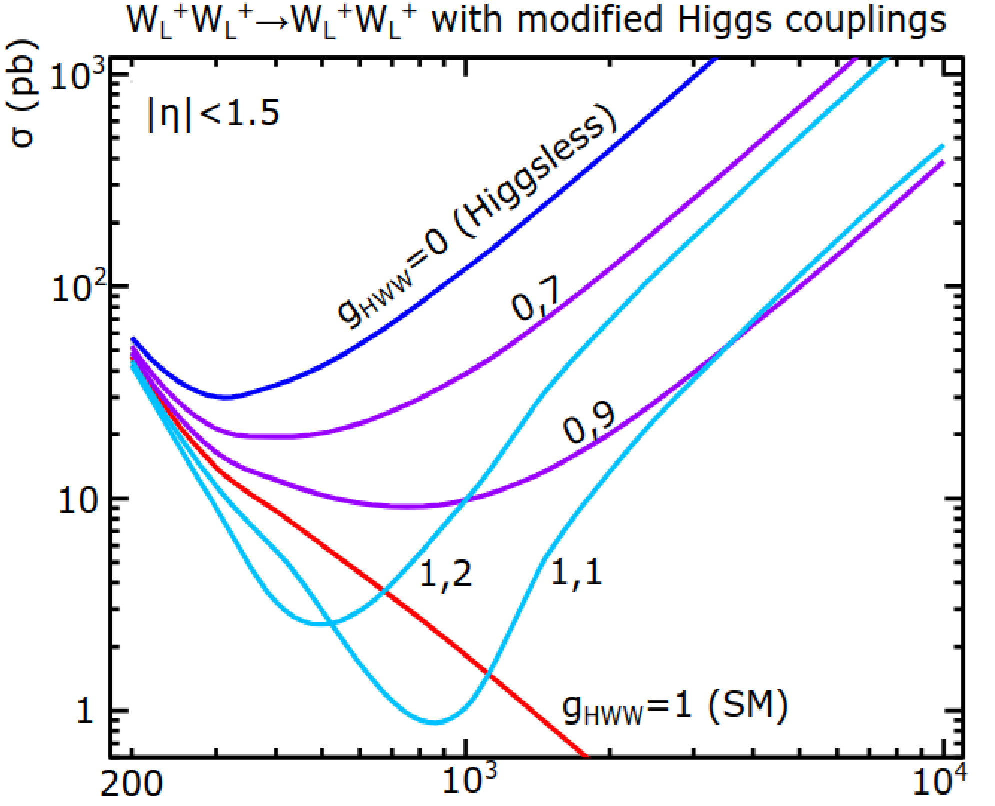

[adapted from arXiv:1412.8367]

Longitudinal VBS: same-sign WW jj

- **Two-stage DNN strategy:**
  - ☐ **DNN$_{\text{inclusive}}$**: inclusive EW ssWW vs backgrounds
  - ☐ **DNN$_{\text{polarization}}$**: polarization separation for $W_L W_L$ vs. $W_T W$, $W_L W$ vs. $W_T W_T$
- **First evidence for ≥1 longitudinally polarized W boson: 3.3σ (4σ exp.)**
- Upper limit for doubly-longitudinal $W_L W_L$ components: 0.45 fb (95% CL)

204 signal:
- LL: 10%
- LT: 21%
- TT: 69%

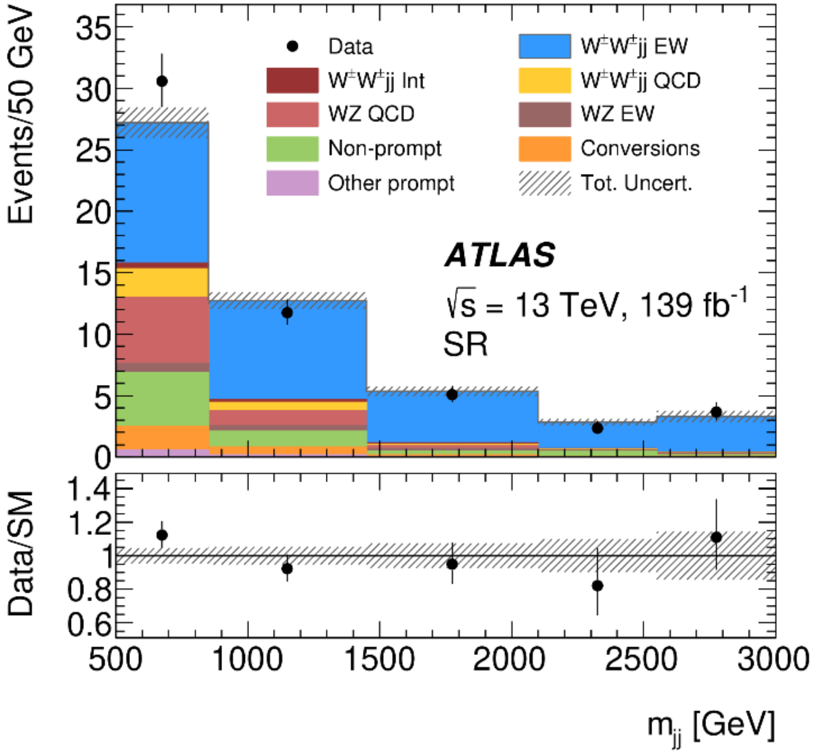

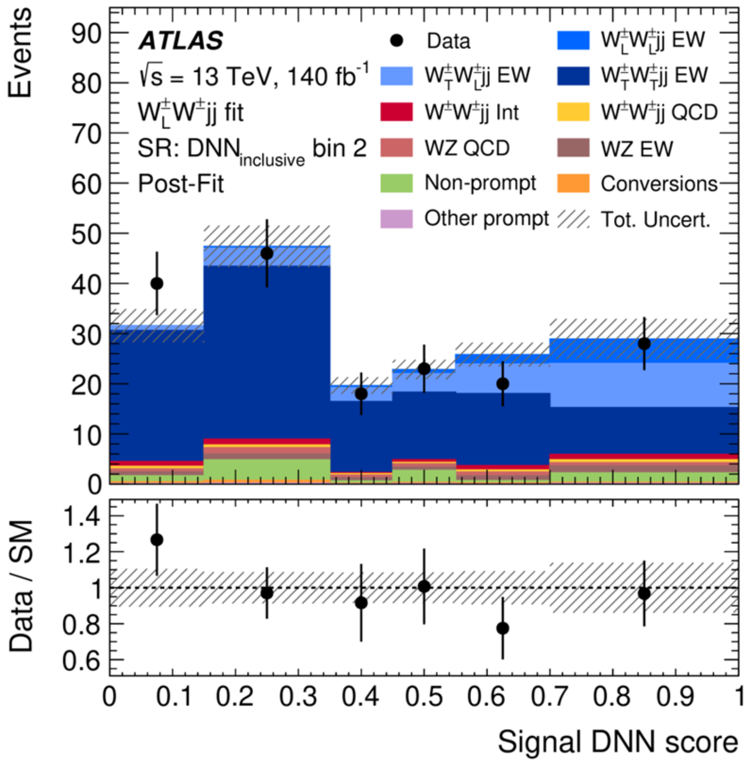

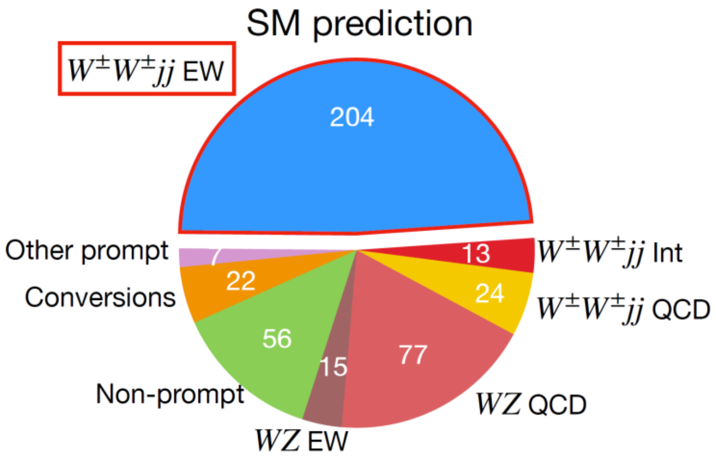

Process	Predicted $\sigma\mathcal{B}$ (fb)	Measured $\sigma\mathcal{B}$ (fb)
$W_L^\pm W_L^\pm jj$	0.29 ± 0.07	0.01 ± 0.21(tot)
$W_T^\pm W^\pm jj$	2.56 ± 0.64	3.39 ± 0.35(tot)
$W_L^\pm W^\pm jj$	1.18 ± 0.29	0.88 ± 0.30(tot)
$W_T^\pm W_T^\pm jj$	1.67 ± 0.40	2.49 ± 0.32(tot)

PRL 135 (2025) 111802

Tri-boson: VVZ Observation

- ATLAS observed VVZ 6.4σ (exp 4.7σ) using 140 fb^{-1} Run-2 data at 13 TeV

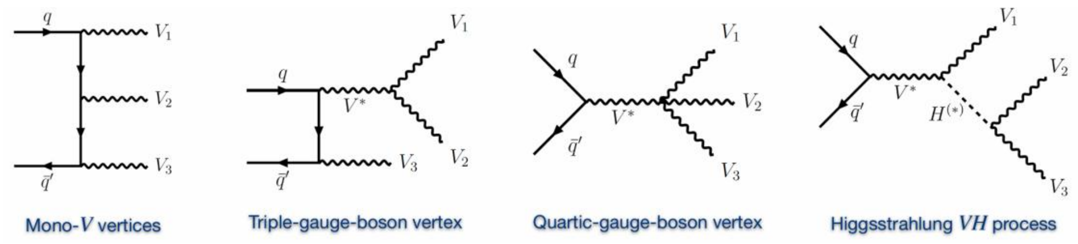

Process	Signal strength	Cross section (fb)	Observed (expected)
VVZ	$1.43 \pm 0.20(\text{stat.})^{+0.21}_{-0.19}(\text{syst.})$	$660^{+93}_{-90}(\text{stat.})^{+88}_{-81}(\text{syst.})$	6.4 (4.7) σ
WWZ	$1.33 \pm 0.28(\text{stat.})^{+0.21}_{-0.17}(\text{syst.})$	$442 \pm 94(\text{stat.})^{+60}_{-52}(\text{syst.})$	4.4 (3.6) σ
WZZ	$2.13^{+1.18}_{-0.96}(\text{stat.})^{+0.76}_{-0.41}(\text{syst.})$	$200^{+111}_{-91}(\text{stat.})^{+65}_{-37}(\text{syst.})$	2.8 (1.6) σ

Coefficient	Expected limit [TeV^{-4}]	Exp. $\sqrt{\hat{s}_c}$ [TeV]	Observed limit [TeV^{-4}]	Obs. $\sqrt{\hat{s}_c}$ [TeV]
f_{M2}/Λ^4	[−18, 17]	1.2	[−19, 19]	1.2
f_{M3}/Λ^4	[−28, 29]	1.5	[−28, 29]	1.5
f_{M4}/Λ^4	[−14, 14]	1.6	[−12, 12]	1.7
f_{M5}/Λ^4	[−11, 11]	2.1	[−9.1, 9.3]	2.2

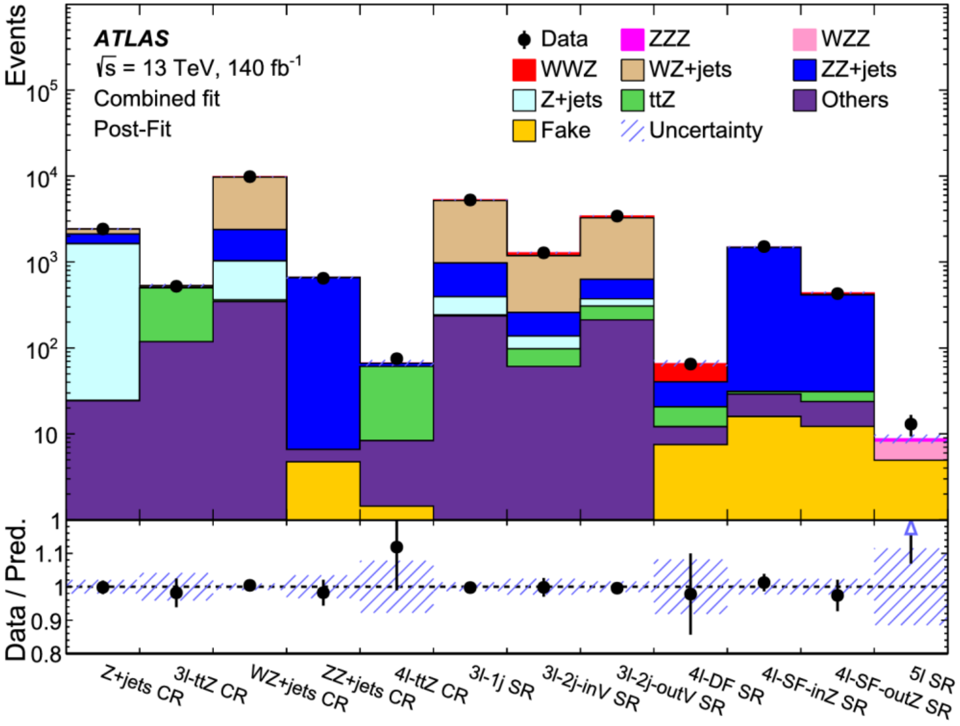

PLB 866 (2025) 139527

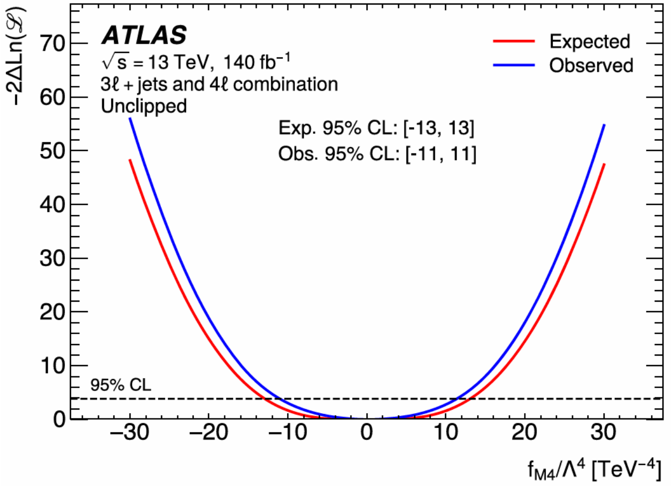

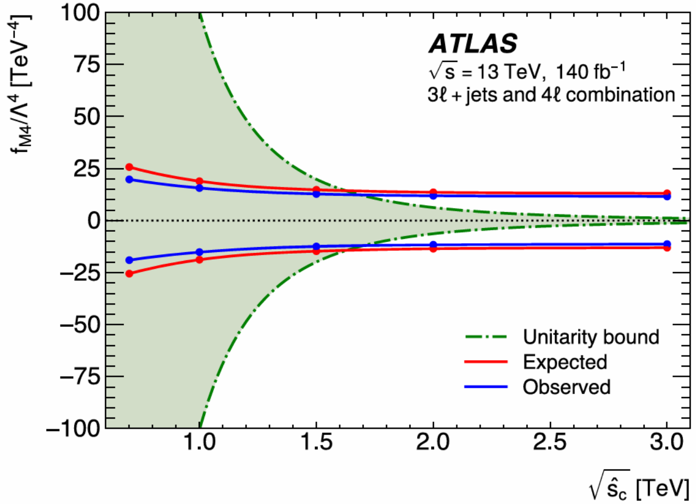

arXiv:2412.15123

Tri-boson: WWγ Observation

- ➢**First observation of WWγ with significance of 5.9σ (6σ exp.)**
- ➢**Measured fiducial cross-section:**

  6.2 ± 0.8 (stat.) ± 0.6 (syst.) fb

  consistent with SM (6.1 fb)

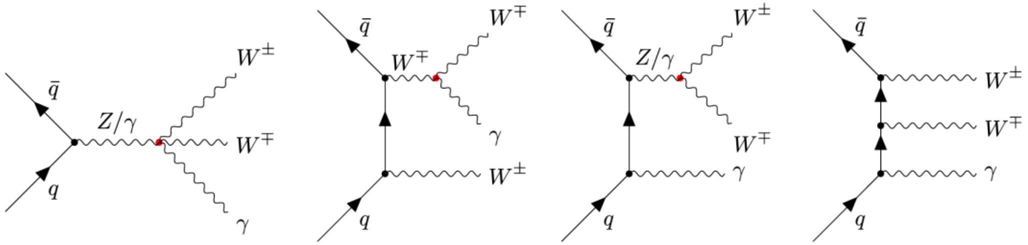

	SR $e^\pm\mu^\mp\nu\bar{\nu}\gamma$
$WW\gamma$	250 ± 40
$VZ\gamma$	31 ± 6
$Z\gamma$	119 ± 7
$t\bar{t}\gamma$	422 ± 34
$j \to \gamma$	89 ± 34
$e \to \gamma$	34 ± 5
Total	941 ± 29
Data	957

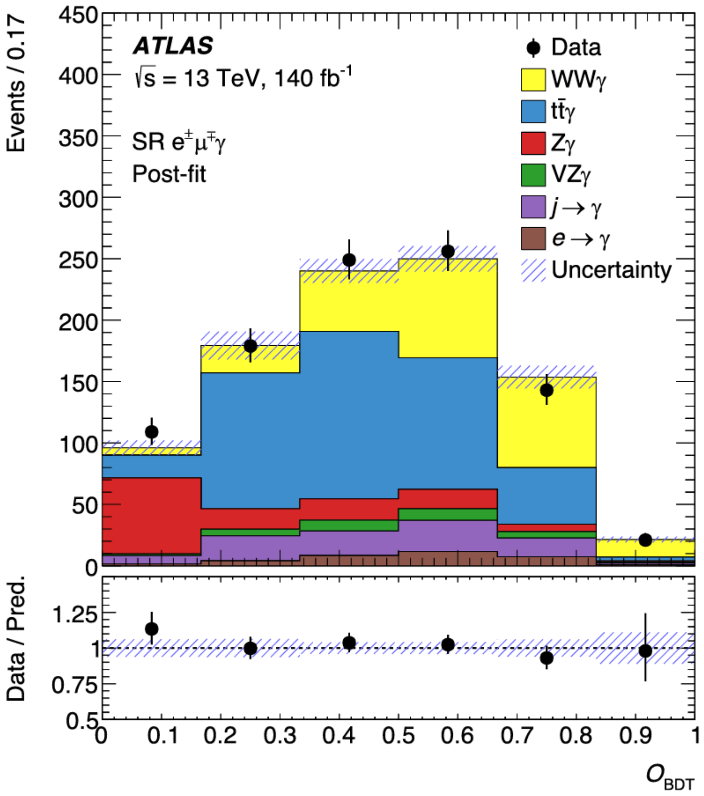

- ➢ Constraints on Wilson coefficients of 13 dim-8 EFT operators via anomalous quartic gauge couplings (**aQGC**):

EFT operator	Expected 95 % CI [TeV^{-4}]	Observed 95 % CI [TeV^{-4}]
f_{M0}/Λ^4	$[-8, 8]$	$[-6, 6]$
f_{M1}/Λ^4	$[-13, 13]$	$[-10, 10]$
f_{M2}/Λ^4	$[-3.1, 3.1]$	$[-2.5, 2.5]$
f_{M3}/Λ^4	$[-5, 5]$	$[-4, 4]$
f_{M4}/Λ^4	$[-8, 8]$	$[-6, 6]$
f_{M5}/Λ^4	$[-6, 6]$	$[-5, 5]$
f_{M7}/Λ^4	$[-26, 26]$	$[-21, 21]$
f_{T0}/Λ^4	$[-1.4, 1.4]$	$[-1.1, 1.1]$
f_{T1}/Λ^4	$[-1.7, 1.7]$	$[-1.4, 1.3]$
f_{T2}/Λ^4	$[-4, 4]$	$[-3.1, 3.0]$
f_{T5}/Λ^4	$[-1.1, 1.1]$	$[-0.9, 0.9]$
f_{T6}/Λ^4	$[-1.3, 1.3]$	$[-1.1, 1.1]$
f_{T7}/Λ^4	$[-3.0, 3.0]$	$[-2.4, 2.4]$

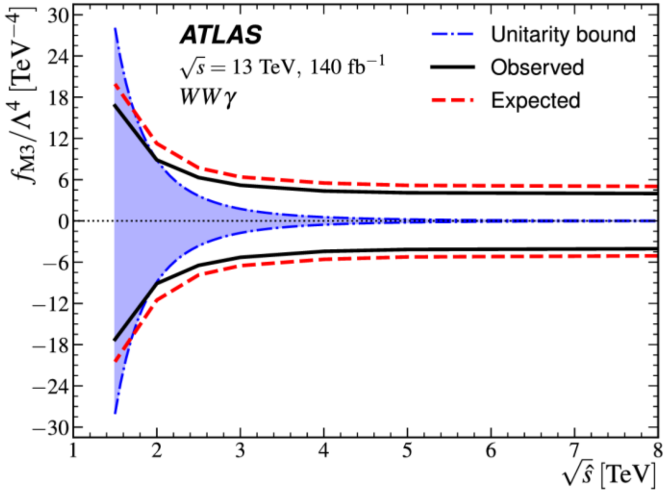

PLB 873 (2026) 140050

Tri-boson: ZZγ evidence

- **ZZγ → 4l+γ** has high S/B ratio (~7)
- **Evidence of ZZγ → 4l+γ (observed 4.4σ)**

$$\sigma_{ZZ\gamma} = 0.144\,^{+0.064}_{-0.051}\,(\text{stat.})\,^{+0.007}_{-0.005}\,(\text{syst.})\text{ fb}$$

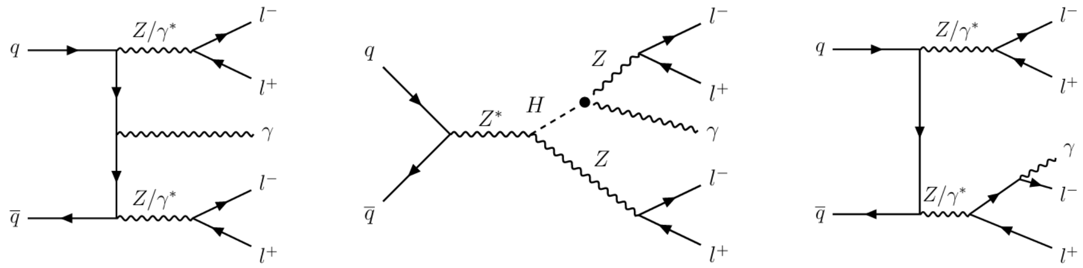

	Number of events
Sherpa 2.2.11 $4\ell\gamma$	6.28 ± 0.09 (stat.) ± 0.18 (syst.)
Powheg+Pythia8 $ZH \rightarrow ZZ\gamma$	0.76 ± 0.03 (stat.) ± 0.03 (syst.)
Signal	7.04 ± 0.09 (stat.) ± 0.18 (syst.)
Fake photons	0.71 ± 0.02 (stat.) ± 0.13 (syst.)
Fake leptons	0.12 ± 0.02 (stat.) ± 0.08 (syst.)
Pileup	0.09 ± 0.002 (stat.) ± 0.02 (syst.)
Total background	0.92 ± 0.03 (stat.) ± 0.15 (syst.)
N_{tot} prediction	7.96 ± 0.09 (stat.) ± 0.23 (syst.)
N_{tot} data	8

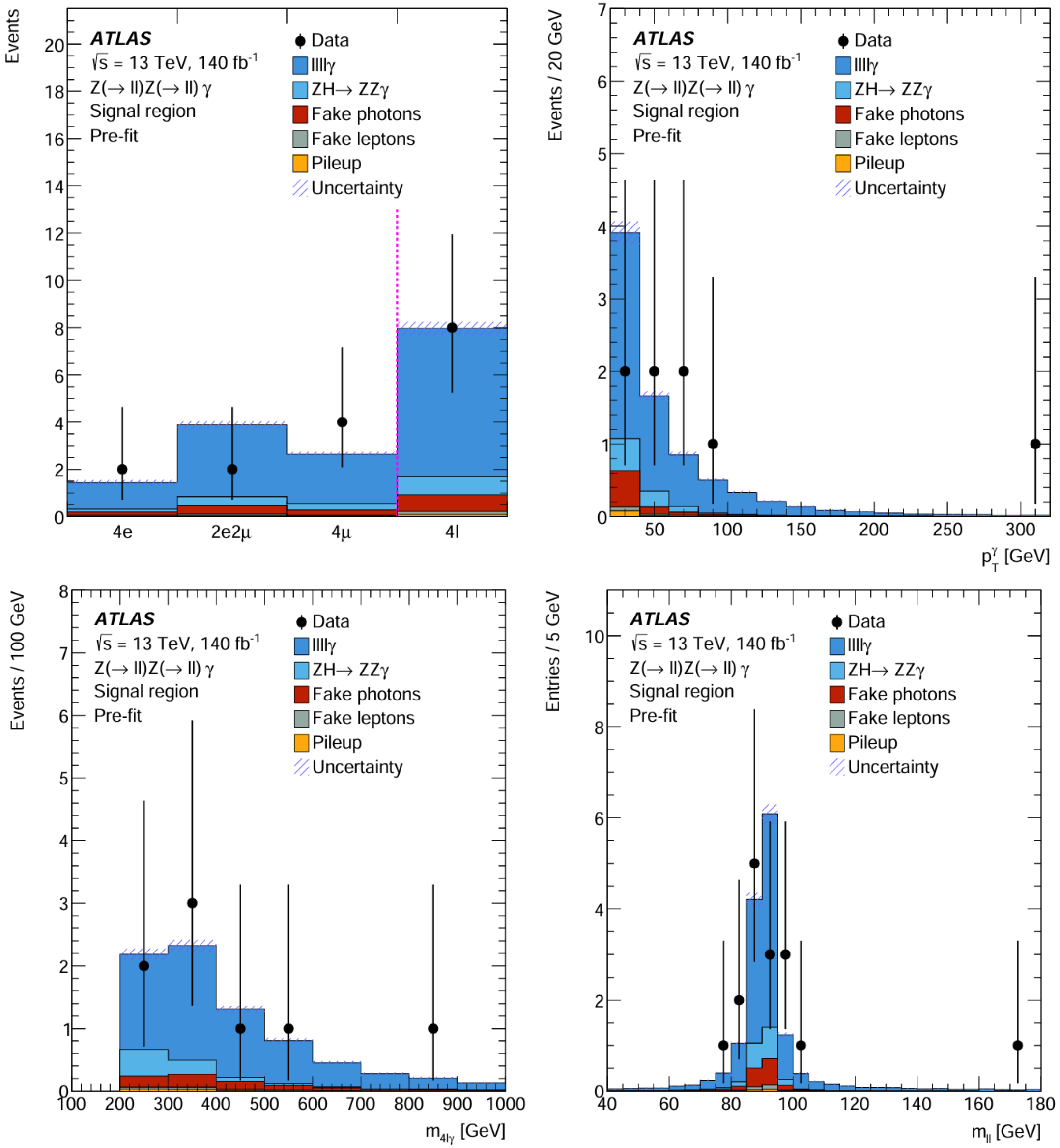

arXiv:2602.17165

Top Pair Production

- Inclusive cross section: $\sigma_{t\bar{t}} = 829.3 \pm 1.3\,(stat) \pm 8.0\,(syst) \pm 7.3\,(lumi) \pm 1.9\,(beam)\; pb$
- Consistent with NNLO+NNLL, precision limited by systematics and luminosity uncertainties.
- Top pole-mass extraction using NNPDF3.1_notop NNLO:

$$m_t^{pole} = 172.8^{+1.5}_{-1.7}\ GeV$$

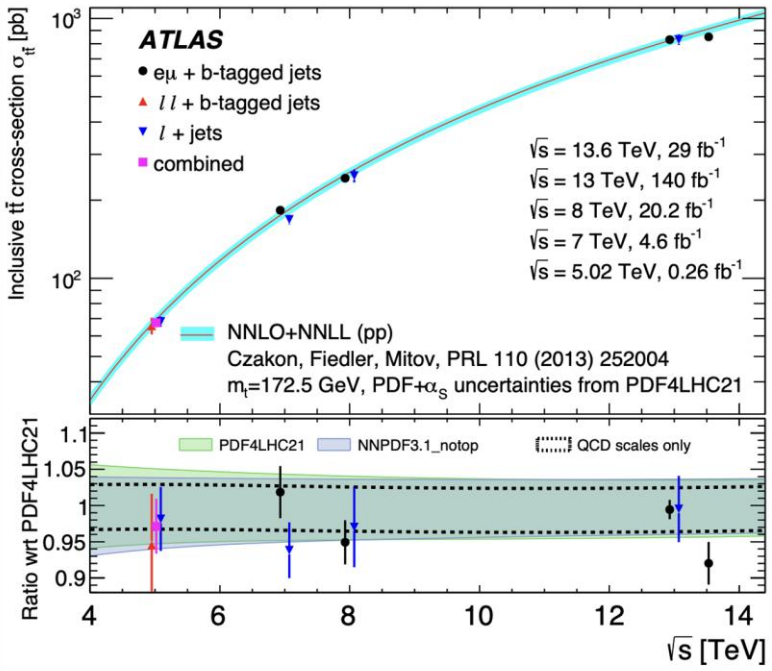

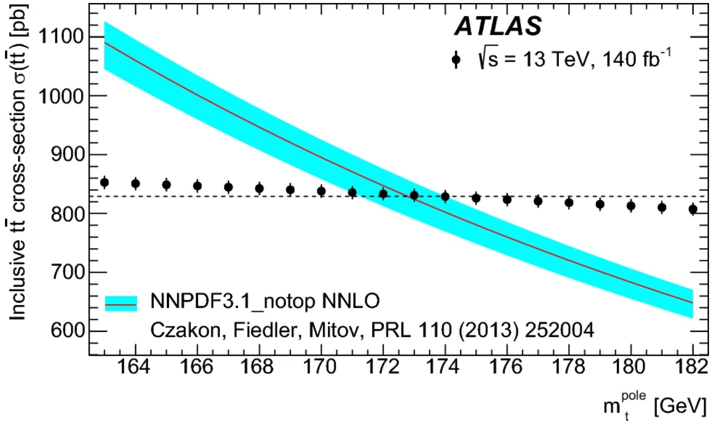

EPJC 86 (2026) 470
arXiv:2605.02341

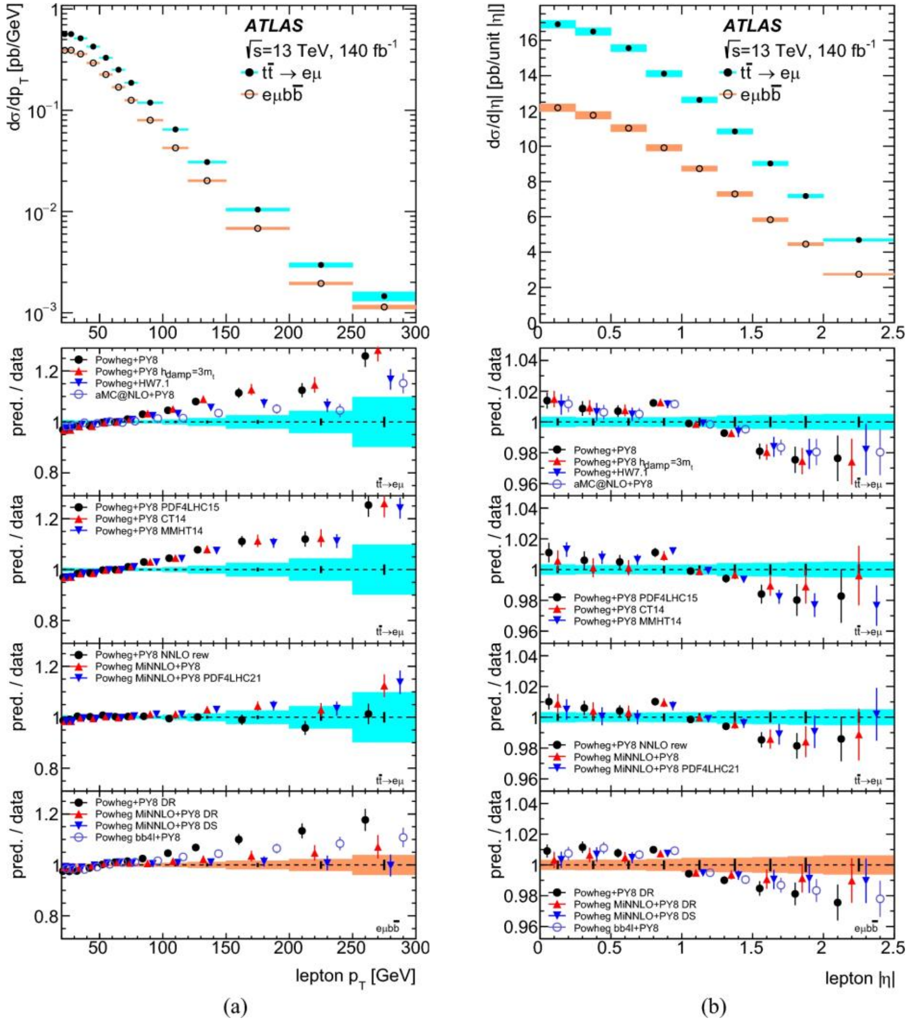

(a)

(b)

Differential cross section in eμ final states

tt quasi-bounding state: Toponium

- tt quasi-bound-state provide a stringent probe of NRQCD.
- tt cross section enhancement near threshold (~345 GeV), ~ 45% larger than SM prediction (6.43pb)

$$\sigma\left(t\bar{t}_{\mathrm{GFRW}}\right) = 9.3^{+1.4}_{-1.3}\,\mathrm{pb} = 9.3^{+1.1}_{-1.0}\ (\mathrm{stat.}) \pm 0.8\ (\mathrm{syst.})\,\mathrm{pb}$$

- **The baseline model without tt quasi-bound-state contribution is excluded with 8σ (6σ expected)**
- Overall statistically dominated, tt GFRW modelling, pQCD modelling are major sources of uncertainty

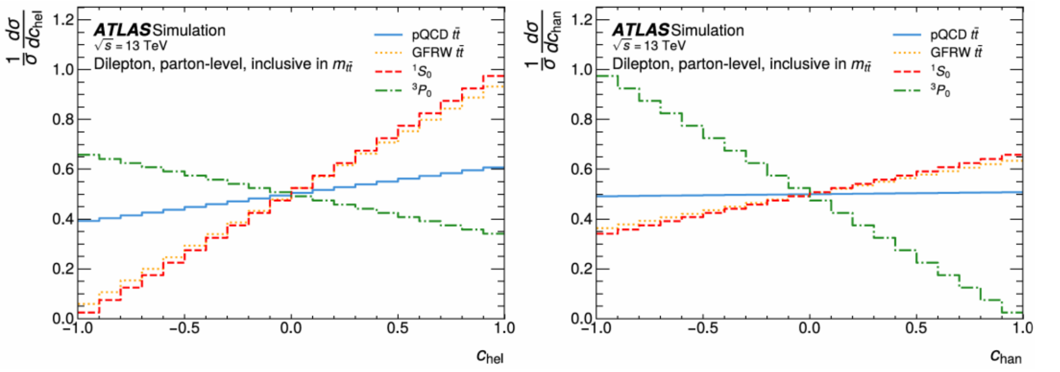

9 orthogonal signal regions based on angular variables

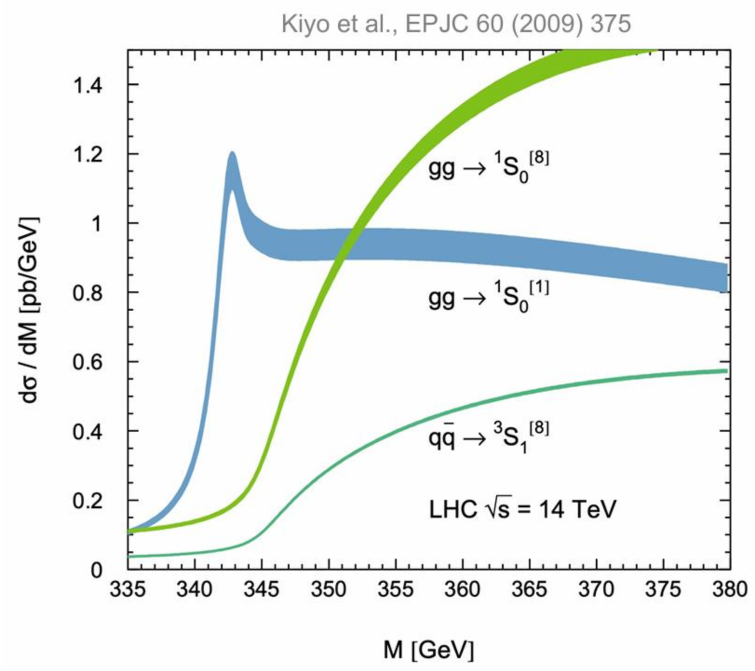
Kiyo et al., EPJC 60 (2009) 375

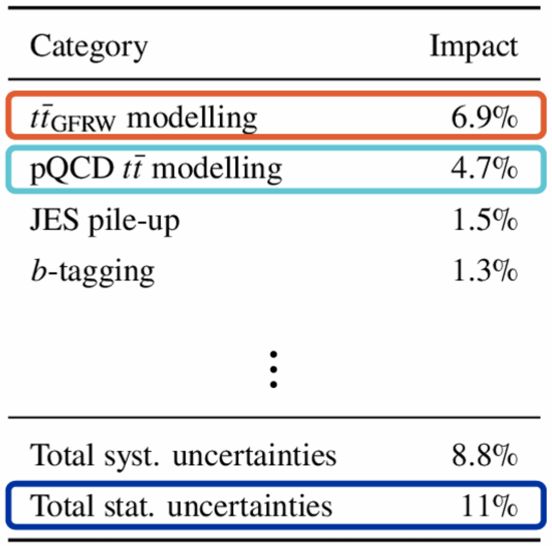

Category	Impact
$t\bar{t}_{\mathrm{GFRW}}$ modelling	6.9%
pQCD $t\bar{t}$ modelling	4.7%
JES pile-up	1.5%
b-tagging	1.3%
⋮	
Total syst. uncertainties	8.8%
Total stat. uncertainties	11%

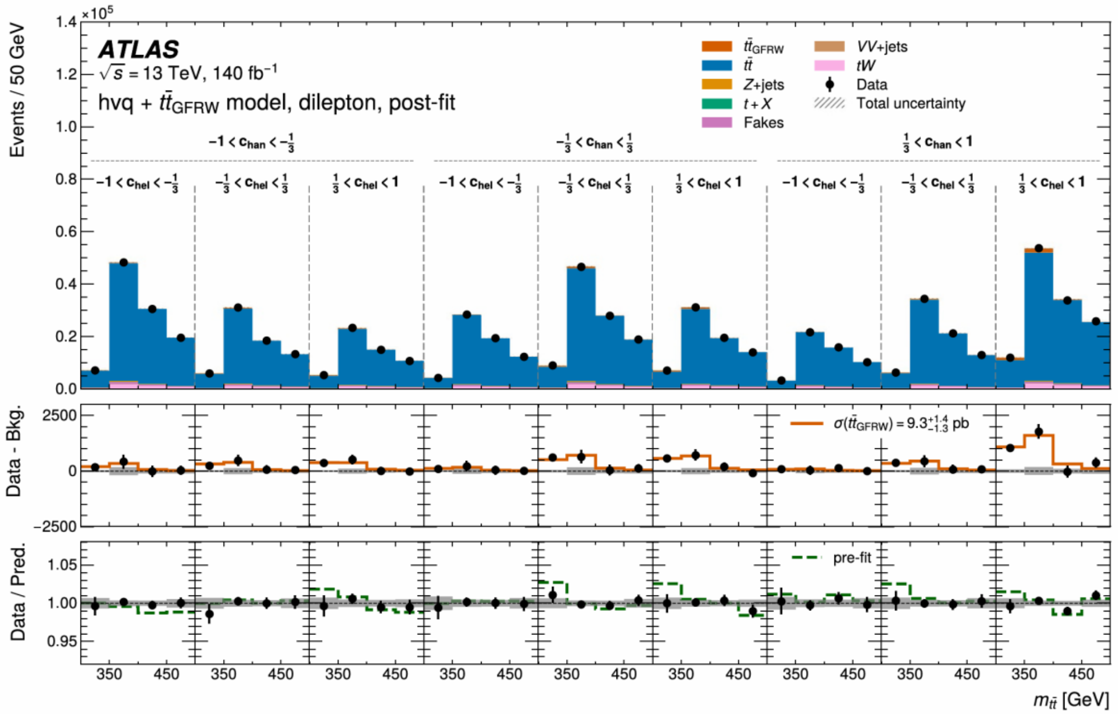

Rep. Prog. Phys. 89 (2026) 057801

Rare Top-Associated Productions

■ tt + diphoton (observation)

PLB 874 (2026) 140195

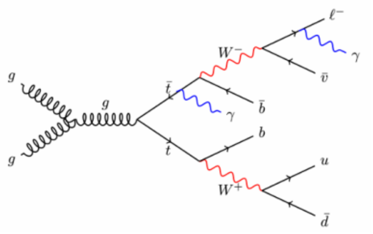

Fiducial cross section

$$\sigma_{\rm fid}(t\bar{t}\gamma\gamma) = 2.42^{+0.58}_{-0.53}\ \text{fb}$$

$$\text{Observed significance} = 5.2\sigma$$

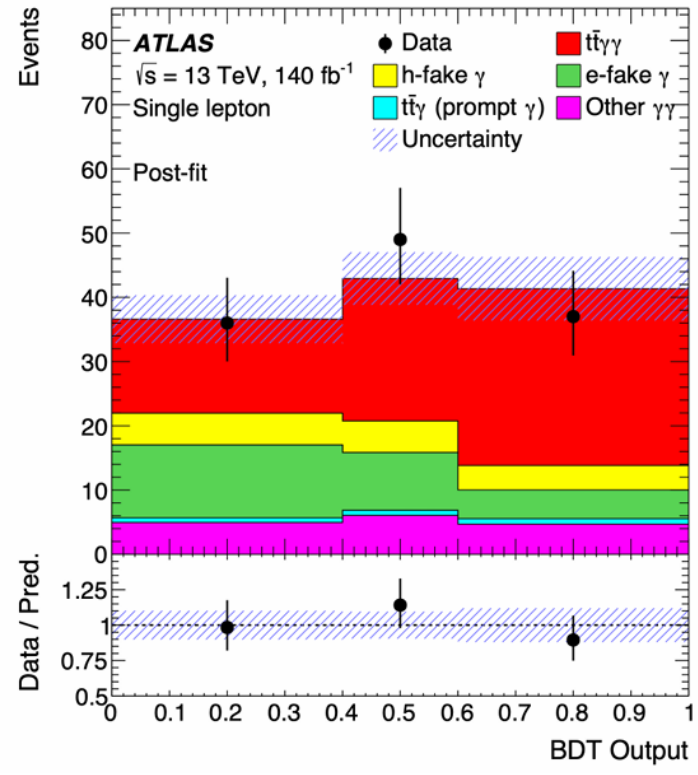

■ tt + dilepton (evidence)

EPJC 85 (2025) 1434

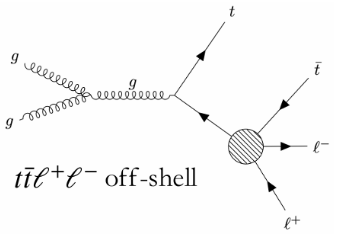

SM signal strength

$$\mu(t\bar{t}\ell^+\ell^-) = 1.0^{+0.4}_{-0.4}$$

$$\text{significance} = 2.9\,(2.8)\sigma$$

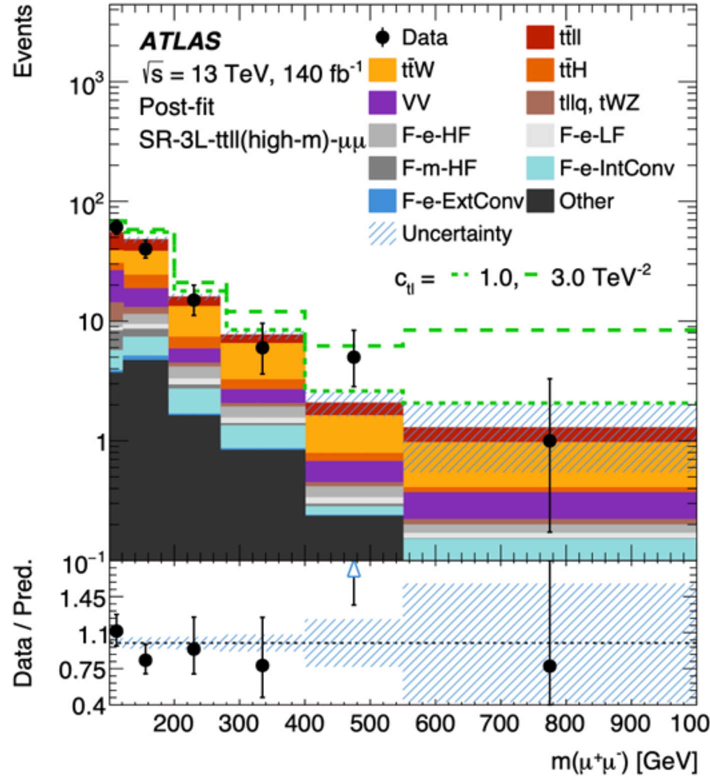

■ tt + Wj (no excess)

arXiv:2509.19038

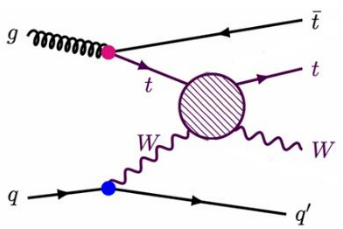

$$\mu_{\text{EW } t\bar{t}Wj} = 0.9^{+2.4}_{-3.0}$$

$$\sigma^{95\%\text{ CL}}_{\text{EW } t\bar{t}Wj} < 251\ \text{fb}$$

$$\text{Expected} : 230\ \text{fb}$$

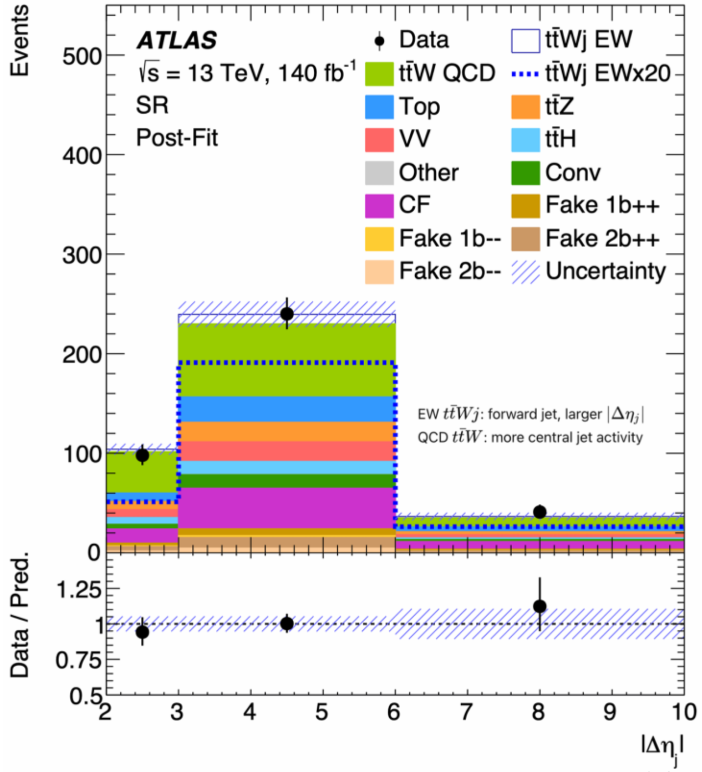

EW $t\bar{t}Wj$: forward jet, larger $|\Delta\eta_j|$

QCD $t\bar{t}W$: more central jet activity

Observation of B_c^{*+} and X(6900)

Observation of meson $B_c^{*+} \to B_c^+\gamma$

arXiv:2605.16228

$$B_c^+ \to J/\psi\mu^+\nu_\mu X$$

$$\Delta m_{B_c^{*+}} = 64.5 \pm 1.4\,(\text{stat.})^{+1.0}_{-1.4}\,(\text{syst.})\,\text{MeV}$$

$$m(B_c^{*+}) = 6339.0 \pm 1.4\,(\text{stat.})^{+1.0}_{-1.4}\,(\text{syst.}) \pm 0.3\,(m_{B_c^+})\,\text{MeV}$$

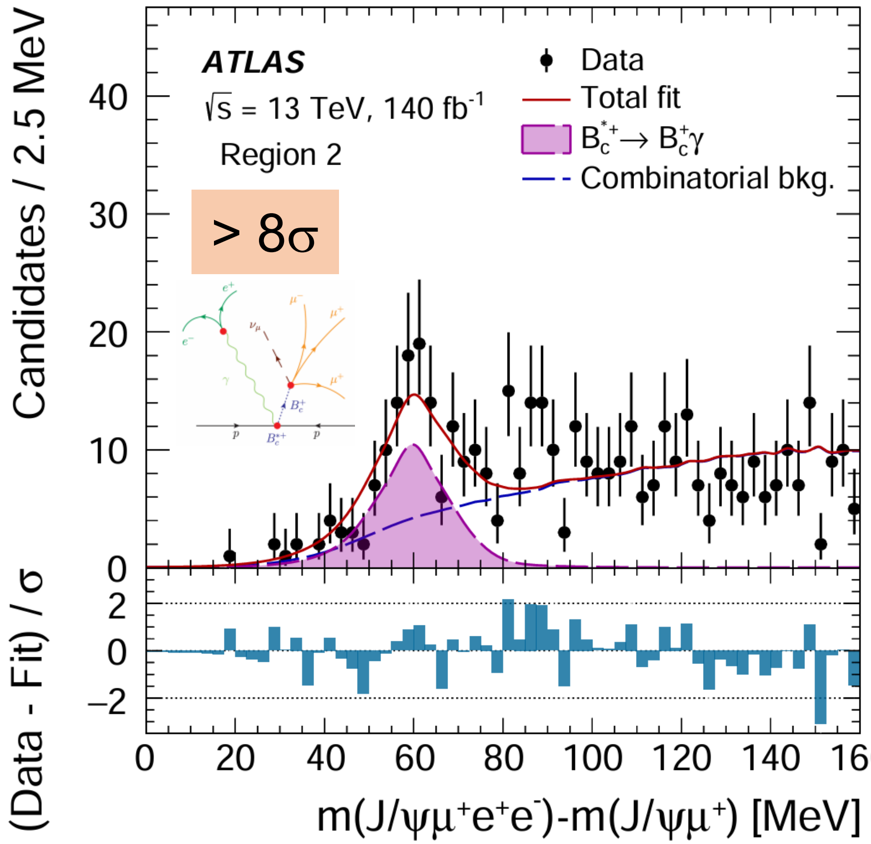

> 8σ

Observation of X(6900) → J/ψ+ψ(2S) → 4μ, 4μ+2π

$$m\,/\,\text{GeV} \quad 6.860 \pm 0.023 \pm 0.010$$

$$\Gamma\,/\,\text{GeV} \quad 0.082 \pm 0.032 \pm 0.015$$

$$R \quad 1.08 \pm 0.20^{+0.40}_{-0.09}$$

$$R = \Gamma_{X(6900)\to J/\psi+\psi(2S)} / \Gamma_{X(6900)\to \text{di-}J/\psi}$$

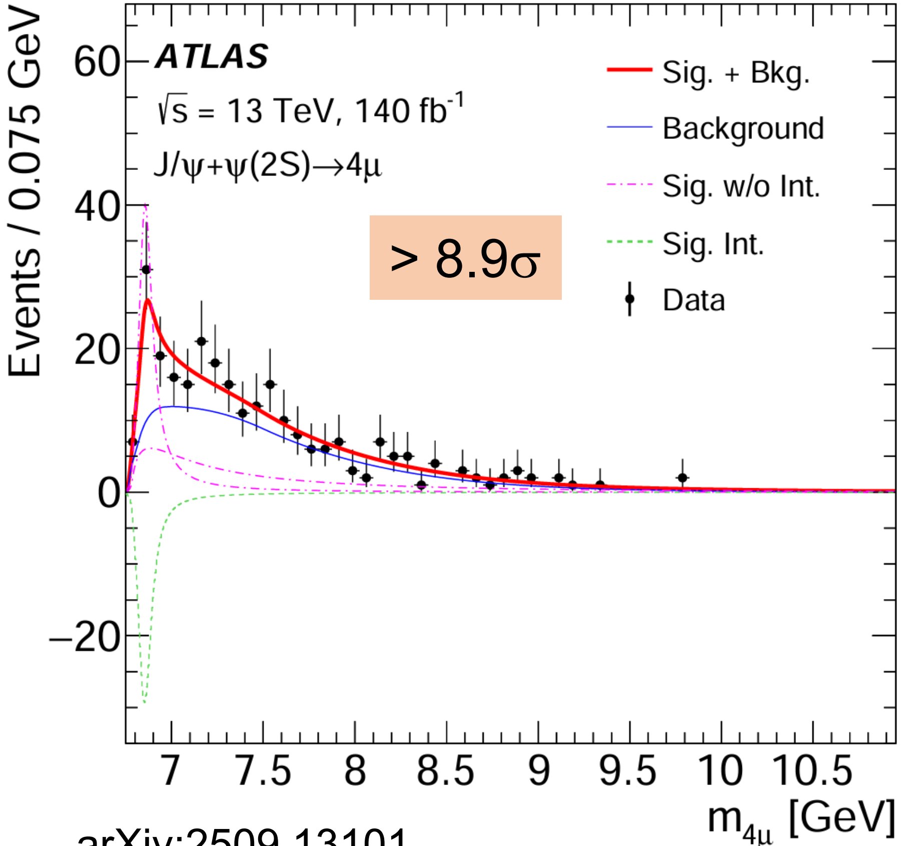

> 8.9σ

arXiv:2509.13101

BSM Searches with τ-lepton

■ Search for leptoquark with τ-lepton

Signal is described by 3 parameters: m_{U_1}, g_U and β_L^{23}

No signal is observed, limits are set on couplings in benchmark U_1 vector-leptoquark model at 95%CL:

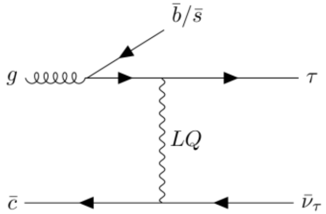

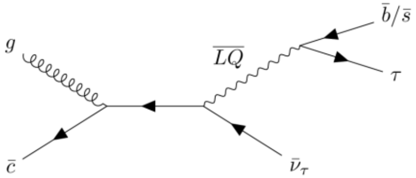

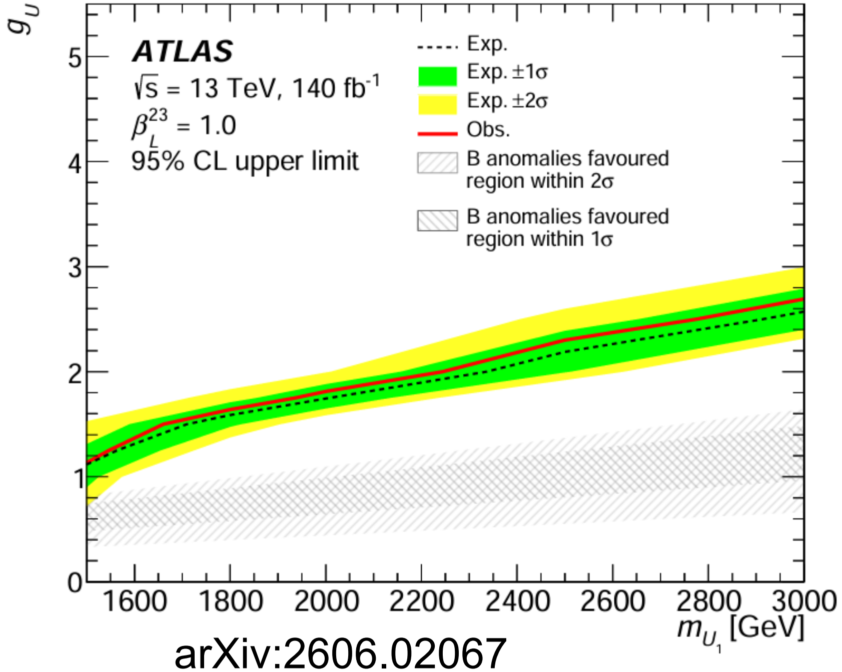

arXiv:2606.02067

■ Search for LFV W→ τν → 3μν

Any observation of LFV would be evidence of BSM

No signal is observed, the best-fit signal strength:

$$B(\tau \rightarrow 3\mu) = (1.5 \pm 4.0) \times 10^{-8}$$

$$B(\tau \rightarrow 3\mu) < 8.7\times10^{-8}\ (7.5\times10^{-8}) \text{ at } 90\%\ \text{CL}$$

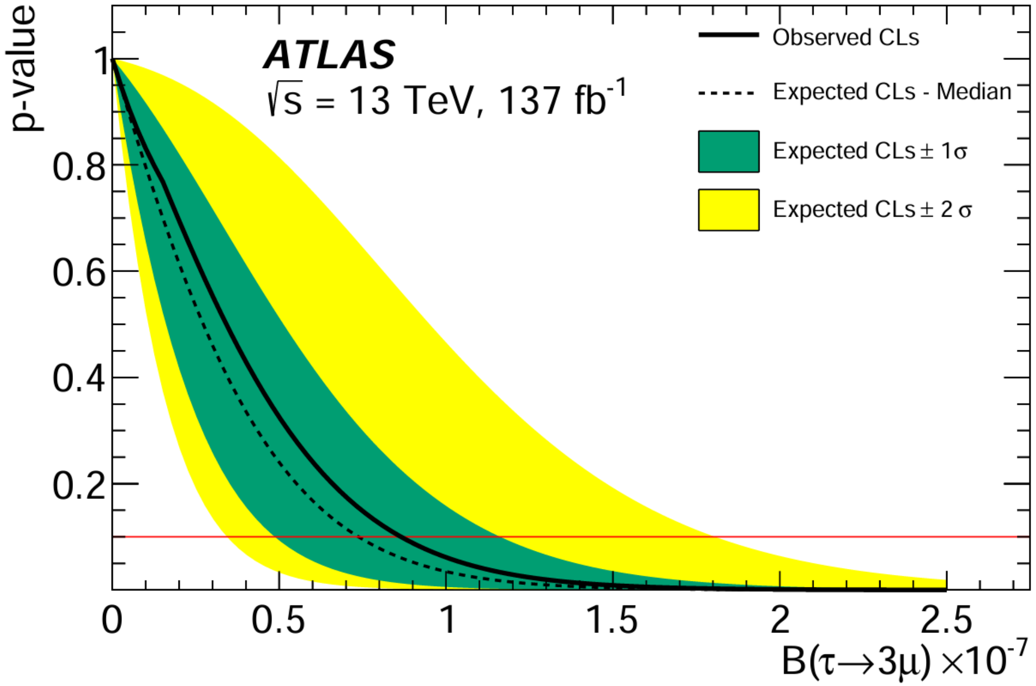

arXiv:2603.18099

Searches for Long-Lived Particles (LLP)

- The long-lived particle (LLP) regime probes particles with decay lengths, supported by theories including LFV, cascade decays through heavy mediators and RPV SUSY etc.
- ATLAS enables sensitive search for LLPs with decay length ($c\tau$) around $10^{-4} \sim 10$ m.

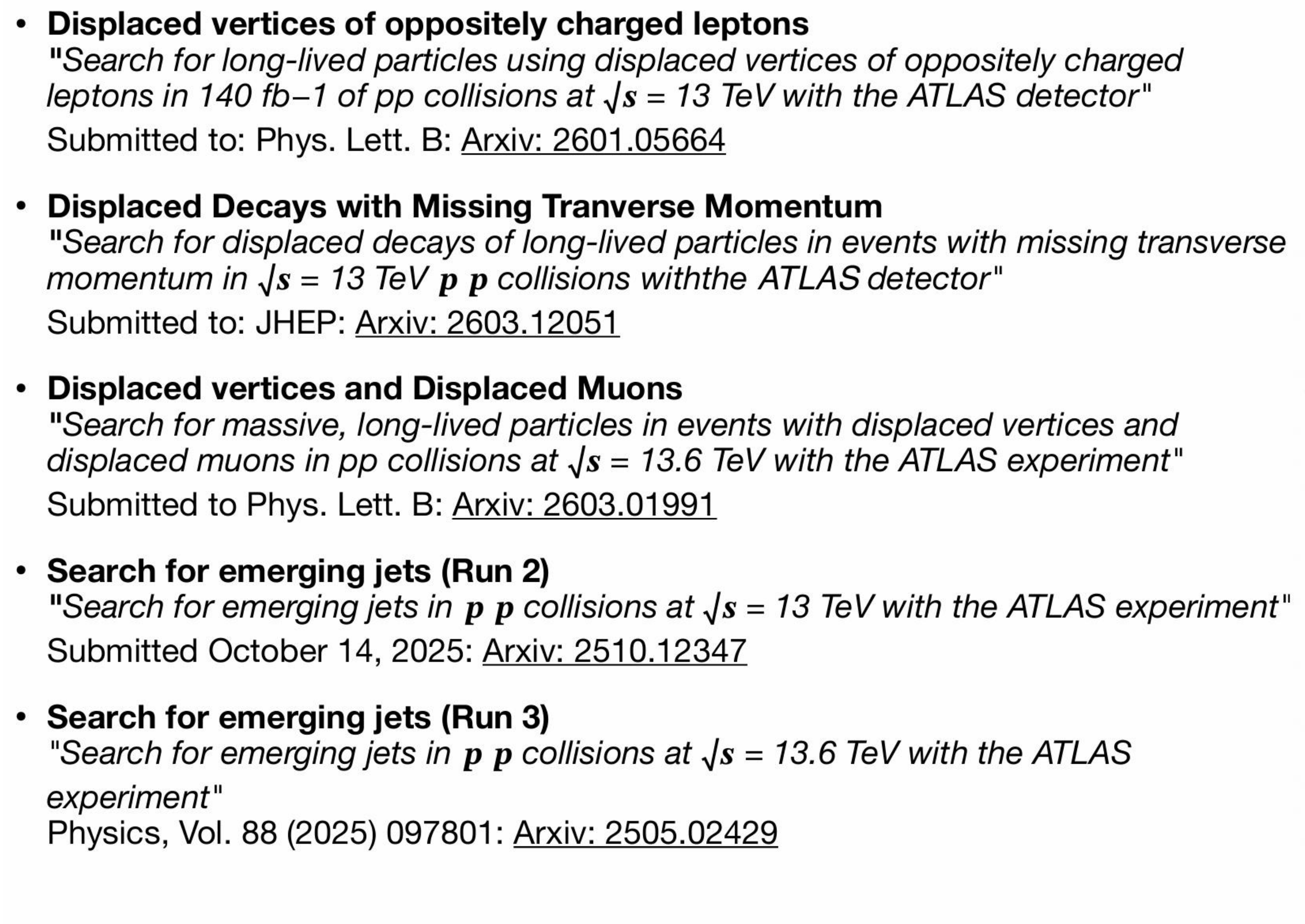

- **Displaced vertices of oppositely charged leptons**
  "Search for long-lived particles using displaced vertices of oppositely charged leptons in 140 fb−1 of pp collisions at $\sqrt{s}$ = 13 TeV with the ATLAS detector"
  Submitted to: Phys. Lett. B: Arxiv: 2601.05664
- **Displaced Decays with Missing Tranverse Momentum**
  "Search for displaced decays of long-lived particles in events with missing transverse momentum in $\sqrt{s}$ = 13 TeV $p\ p$ collisions withthe ATLAS detector"
  Submitted to: JHEP: Arxiv: 2603.12051
- **Displaced vertices and Displaced Muons**
  "Search for massive, long-lived particles in events with displaced vertices and displaced muons in pp collisions at $\sqrt{s}$ = 13.6 TeV with the ATLAS experiment"
  Submitted to Phys. Lett. B: Arxiv: 2603.01991
- **Search for emerging jets (Run 2)**
  "Search for emerging jets in $p\ p$ collisions at $\sqrt{s}$ = 13 TeV with the ATLAS experiment"
  Submitted October 14, 2025: Arxiv: 2510.12347
- **Search for emerging jets (Run 3)**
  "Search for emerging jets in $p\ p$ collisions at $\sqrt{s}$ = 13.6 TeV with the ATLAS experiment"
  Physics, Vol. 88 (2025) 097801: Arxiv: 2505.02429

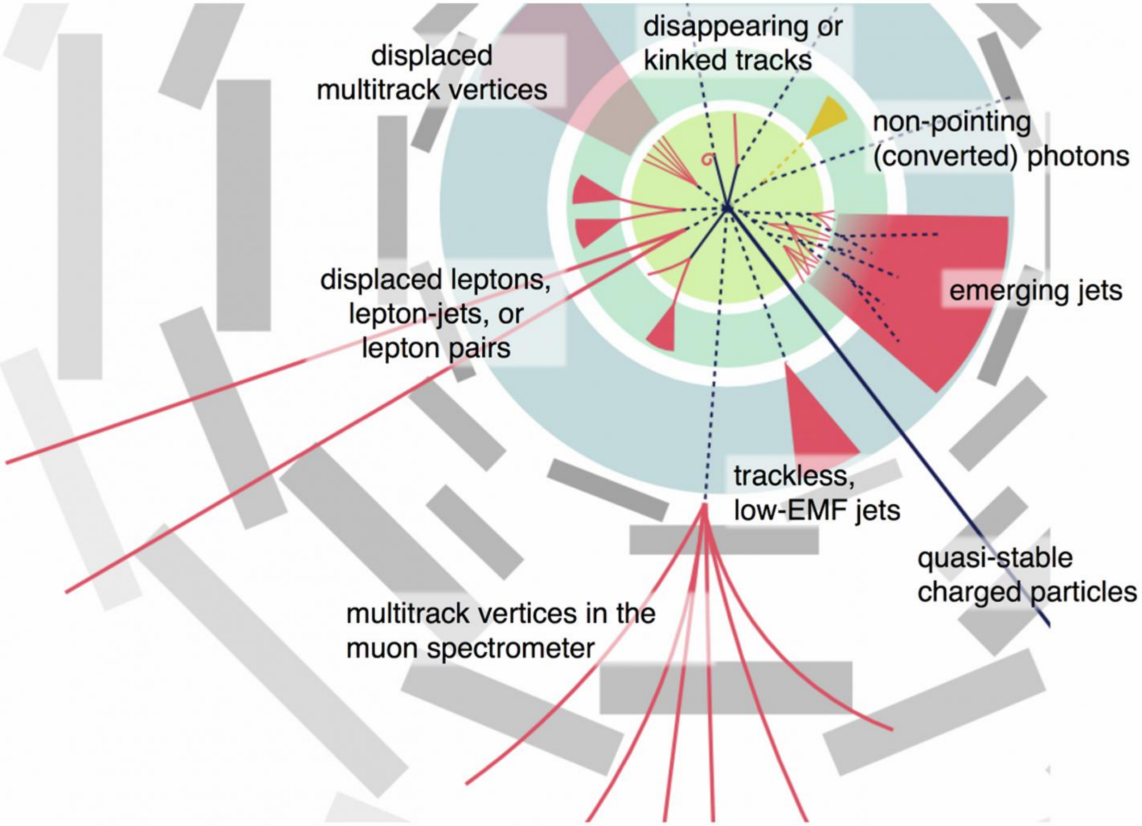

Graphics by Heather Russell

Searches for Long-Lived Particles (LLP)

■ LLP: DV + MET

arXiv:2603.12051

Four models: Gluinos R-hadron

Neutralinos Bino-Wino coannihilation

Higgsinos decaying to axinos

Higgs portal model: light pseudoscalars

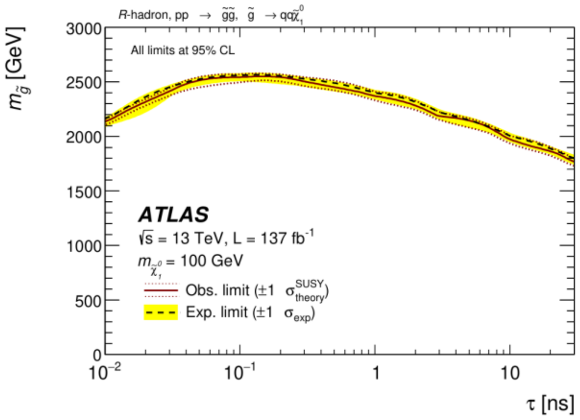

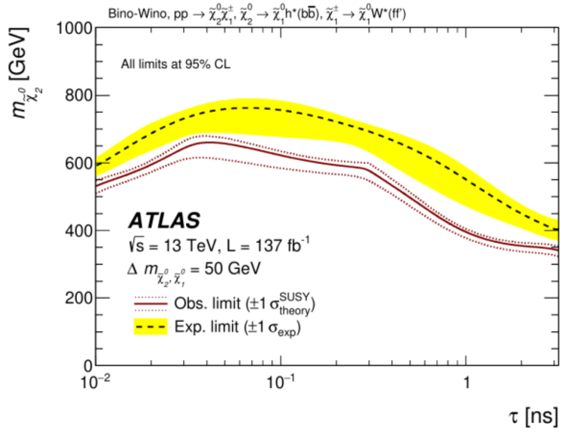

■ LLP: DV + leptons

PLB 878 (2026) 14097

Z', Gluino and Electroweakino models

Cross section limits with cτ (1-10000) mm

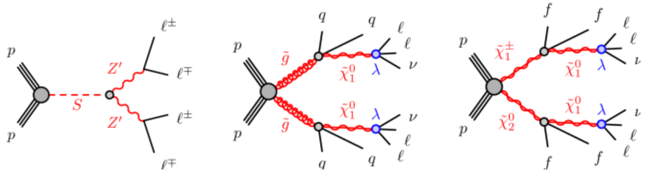

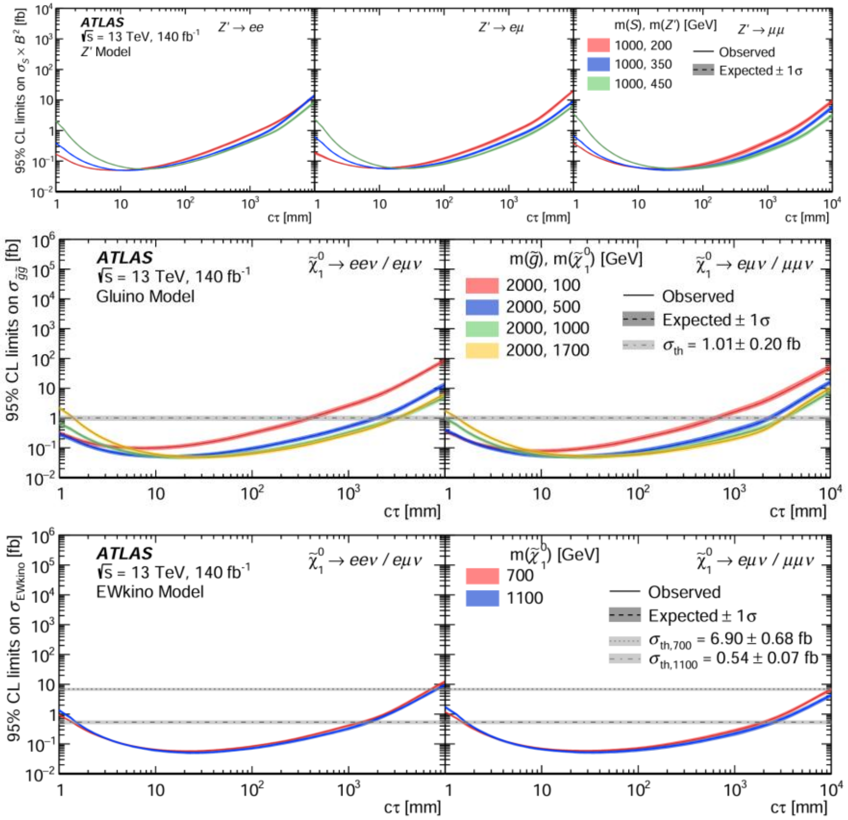

■ LLP: DV + Muons

PLB 878 (2026) 140509

RPV SUSY model: higgsino pair production

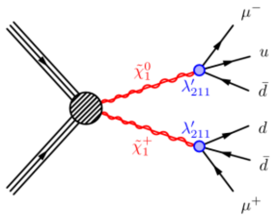

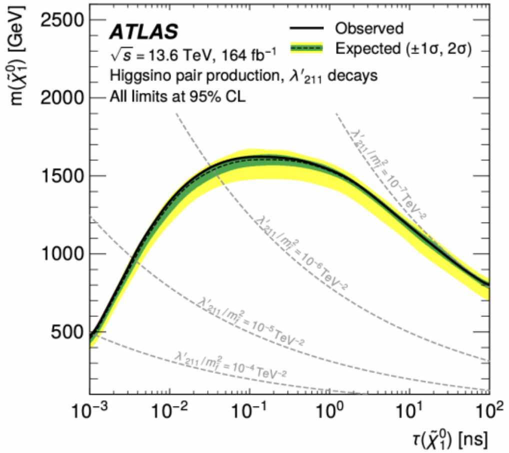

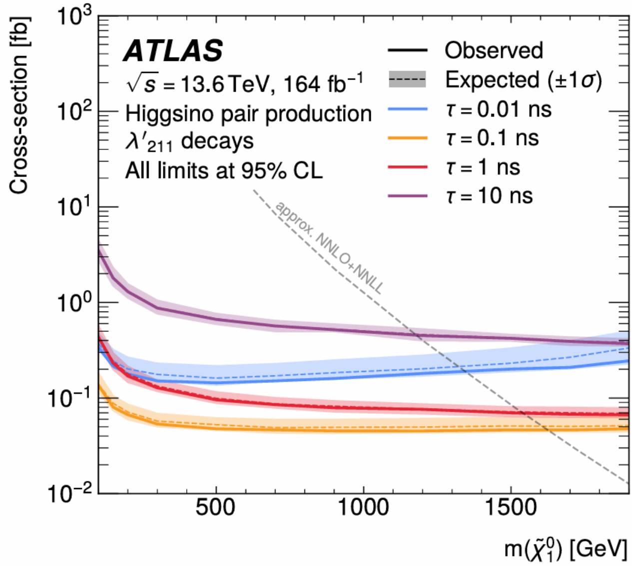

SUSY Searches

■ Search for RPV Chargino and Neutralinos

Charginos and neutralinos (via Higgs decay) with masses between 150 and 1100 GeV are excluded at 95% CL.

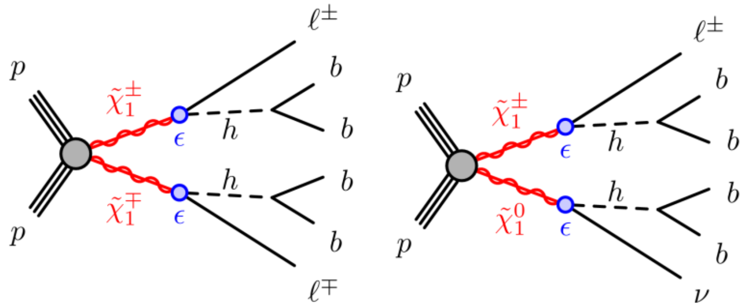

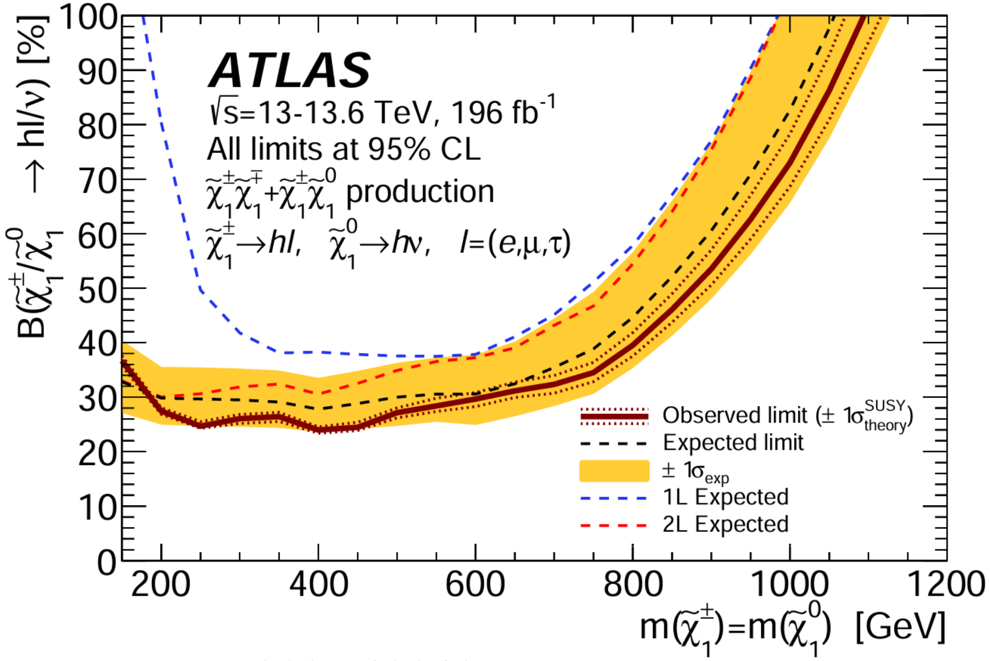

arXiv:2605.13819

■ Search for pair of top squarks

Top squark mass limits improving 10%: >1060 GeV at 95% CL

Neutralino mass: >560 GeV for $m(\tilde{t}_1)$ of 900 GeV at 95% CL

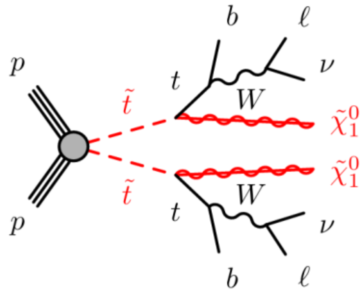

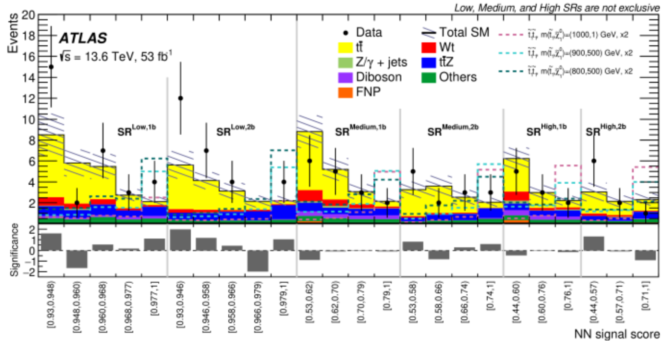

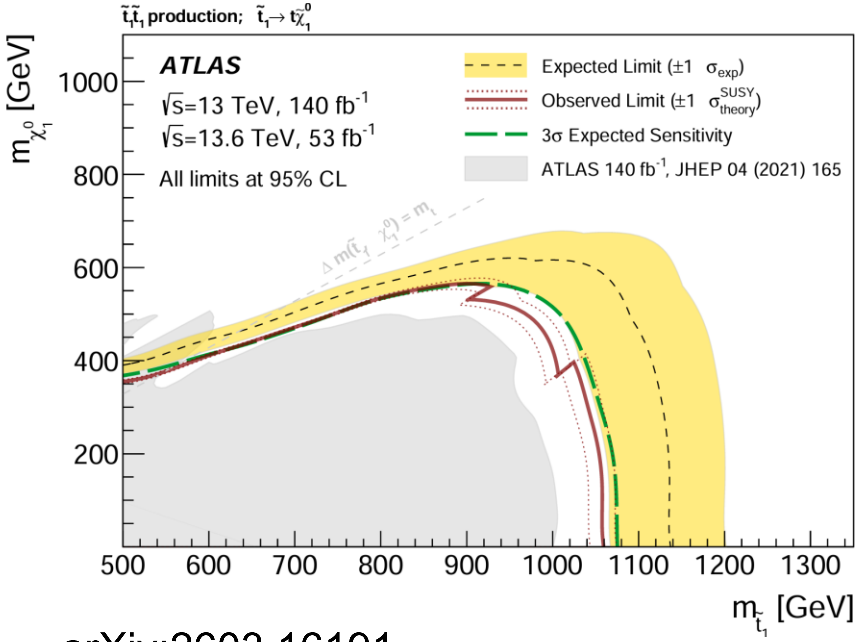

arXiv:2603.16191

Hunting for New Particles

- Search for dark Higgs boson (s) in Z' mediator model
- Dxbb to improve b-tagging calibration efficiency
- Best limit on dark Higgs search which satisfy observed cosmological constraint on freeze-out relic density $\Omega h^2=0.1200\pm 0.0012$ [PLANCK218]
- Dark Higgs mass between [30,150] GeV with Z' mass up to 4.8 TeV is excluded at 95% CL

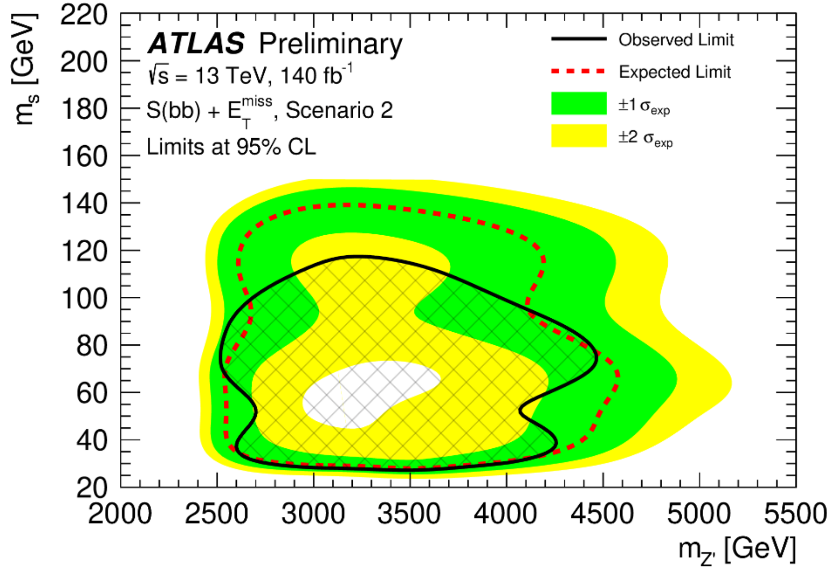

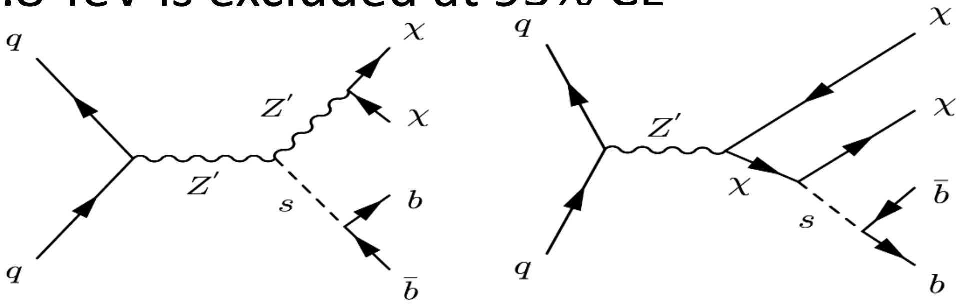

Resolved Topo.

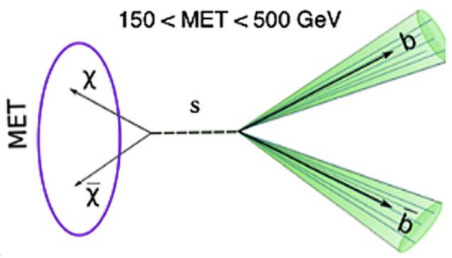

Good statistics

Boosted Topo.

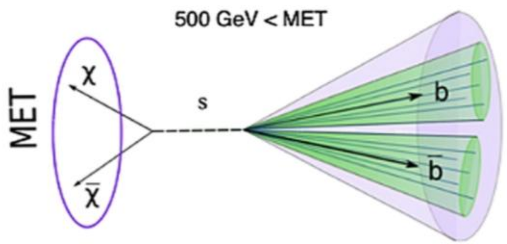

Sensitive to high mZ'
dominates for mZ'>2 TeV

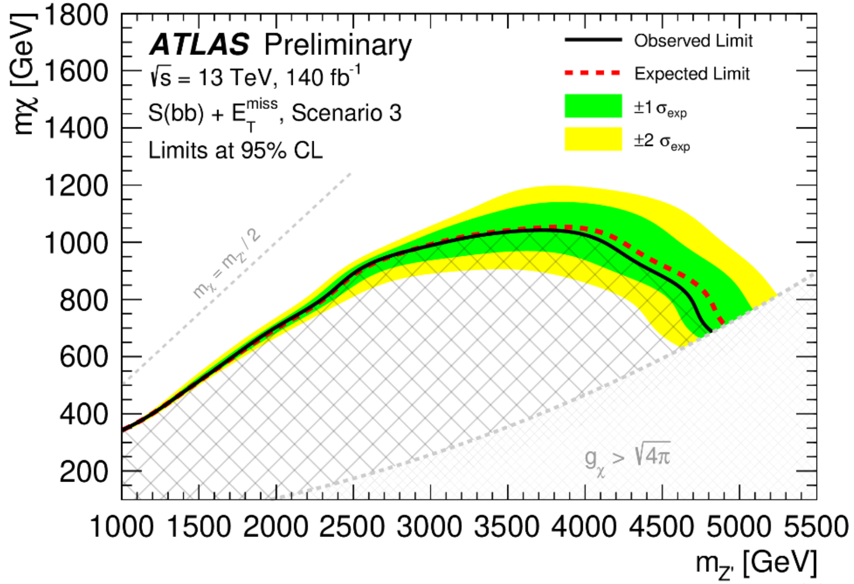

PRL 134 (2025) 121801

Hunting for New Particles

- Search for dark photon in Higgs decays (ggF $H \rightarrow \gamma\gamma_d$)
- Predicted as the gauge boson of dark U(1) group in hidden sector
- Dedicated new trigger improve acceptance x2 – Run3 (2023+2024)
- Primary vertex with dedicated BDT_{vertex}
- Observed (exp.) upper limit on BR ($H \rightarrow \gamma\gamma_d$): 0.9% (0.9%) at 95%CL

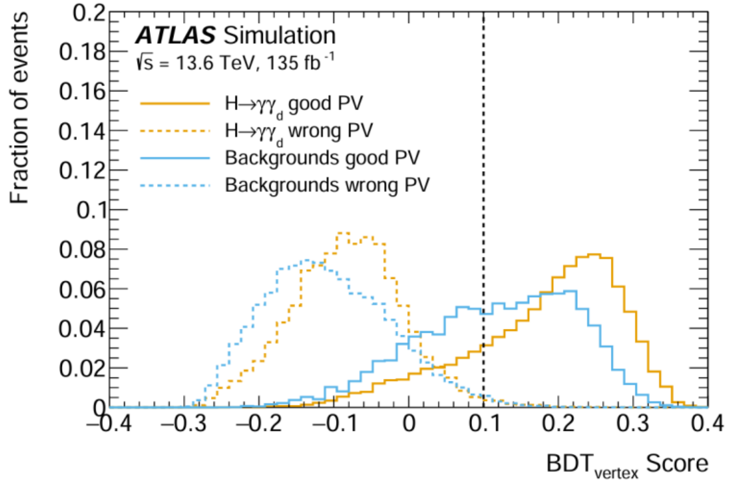

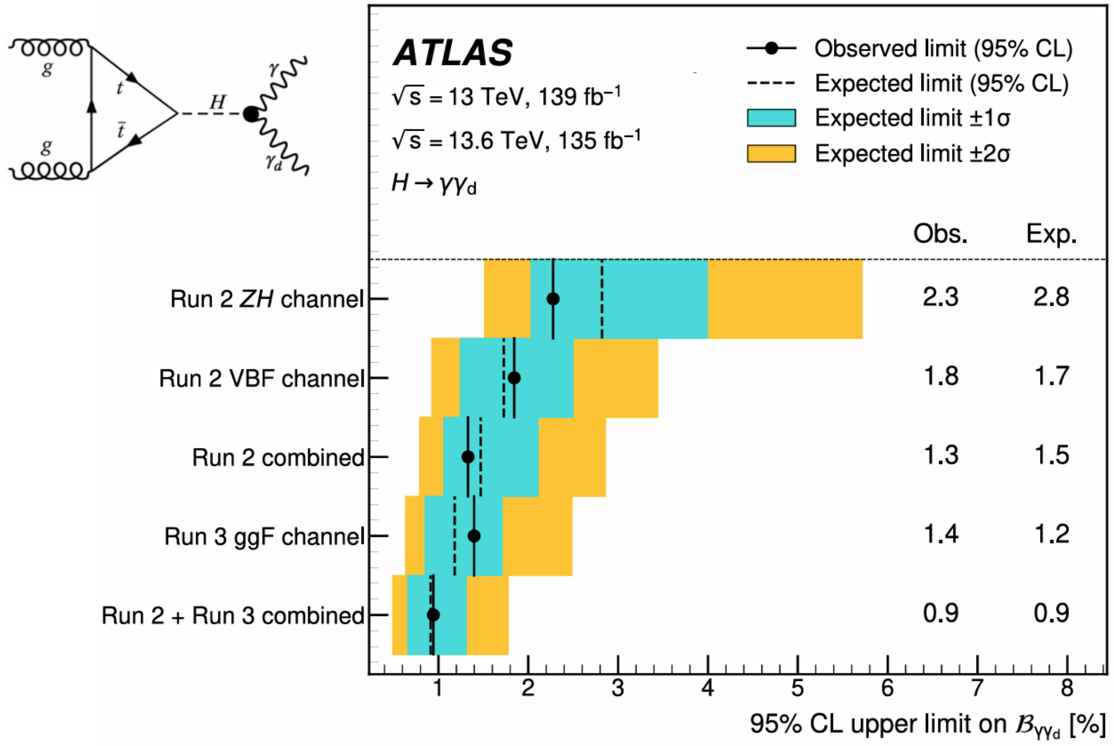

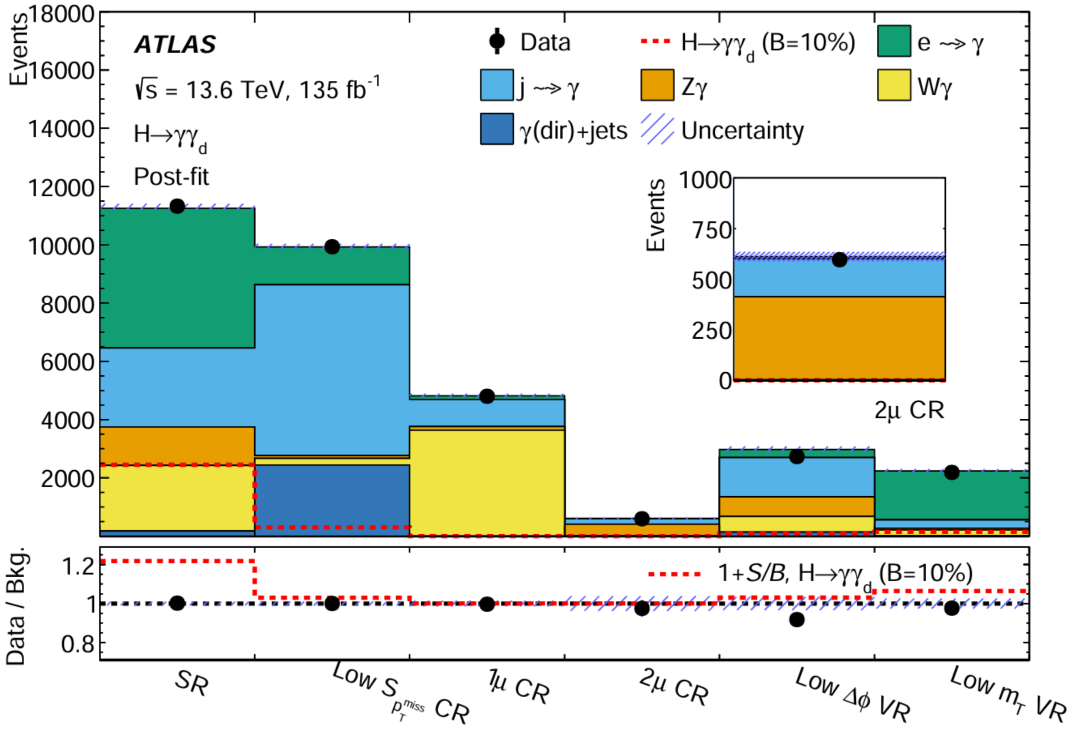

arXiv:2606.14362

Transforming Flavor Tagging: GN2 → GN3

Briefing: ATLAS enters a new era of jet flavour tagging – powered by AI

- GN3 combines inputs from jets, tracks (with looser selection), charged/neutral PFO with dedicated initialisation network before a transformer encoder
- Jet flavor classification for b/c/ud/s/g-jet with 4 auxiliary tasks
- For a given b-jet signal efficiency, significant improvement for background rejection

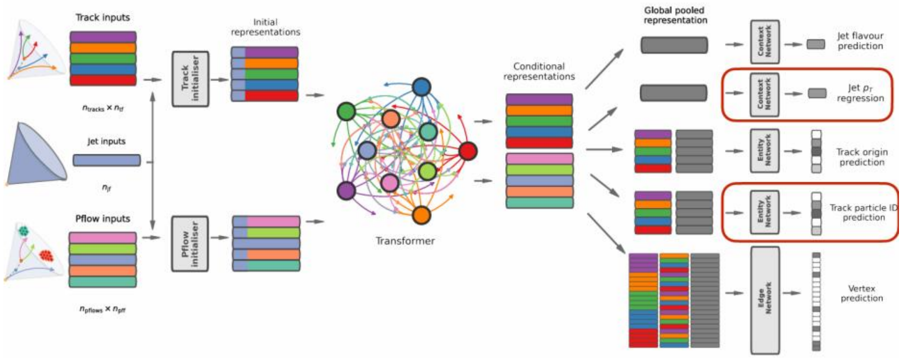

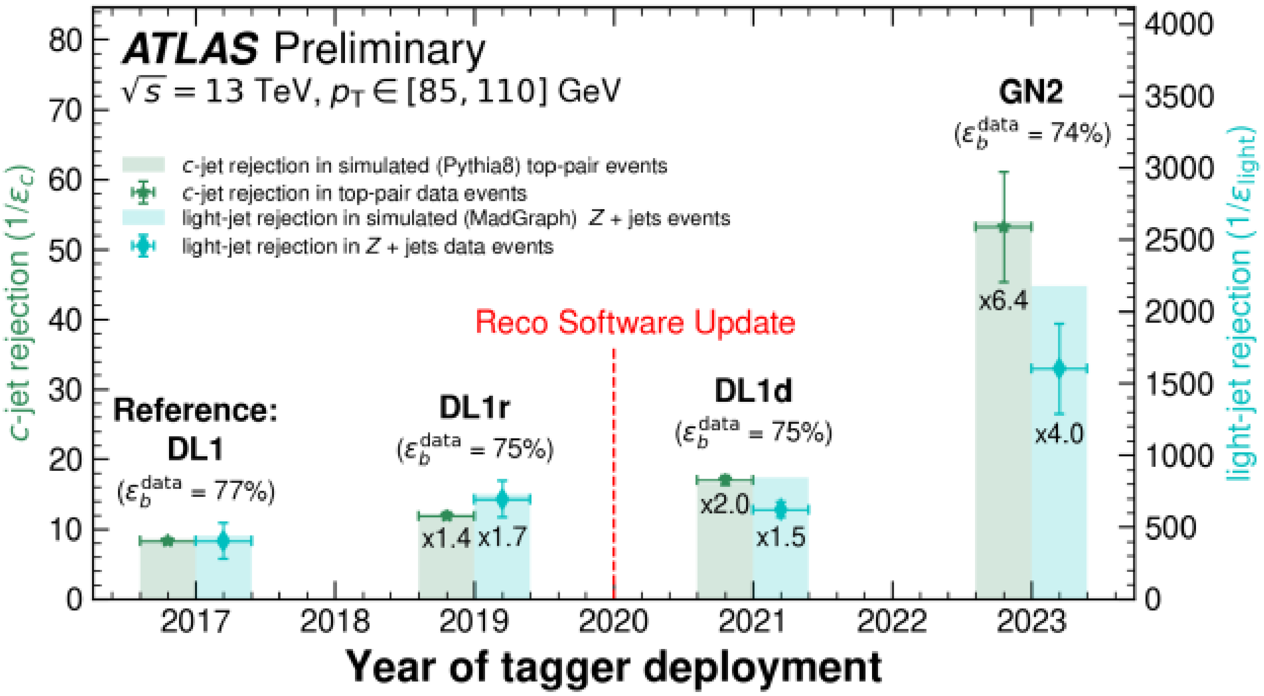

Nature Commun. 17 (2026) 541

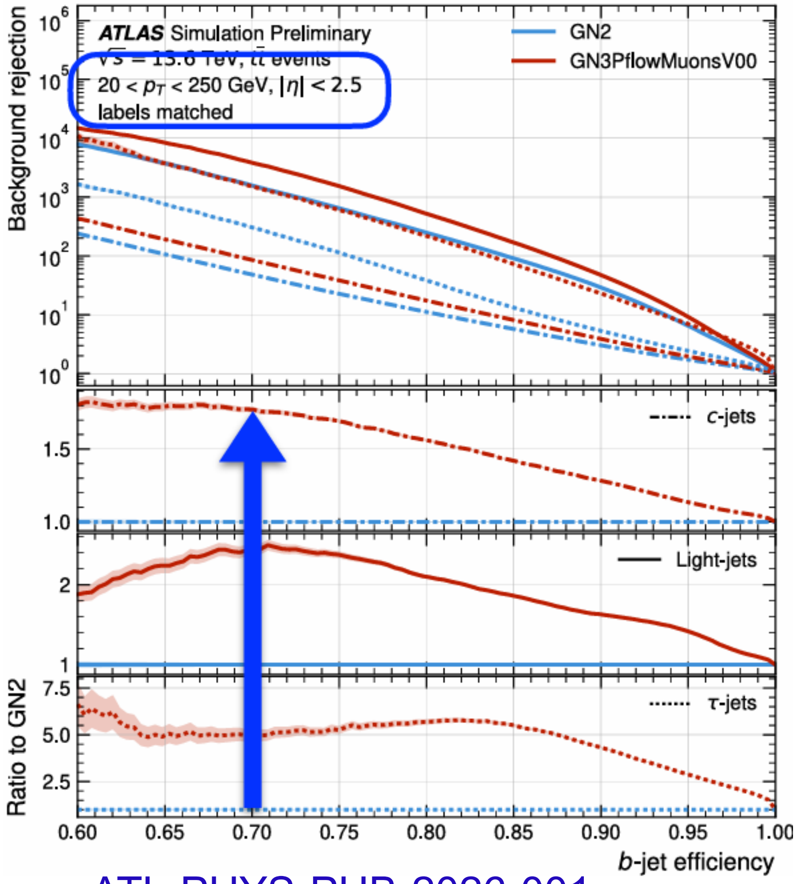

ATL-PHYS-PUB-2026-001

Impact of Flavor Tagging

■Improved sensitivity for better flavor tagging: HH→bbγγ, VH (H→bb, cc)

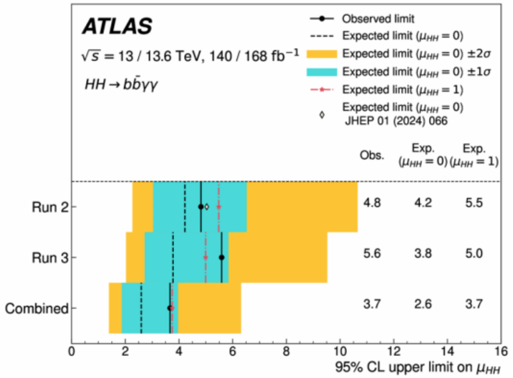

HH → bbγγ **Run 2+ Run 3 (2022-2024)** comparable to full Run 2 combination, made possible by improved b-tagging and kinematic fit

20% sensitivity improvement just from new b-tagging capability

Phys. Lett. B 876 (2026) 140280

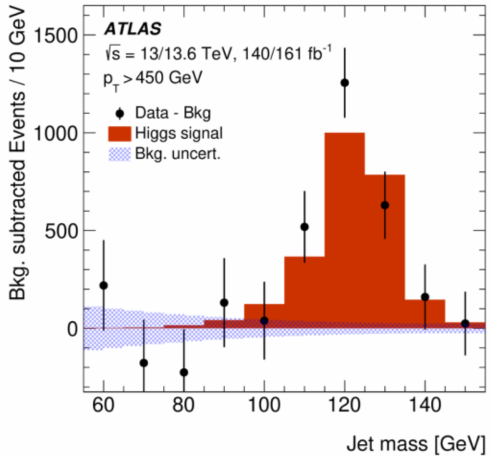

High pT Higgs measurements made possible by optimised **GN2X H → bb tagger** and **jet regression for resolution improvement**

x 7-10 sensitivity improvement compared to Run 2 result

arXiv: 2603.19369 vs Phys. Rev. D 105, 092003

3.8σ (2.5σ exp.)

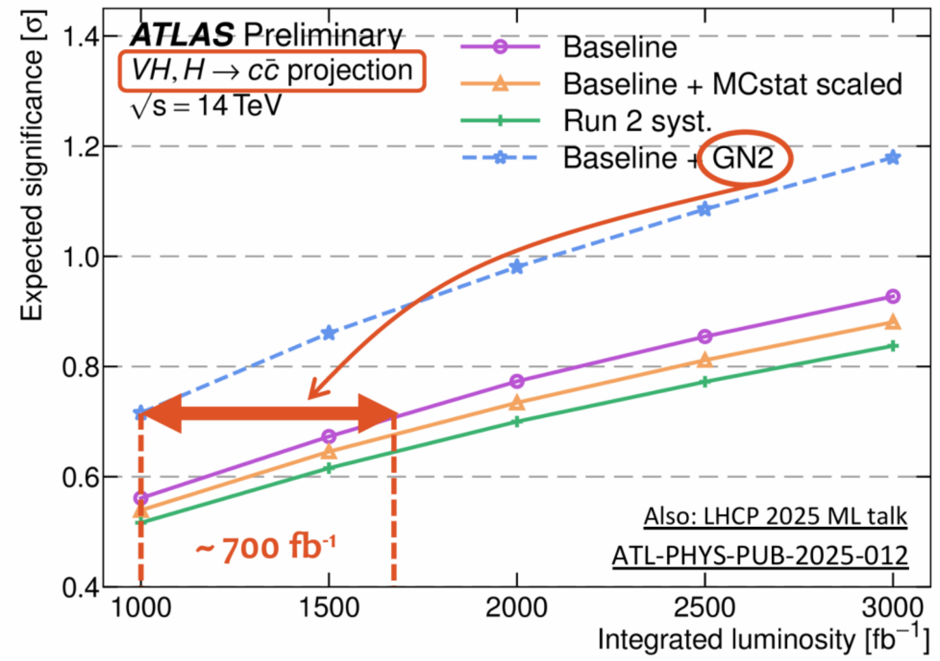

Also: LHCP 2025 ML talk

ATL-PHYS-PUB-2025-012

Improved sensitivity for same luminosity, or a data-size booster!

Also: keeps HEP computationally cutting-edge, attracting talent and innovation

Cosmic-ray Lab with Proton-Oxygen Collisions

- Revealing origins of cosmic rays is a crucial goal in astroparticle physics
- First collider measurement mimicking cosmic-ray atmospheric interactions
- Fiducial p-O (6.8+3.4TeV) cross section consistent with MC (EPOS LHC-R and HIJING)

$$\sigma^{pO}_{\text{fid.}} = 396 \pm 6\ (\text{exp.}) \pm 9\ (\text{lumi.})\ \text{mb}$$

$$\sigma^{p+\text{air}}_{\text{inel.}} = 406 \pm 6\ (\text{exp.}) \pm 9\ (\text{lumi.}) \pm 28\ (\text{th.})\ \text{mb}$$

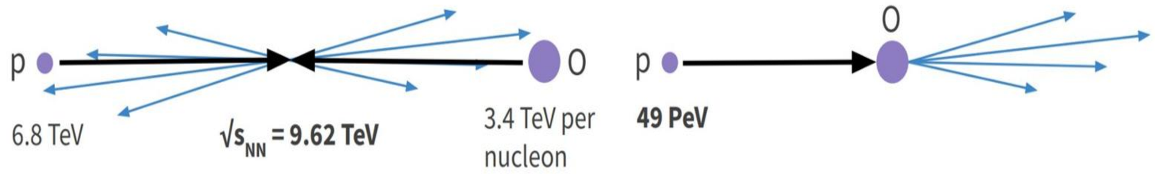

$634\ \mu\text{b}^{-1}$

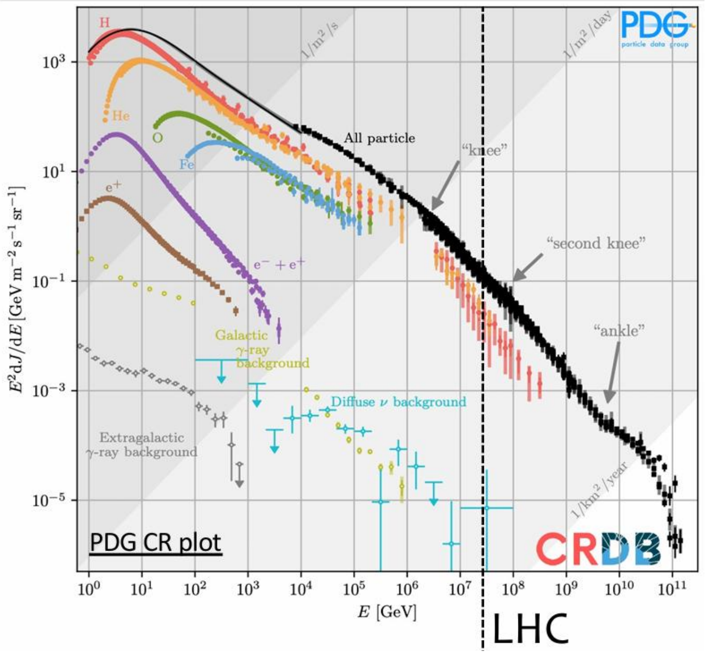

PDG CR plot

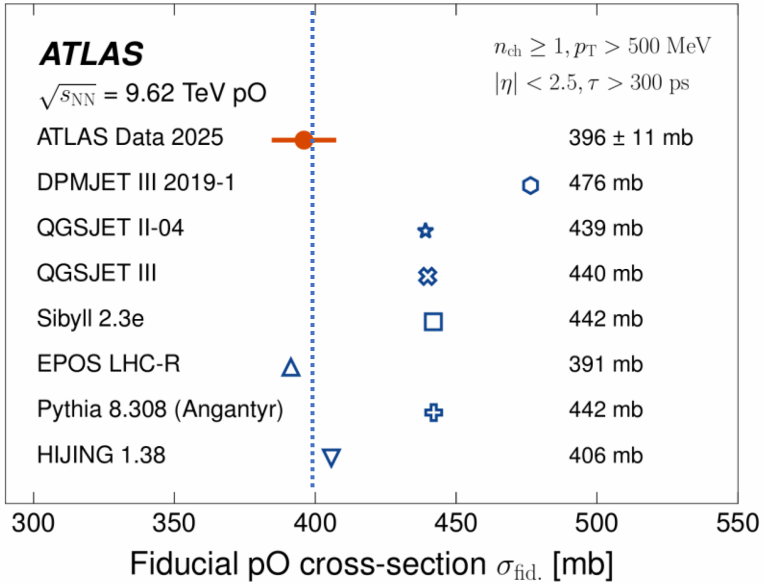

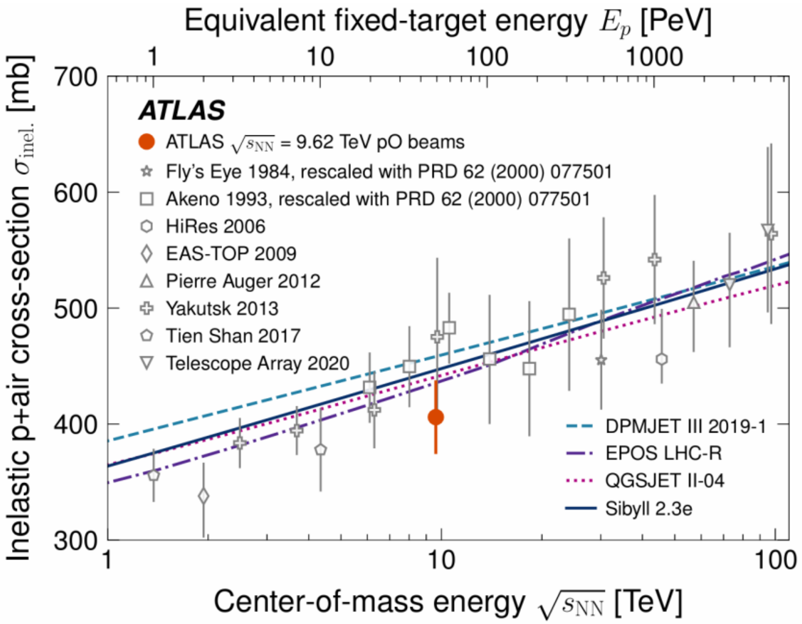

arXiv:2604.05512

HION: O+O and Ne+Ne @ 5.36 TeV

■ Centrality dependence of dn/dη or <p_T>

- ✓ Particle multiplicity rises towards central collisions
- ✓ dN/dη ratio: models comparable in central collisions
- ✓ <p_T> ratio: models predictions within 1-2% of data.

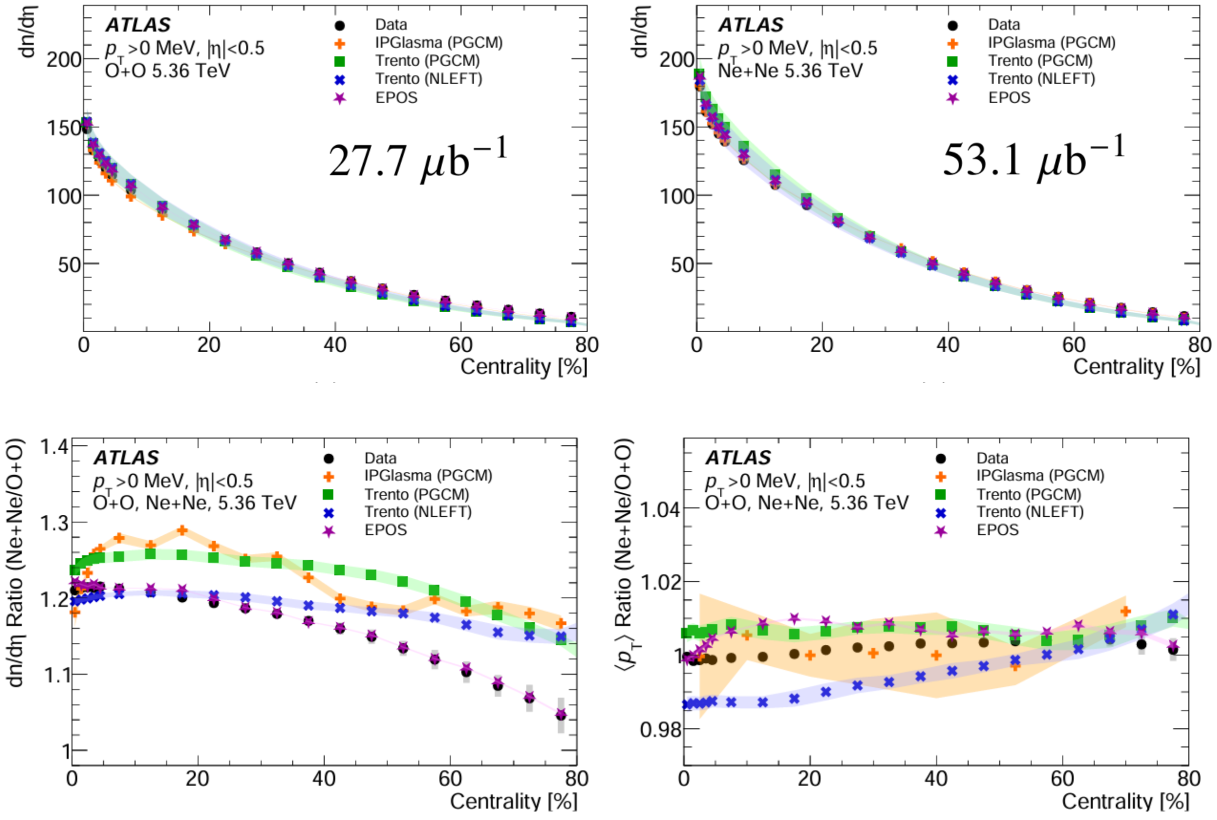

arXiv:2606.20257

■ Observation of centrality-dependence p_T imbalance

- ✓ Centrality-dependent dijet p_T imbalance $x_J = \frac{p_{T_2}}{p_{T_1}}$
- ✓ Large deviations from pp ref in central collisions
- ✓ New regime for path-length dep. of jet quenching

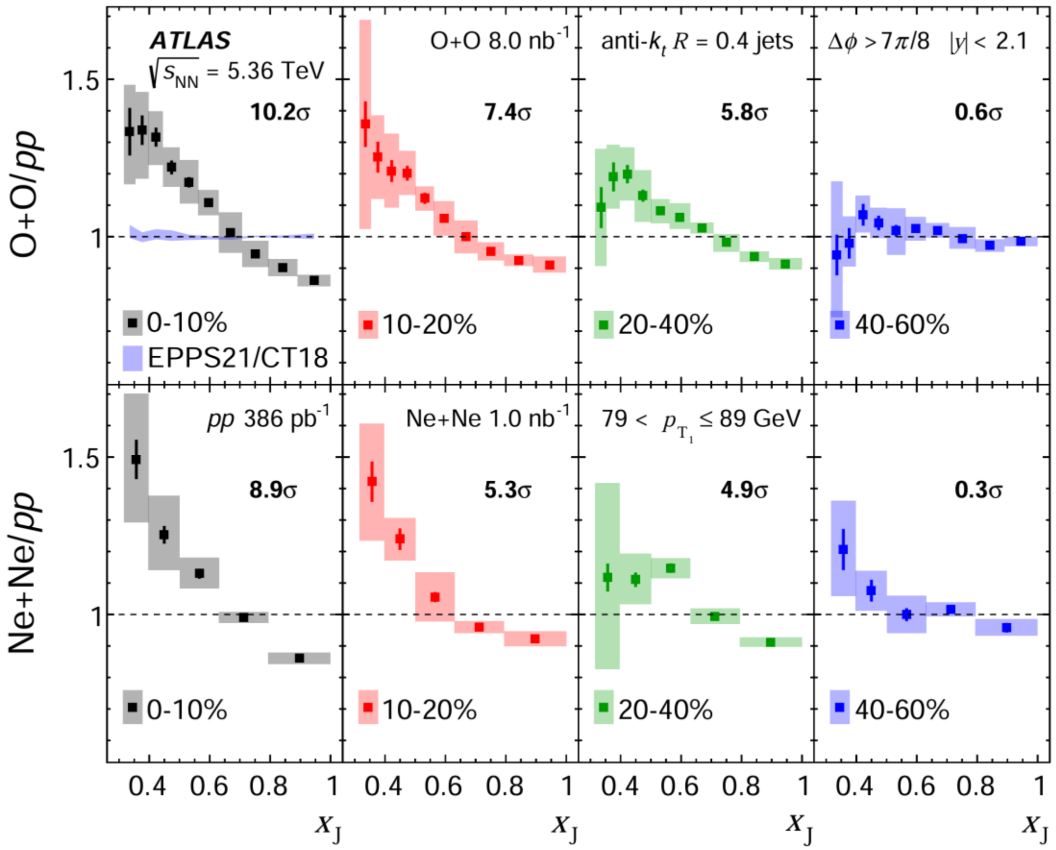

arXiv:2606.20463

Summary and Outlook

- **Data**: Successful Run3 collected 332 fb^{-1} at 13.6 TeV, more results are coming
- **AI/ML**: GN transformer flavour tagger greatly enhances physics sensitivity
- **Higgs**: Precise cross-section, couplings and width; rare decays $H \to \mu\mu$ (3.4σ), $H \to Z\gamma$ (2.5σ); tight limits on Higgs self-coupling κ_λ and Higgs CPV
- **Diboson/VBS**: First 3.3σ evidence of at least one longitudinal WW scattering;

  tribosons WWγ/VVZ observed, strong SMEFT aQGC constraints
- **Top & heavy flavour**: Observation of toponium quasi-bounding state;
  top quark mass, new mesons B_c^{*+}, X(6900) discovered
- **BSM**: No SUSY/LLP/dark particle excess
- **HION**: p-O/O-O/Ne-Ne collision for cosmic/jet-quenching studies

Thanks for your attention, please stay tuned !

17th Workshop of the

FCPPN/L

France-China Particle Physics Network and Laboratory

Lyon, France • 29 June – 3 July 2026

Highlights from the ATLAS Experiment

Haijun Yang (SJTU/TDLI)

上海交通大學 SHANGHAI JIAO TONG UNIVERSITY | 李政道研究所 Tsung-Dao Lee Institute

The 17th Workshop of the FCPPN/L at Lyon, France
June 29 – July 3, 2026

Heavy Particle Searches

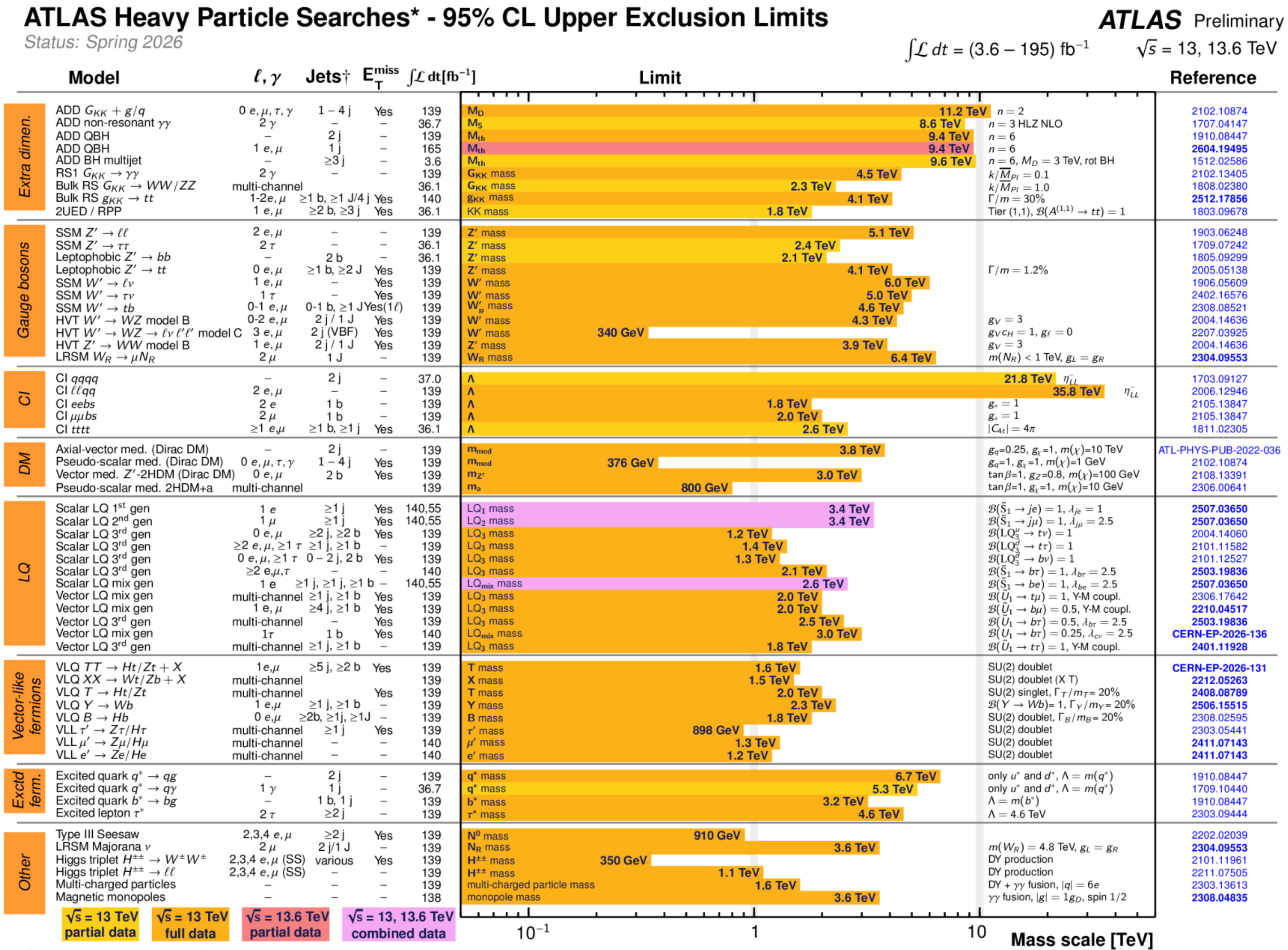

ATLAS Heavy Particle Searches* - 95% CL Upper Exclusion Limits

Status: Spring 2026

ATLAS Preliminary

$\int\mathcal{L}\,dt = (3.6 - 195)\ \mathrm{fb}^{-1}$ $\sqrt{s} = 13,\ 13.6$ TeV

	Model	ℓ, γ	Jets†	E_T^{miss}	$\int\mathcal{L}\,dt[\mathrm{fb}^{-1}]$	Limit			Reference
Extra dimen.	ADD $G_{KK} + g/q$	0 e, μ, τ, γ	1 – 4 j	Yes	139	$\mathrm{M_D}$	11.2 TeV	$n = 2$	2102.10874
	ADD non-resonant $\gamma\gamma$	2 γ	–	–	36.7	$\mathrm{M_S}$	8.6 TeV	$n = 3$ HLZ NLO	1707.04147
	ADD QBH	–	2 j	–	139	$\mathrm{M_{th}}$	9.4 TeV	$n = 6$	1910.08447
	ADD QBH	1 e, μ	1 j	–	165	$\mathrm{M_{th}}$	9.4 TeV	$n = 6$	**2604.19495**
	ADD BH multijet	–	≥3 j	–	3.6	$\mathrm{M_{th}}$	9.6 TeV	$n = 6$, $M_D = 3$ TeV, rot BH	1512.02586
	RS1 $G_{KK} \to \gamma\gamma$	2 γ	–	–	139	$\mathrm{G_{KK}}$ mass	4.5 TeV	$k/\overline{M}_{Pl} = 0.1$	2102.13405
	Bulk RS $G_{KK} \to WW/ZZ$	multi-channel			36.1	$\mathrm{G_{KK}}$ mass	2.3 TeV	$k/\overline{M}_{Pl} = 1.0$	1808.02380
	Bulk RS $g_{KK} \to tt$	1-2e, μ	≥1 b, ≥1 J/4 j	Yes	140	$\mathrm{g_{KK}}$ mass	4.1 TeV	$\Gamma/m = 30\%$	**2512.17856**
	2UED / RPP	1 e, μ	≥2 b, ≥3 j	Yes	36.1	KK mass	1.8 TeV	Tier (1,1), $\mathcal{B}(A^{(1,1)} \to tt) = 1$	1803.09678
Gauge bosons	SSM $Z' \to \ell\ell$	2 e, μ	–	–	139	Z' mass	5.1 TeV		1903.06248
	SSM $Z' \to \tau\tau$	2 τ	–	–	36.1	Z' mass	2.4 TeV		1709.07242
	Leptophobic $Z' \to bb$	–	2 b	–	36.1	Z' mass	2.1 TeV		1805.09299
	Leptophobic $Z' \to tt$	0 e, μ	≥1 b, ≥2 J	Yes	139	Z' mass	4.1 TeV	$\Gamma/m = 1.2\%$	2005.05138
	SSM $W' \to \ell\nu$	1 e, μ	–	Yes	139	W' mass	6.0 TeV		1906.05609
	SSM $W' \to \tau\nu$	1 τ	–	Yes	139	W' mass	5.0 TeV		2402.16576
	SSM $W' \to tb$	0-1 e, μ	0-1 b, ≥1 J	Yes(1ℓ)	139	W'_R mass	4.6 TeV		2308.08521
	HVT $W' \to WZ$ model B	0-2 e, μ	2 j / 1 J	Yes	139	W' mass	4.3 TeV	$g_V = 3$	2004.14636
	HVT $W' \to WZ \to \ell\nu\,\ell'\ell'$ model C	3 e, μ	2 j (VBF)	Yes	139	W' mass	340 GeV	$g_V c_H = 1$, $g_f = 0$	2207.03925
	HVT $Z' \to WW$ model B	1 e, μ	2 j / 1 J	Yes	139	Z' mass	3.9 TeV	$g_V = 3$	2004.14636
	LRSM $W_R \to \mu N_R$	2 μ	1 J	–	139	$\mathrm{W_R}$ mass	6.4 TeV	$m(N_R) < 1$ TeV, $g_L = g_R$	**2304.09553**
CI	CI $qqqq$	–	2 j	–	37.0	Λ	21.8 TeV	η_{LL}^{-}	1703.09127
	CI $\ell\ell qq$	2 e, μ	–	–	139	Λ	35.8 TeV	η_{LL}^{-}	2006.12946
	CI $eebs$	2 e	1 b	–	139	Λ	1.8 TeV	$g_* = 1$	2105.13847
	CI $\mu\mu bs$	2 μ	1 b	–	139	Λ	2.0 TeV	$g_* = 1$	2105.13847
	CI $tttt$	≥1 e,μ	≥1 b, ≥1 j	Yes	36.1	Λ	2.6 TeV	$\lvert C_{4t}\rvert = 4\pi$	1811.02305
DM	Axial-vector med. (Dirac DM)	–	2 j	–	139	$\mathrm{m_{med}}$	3.8 TeV	g_q=0.25, g_χ=1, $m(\chi)$=10 TeV	ATL-PHYS-PUB-2022-036
	Pseudo-scalar med. (Dirac DM)	0 e, μ, τ, γ	1 – 4 j	Yes	139	$\mathrm{m_{med}}$	376 GeV	g_q=1, g_χ=1, $m(\chi)$=1 GeV	2102.10874
	Vector med. Z'-2HDM (Dirac DM)	0 e, μ	2 b	Yes	139	$\mathrm{m_{Z'}}$	3.0 TeV	$\tan\beta$=1, g_Z=0.8, $m(\chi)$=100 GeV	2108.13391
	Pseudo-scalar med. 2HDM+a	multi-channel			139	$\mathrm{m_a}$	800 GeV	$\tan\beta$=1, g_χ=1, $m(\chi)$=10 GeV	2306.00641
LQ	Scalar LQ 1st gen	1 e	≥1 j	Yes	140,55	$\mathrm{LQ_1}$ mass	3.4 TeV	$\mathcal{B}(\tilde{S}_1 \to je) = 1$, $\lambda_{je} = 1$	**2507.03650**
	Scalar LQ 2nd gen	1 μ	≥1 j	Yes	140,55	$\mathrm{LQ_2}$ mass	3.4 TeV	$\mathcal{B}(\tilde{S}_1 \to j\mu) = 1$, $\lambda_{j\mu} = 2.5$	**2507.03650**
	Scalar LQ 3rd gen	0 e, μ	≥2 j, ≥2 b	Yes	139	$\mathrm{LQ_3}$ mass	1.2 TeV	$\mathcal{B}(\mathrm{LQ}_3^u \to t\nu) = 1$	2004.14060
	Scalar LQ 3rd gen	≥2 e, μ, ≥1 τ	≥1 j, ≥1 b	–	139	$\mathrm{LQ_3}$ mass	1.4 TeV	$\mathcal{B}(\mathrm{LQ}_3^d \to t\tau) = 1$	2101.11582
	Scalar LQ 3rd gen	0 e, μ, ≥1 τ	0 – 2 j, 2 b	Yes	139	$\mathrm{LQ_3}$ mass	1.3 TeV	$\mathcal{B}(\mathrm{LQ}_3^d \to b\nu) = 1$	2101.12527
	Scalar LQ 3rd gen	≥2 e,μ,τ	–	–	140	$\mathrm{LQ_3}$ mass	2.1 TeV	$\mathcal{B}(\tilde{S}_1 \to b\tau) = 1$, $\lambda_{b\tau} = 2.5$	**2503.19836**
	Scalar LQ mix gen	1 e	≥1 j, ≥1 j, ≥1 b	–	140,55	$\mathrm{LQ_{mix}}$ mass	2.6 TeV	$\mathcal{B}(\tilde{S}_1 \to be) = 1$, $\lambda_{be} = 2.5$	**2507.03650**
	Vector LQ mix gen	multi-channel	≥1 j, ≥1 b	Yes	139	$\mathrm{LQ_3}$ mass	2.0 TeV	$\mathcal{B}(\tilde{U}_1 \to t\mu) = 1$, Y-M coupl.	2306.17642
	Vector LQ mix gen	1 e, μ	≥4 j, ≥1 b	Yes	139	$\mathrm{LQ_3}$ mass	2.0 TeV	$\mathcal{B}(\tilde{U}_1 \to b\mu) = 0.5$, Y-M coupl.	**2210.04517**
	Vector LQ 3rd gen	multi-channel	–	Yes	139	$\mathrm{LQ_3}$ mass	2.5 TeV	$\mathcal{B}(\tilde{U}_1 \to b\tau) = 0.5$, $\lambda_{b\tau} = 2.5$	**2503.19836**
	Vector LQ mix gen	1τ	1 b	Yes	140	$\mathrm{LQ_{mix}}$ mass	3.0 TeV	$\mathcal{B}(U_1 \to b\tau) = 0.25$, $\lambda_{c\nu} = 2.5$	**CERN-EP-2026-136**
	Vector LQ 3rd gen	multi-channel	≥1 j, ≥1 b	–	139	$\mathrm{LQ_3}$ mass	1.8 TeV	$\mathcal{B}(\tilde{U}_1 \to t\tau) = 1$, Y-M coupl.	**2401.11928**
Vector-like fermions	VLQ $TT \to Ht/Zt + X$	1e,μ	≥5 j, ≥2 b	Yes	139	T mass	1.6 TeV	SU(2) doublet	**CERN-EP-2026-131**
	VLQ $XX \to Wt/Zb + X$	multi-channel			139	X mass	1.5 TeV	SU(2) doublet (X T)	**2212.05263**
	VLQ $T \to Ht/Zt$	multi-channel		Yes	139	T mass	2.0 TeV	SU(2) singlet, Γ_T/m_T= 20%	**2408.08789**
	VLQ $Y \to Wb$	1 e,μ	≥1 j, ≥1 b	–	139	Y mass	2.3 TeV	$\mathcal{B}(Y \to Wb)$= 1, Γ_Y/m_Y= 20%	**2506.15515**
	VLQ $B \to Hb$	0 e,μ	≥2b, ≥1j, ≥1J	–	139	B mass	1.8 TeV	SU(2) doublet, Γ_B/m_B= 20%	2308.02595
	VLL $\tau' \to Z\tau/H\tau$	multi-channel	≥1 j	Yes	139	τ' mass	898 GeV	SU(2) doublet	2303.05441
	VLL $\mu' \to Z\mu/H\mu$	multi-channel	–	–	140	μ' mass	1.3 TeV	SU(2) doublet	**2411.07143**
	VLL $e' \to Ze/He$	multi-channel	–	–	140	e' mass	1.2 TeV	SU(2) doublet	**2411.07143**
Exctd ferm.	Excited quark $q^* \to qg$	–	2 j	–	139	$\mathrm{q^*}$ mass	6.7 TeV	only u^* and d^*, $\Lambda = m(q^*)$	1910.08447
	Excited quark $q^* \to q\gamma$	1 γ	1 j	–	36.7	$\mathrm{q^*}$ mass	5.3 TeV	only u^* and d^*, $\Lambda = m(q^*)$	1709.10440
	Excited quark $b^* \to bg$	–	1 b, 1 j	–	139	$\mathrm{b^*}$ mass	3.2 TeV	$\Lambda = m(b^*)$	1910.08447
	Excited lepton τ^*	2 τ	≥2 j	–	139	τ^* mass	4.6 TeV	$\Lambda = 4.6$ TeV	2303.09444
Other	Type III Seesaw	2,3,4 e, μ	≥2 j	Yes	139	$\mathrm{N^0}$ mass	910 GeV		2202.02039
	LRSM Majorana ν	2 μ	2 j/1 J	–	139	$\mathrm{N_R}$ mass	3.6 TeV	$m(W_R) = 4.8$ TeV, $g_L = g_R$	**2304.09553**
	Higgs triplet $H^{\pm\pm} \to W^\pm W^\pm$	2,3,4 e, μ (SS)	various	Yes	139	$\mathrm{H^{\pm\pm}}$ mass	350 GeV	DY production	2101.11961
	Higgs triplet $H^{\pm\pm} \to \ell\ell$	2,3,4 e, μ (SS)	–	–	139	$\mathrm{H^{\pm\pm}}$ mass	1.1 TeV	DY production	2211.07505
	Multi-charged particles	–	–	–	139	multi-charged particle mass	1.6 TeV	DY + $\gamma\gamma$ fusion, $\lvert q\rvert = 6e$	2303.13613
	Magnetic monopoles	–	–	–	138	monopole mass	3.6 TeV	$\gamma\gamma$ fusion, $\lvert g\rvert = 1g_D$, spin 1/2	**2308.04835**

**Only a selection of the available mass limits on new states or phenomena is shown.*

†Small-radius (large-radius) jets are denoted by the letter j (J).

SUSY Searches

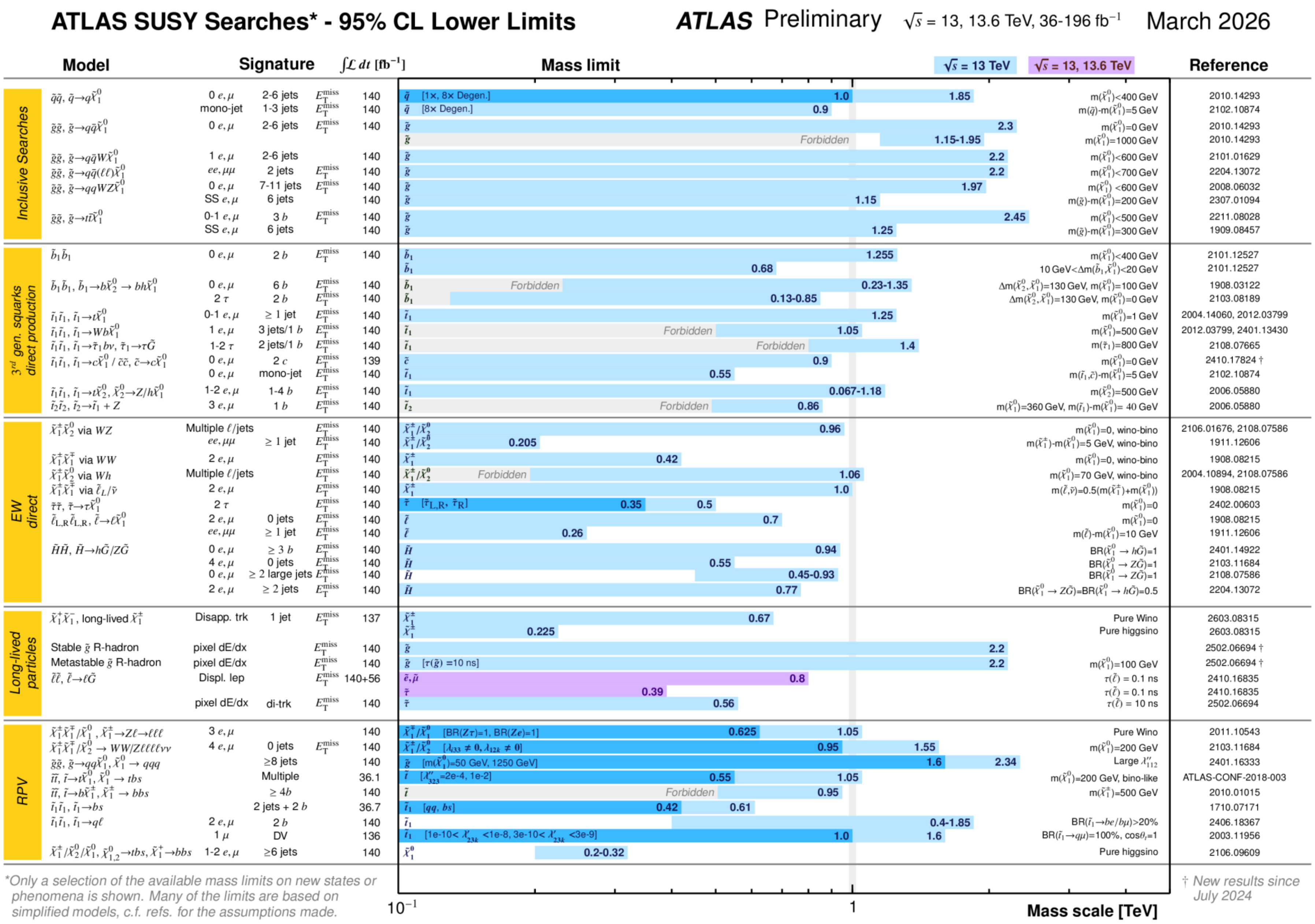

ATLAS SUSY Searches* - 95% CL Lower Limits

ATLAS Preliminary $\sqrt{s}$ = 13, 13.6 TeV, 36-196 fb^{-1}

March 2026

	Model	Signature			$\int\mathcal{L}\,dt$ [fb^{-1}]	Mass limit			Reference
Inclusive Searches	$\tilde{q}\tilde{q}$, $\tilde{q}\to q\tilde{\chi}^0_1$	0 e,μ	2-6 jets	E_T^{miss}	140	$\tilde{q}$ [1×, 8× Degen.]	1.0 1.85	m($\tilde{\chi}^0_1$)<400 GeV	2010.14293
		mono-jet	1-3 jets	E_T^{miss}	140	$\tilde{q}$ [8× Degen.]	0.9	m($\tilde{q}$)-m($\tilde{\chi}^0_1$)=5 GeV	2102.10874
	$\tilde{g}\tilde{g}$, $\tilde{g}\to q\bar{q}\tilde{\chi}^0_1$	0 e,μ	2-6 jets	E_T^{miss}	140	$\tilde{g}$	2.3	m($\tilde{\chi}^0_1$)=0 GeV	2010.14293
						$\tilde{g}$	Forbidden 1.15-1.95	m($\tilde{\chi}^0_1$)=1000 GeV	2010.14293
	$\tilde{g}\tilde{g}$, $\tilde{g}\to q\bar{q}W\tilde{\chi}^0_1$	1 e,μ	2-6 jets		140	$\tilde{g}$	2.2	m($\tilde{\chi}^0_1$)<600 GeV	2101.01629
	$\tilde{g}\tilde{g}$, $\tilde{g}\to q\bar{q}(\ell\ell)\tilde{\chi}^0_1$	$ee,\mu\mu$	2 jets	E_T^{miss}	140	$\tilde{g}$	2.2	m($\tilde{\chi}^0_1$)<700 GeV	2204.13072
	$\tilde{g}\tilde{g}$, $\tilde{g}\to qqWZ\tilde{\chi}^0_1$	0 e,μ	7-11 jets	E_T^{miss}	140	$\tilde{g}$	1.97	m($\tilde{\chi}^0_1$) <600 GeV	2008.06032
		SS e,μ	6 jets		140	$\tilde{g}$	1.15	m($\tilde{g}$)-m($\tilde{\chi}^0_1$)=200 GeV	2307.01094
	$\tilde{g}\tilde{g}$, $\tilde{g}\to t\bar{t}\tilde{\chi}^0_1$	0-1 e,μ	3 b	E_T^{miss}	140	$\tilde{g}$	2.45	m($\tilde{\chi}^0_1$)<500 GeV	2211.08028
		SS e,μ	6 jets		140	$\tilde{g}$	1.25	m($\tilde{g}$)-m($\tilde{\chi}^0_1$)=300 GeV	1909.08457
3^{rd} gen. squarks direct production	$\tilde{b}_1\tilde{b}_1$	0 e,μ	2 b	E_T^{miss}	140	$\tilde{b}_1$	1.255	m($\tilde{\chi}^0_1$)<400 GeV	2101.12527
						$\tilde{b}_1$	0.68	10 GeV<Δm($\tilde{b}_1$,$\tilde{\chi}^0_1$)<20 GeV	2101.12527
	$\tilde{b}_1\tilde{b}_1$, $\tilde{b}_1\to b\tilde{\chi}^0_2\to bh\tilde{\chi}^0_1$	0 e,μ	6 b	E_T^{miss}	140	$\tilde{b}_1$	Forbidden 0.23-1.35	Δm($\tilde{\chi}^0_2$,$\tilde{\chi}^0_1$)=130 GeV, m($\tilde{\chi}^0_1$)=100 GeV	1908.03122
		2 τ	2 b	E_T^{miss}	140	$\tilde{b}_1$	0.13-0.85	Δm($\tilde{\chi}^0_2$,$\tilde{\chi}^0_1$)=130 GeV, m($\tilde{\chi}^0_1$)=0 GeV	2103.08189
	$\tilde{t}_1\tilde{t}_1$, $\tilde{t}_1\to t\tilde{\chi}^0_1$	0-1 e,μ	≥ 1 jet	E_T^{miss}	140	$\tilde{t}_1$	1.25	m($\tilde{\chi}^0_1$)=1 GeV	2004.14060, 2012.03799
	$\tilde{t}_1\tilde{t}_1$, $\tilde{t}_1\to Wb\tilde{\chi}^0_1$	1 e,μ	3 jets/1 b	E_T^{miss}	140	$\tilde{t}_1$	Forbidden 1.05	m($\tilde{\chi}^0_1$)=500 GeV	2012.03799, 2401.13430
	$\tilde{t}_1\tilde{t}_1$, $\tilde{t}_1\to\tilde{\tau}_1 b\nu$, $\tilde{\tau}_1\to\tau\tilde{G}$	1-2 τ	2 jets/1 b	E_T^{miss}	140	$\tilde{t}_1$	Forbidden 1.4	m($\tilde{\tau}_1$)=800 GeV	2108.07665
	$\tilde{t}_1\tilde{t}_1$, $\tilde{t}_1\to c\tilde{\chi}^0_1$ / $\tilde{c}\tilde{c}$, $\tilde{c}\to c\tilde{\chi}^0_1$	0 e,μ	2 c	E_T^{miss}	139	$\tilde{c}$	0.9	m($\tilde{\chi}^0_1$)=0 GeV	2410.17824 †
		0 e,μ	mono-jet	E_T^{miss}	140	$\tilde{t}_1$	0.55	m($\tilde{t}_1$,$\tilde{c}$)-m($\tilde{\chi}^0_1$)=5 GeV	2102.10874
	$\tilde{t}_1\tilde{t}_1$, $\tilde{t}_1\to t\tilde{\chi}^0_2$, $\tilde{\chi}^0_2\to Z/h\tilde{\chi}^0_1$	1-2 e,μ	1-4 b	E_T^{miss}	140	$\tilde{t}_1$	0.067-1.18	m($\tilde{\chi}^0_2$)=500 GeV	2006.05880
	$\tilde{t}_2\tilde{t}_2$, $\tilde{t}_2\to\tilde{t}_1+Z$	3 e,μ	1 b	E_T^{miss}	140	$\tilde{t}_2$	Forbidden 0.86	m($\tilde{\chi}^0_1$)=360 GeV, m($\tilde{t}_1$)-m($\tilde{\chi}^0_1$)= 40 GeV	2006.05880
EW direct	$\tilde{\chi}^{\pm}_1\tilde{\chi}^0_2$ via WZ	Multiple ℓ/jets		E_T^{miss}	140	$\tilde{\chi}^{\pm}_1/\tilde{\chi}^0_2$	0.96	m($\tilde{\chi}^0_1$)=0, wino-bino	2106.01676, 2108.07586
		$ee,\mu\mu$	≥ 1 jet	E_T^{miss}	140	$\tilde{\chi}^{\pm}_1/\tilde{\chi}^0_2$	0.205	m($\tilde{\chi}^{\pm}_1$)-m($\tilde{\chi}^0_1$)=5 GeV, wino-bino	1911.12606
	$\tilde{\chi}^{\pm}_1\tilde{\chi}^{\mp}_1$ via WW	2 e,μ		E_T^{miss}	140	$\tilde{\chi}^{\pm}_1$	0.42	m($\tilde{\chi}^0_1$)=0, wino-bino	1908.08215
	$\tilde{\chi}^{\pm}_1\tilde{\chi}^0_2$ via Wh	Multiple ℓ/jets		E_T^{miss}	140	$\tilde{\chi}^{\pm}_1/\tilde{\chi}^0_2$	Forbidden 1.06	m($\tilde{\chi}^0_1$)=70 GeV, wino-bino	2004.10894, 2108.07586
	$\tilde{\chi}^{\pm}_1\tilde{\chi}^{\mp}_1$ via $\tilde{\ell}_L/\tilde{\nu}$	2 e,μ		E_T^{miss}	140	$\tilde{\chi}^{\pm}_1$	1.0	m($\tilde{\ell}$,$\tilde{\nu}$)=0.5(m($\tilde{\chi}^{\pm}_1$)+m($\tilde{\chi}^0_1$))	1908.08215
	$\tilde{\tau}\tilde{\tau}$, $\tilde{\tau}\to\tau\tilde{\chi}^0_1$	2 τ		E_T^{miss}	140	$\tilde{\tau}$ [$\tilde{\tau}_{L,R}$, $\tilde{\tau}_R$]	0.35 0.5	m($\tilde{\chi}^0_1$)=0	2402.00603
	$\tilde{\ell}_{L,R}\tilde{\ell}_{L,R}$, $\tilde{\ell}\to\ell\tilde{\chi}^0_1$	2 e,μ	0 jets	E_T^{miss}	140	$\tilde{\ell}$	0.7	m($\tilde{\chi}^0_1$)=0	1908.08215
		$ee,\mu\mu$	≥ 1 jet	E_T^{miss}	140	$\tilde{\ell}$	0.26	m($\tilde{\ell}$)-m($\tilde{\chi}^0_1$)=10 GeV	1911.12606
	$\tilde{H}\tilde{H}$, $\tilde{H}\to h\tilde{G}/Z\tilde{G}$	0 e,μ	≥ 3 b	E_T^{miss}	140	$\tilde{H}$	0.94	BR($\tilde{\chi}^0_1\to h\tilde{G}$)=1	2401.14922
		4 e,μ	0 jets	E_T^{miss}	140	$\tilde{H}$	0.55	BR($\tilde{\chi}^0_1\to Z\tilde{G}$)=1	2103.11684
		0 e,μ	≥ 2 large jets	E_T^{miss}	140	$\tilde{H}$	0.45-0.93	BR($\tilde{\chi}^0_1\to Z\tilde{G}$)=1	2108.07586
		2 e,μ	≥ 2 jets	E_T^{miss}	140	$\tilde{H}$	0.77	BR($\tilde{\chi}^0_1\to Z\tilde{G}$)=BR($\tilde{\chi}^0_1\to h\tilde{G}$)=0.5	2204.13072
Long-lived particles	$\tilde{\chi}^+_1\tilde{\chi}^-_1$, long-lived $\tilde{\chi}^{\pm}_1$	Disapp. trk	1 jet	E_T^{miss}	137	$\tilde{\chi}^{\pm}_1$	0.67	Pure Wino	2603.08315
						$\tilde{\chi}^{\pm}_1$	0.225	Pure higgsino	2603.08315
	Stable $\tilde{g}$ R-hadron	pixel dE/dx		E_T^{miss}	140	$\tilde{g}$	2.2		2502.06694 †
	Metastable $\tilde{g}$ R-hadron	pixel dE/dx		E_T^{miss}	140	$\tilde{g}$ [$\tau(\tilde{g})$ =10 ns]	2.2	m($\tilde{\chi}^0_1$)=100 GeV	2502.06694 †
	$\tilde{\ell}\tilde{\ell}$, $\tilde{\ell}\to\ell\tilde{G}$	Displ. lep		E_T^{miss}	140+56	$\tilde{e},\tilde{\mu}$	0.8	$\tau(\tilde{\ell})$ = 0.1 ns	2410.16835
						$\tilde{\tau}$	0.39	$\tau(\tilde{\ell})$ = 0.1 ns	2410.16835
		pixel dE/dx	di-trk	E_T^{miss}	140	$\tilde{\tau}$	0.56	$\tau(\tilde{\ell})$ = 10 ns	2502.06694
RPV	$\tilde{\chi}^{\pm}_1\tilde{\chi}^{\mp}_1/\tilde{\chi}^0_1$, $\tilde{\chi}^{\pm}_1\to Z\ell\to\ell\ell\ell$	3 e,μ			140	$\tilde{\chi}^{\mp}_1/\tilde{\chi}^0_1$ [BR($Z\tau$)=1, BR(Ze)=1]	0.625 1.05	Pure Wino	2011.10543
	$\tilde{\chi}^{\pm}_1\tilde{\chi}^{\mp}_1/\tilde{\chi}^0_2\to WW/Z\ell\ell\ell\ell\nu\nu$	4 e,μ	0 jets	E_T^{miss}	140	$\tilde{\chi}^{\pm}_1/\tilde{\chi}^0_2$ [$\lambda_{i33}\neq 0, \lambda_{12k}\neq 0$]	0.95 1.55	m($\tilde{\chi}^0_1$)=200 GeV	2103.11684
	$\tilde{g}\tilde{g}$, $\tilde{g}\to qq\tilde{\chi}^0_1$, $\tilde{\chi}^0_1\to qqq$		≥8 jets		140	$\tilde{g}$ [m($\tilde{\chi}^0_1$)=50 GeV, 1250 GeV]	1.6 2.34	Large λ''_{112}	2401.16333
	$\tilde{t}\tilde{t}$, $\tilde{t}\to t\tilde{\chi}^0_1$, $\tilde{\chi}^0_1\to tbs$		Multiple		36.1	$\tilde{t}$ [λ''_{323}=2e-4, 1e-2]	0.55 1.05	m($\tilde{\chi}^0_1$)=200 GeV, bino-like	ATLAS-CONF-2018-003
	$\tilde{t}\tilde{t}$, $\tilde{t}\to b\tilde{\chi}^{\pm}_1$, $\tilde{\chi}^{\pm}_1\to bbs$		≥ 4b		140	$\tilde{t}$	Forbidden 0.95	m($\tilde{\chi}^{\pm}_1$)=500 GeV	2010.01015
	$\tilde{t}_1\tilde{t}_1$, $\tilde{t}_1\to bs$		2 jets + 2 b		36.7	$\tilde{t}_1$ [qq, bs]	0.42 0.61		1710.07171
	$\tilde{t}_1\tilde{t}_1$, $\tilde{t}_1\to q\ell$	2 e,μ	2 b		140	$\tilde{t}_1$	0.4-1.85	BR($\tilde{t}_1\to be/b\mu$)>20%	2406.18367
		1 μ	DV		136	$\tilde{t}_1$ [1e-10< λ'_{23k} <1e-8, 3e-10< λ'_{23k} <3e-9]	1.0 1.6	BR($\tilde{t}_1\to q\mu$)=100%, cosθ_t=1	2003.11956
	$\tilde{\chi}^{\pm}_1/\tilde{\chi}^0_2/\tilde{\chi}^0_1$, $\tilde{\chi}^0_{1,2}\to tbs$, $\tilde{\chi}^+_1\to bbs$	1-2 e,μ	≥6 jets		140	$\tilde{\chi}^0_1$	0.2-0.32	Pure higgsino	2106.09609

*Only a selection of the available mass limits on new states or phenomena is shown. Many of the limits are based on simplified models, c.f. refs. for the assumptions made.

† New results since July 2024

LLP Searches

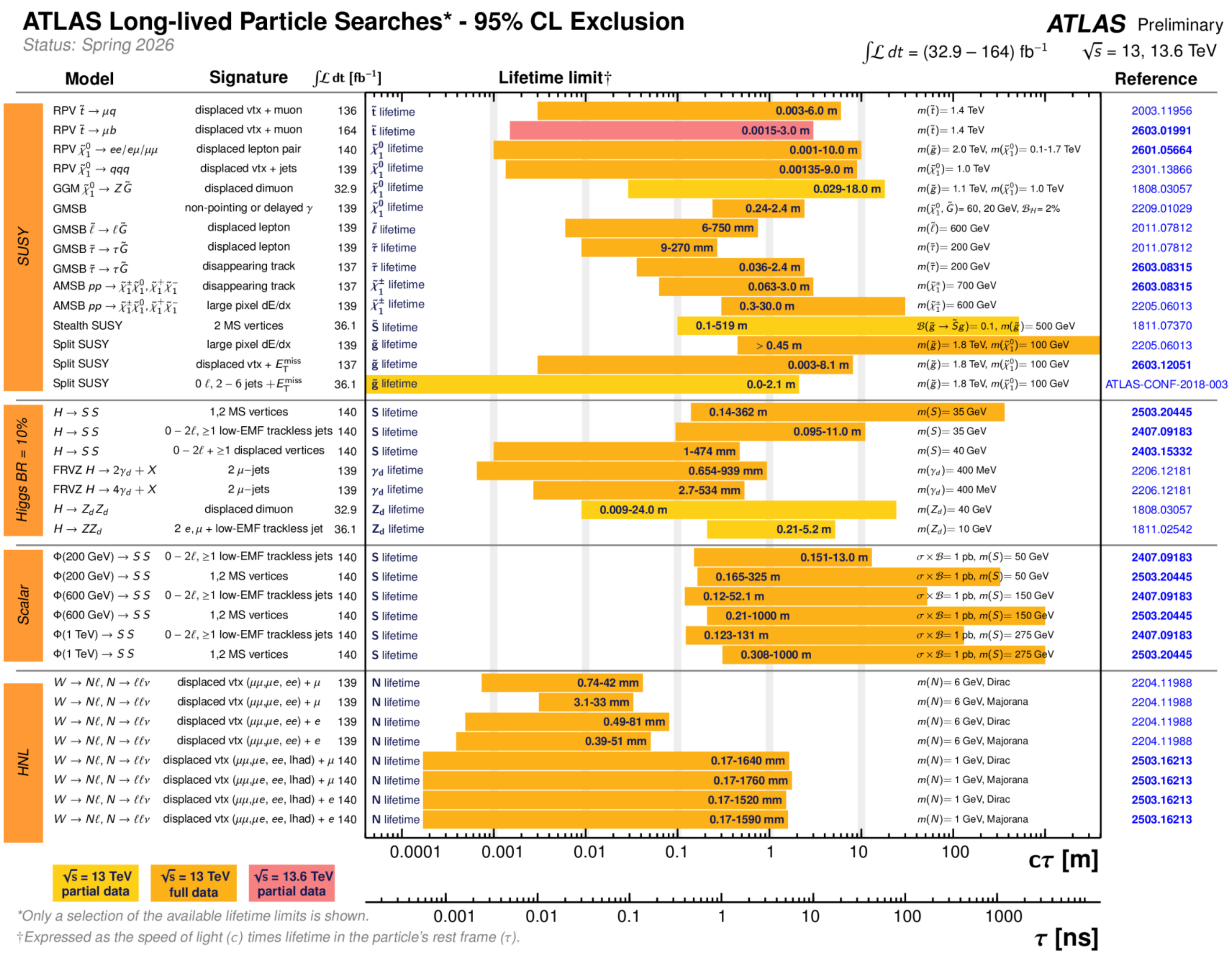

ATLAS Long-lived Particle Searches* - 95% CL Exclusion

Status: Spring 2026

ATLAS Preliminary

$\int\mathcal{L}\,dt$ = (32.9 – 164) fb^{-1} $\sqrt{s}$ = 13, 13.6 TeV

	Model	Signature	$\int\mathcal{L}\,dt$ [fb^{-1}]	Lifetime limit†		Reference
SUSY	RPV $\tilde{t} \to \mu q$	displaced vtx + muon	136	$\tilde{t}$ lifetime 0.003-6.0 m	$m(\tilde{t})$= 1.4 TeV	2003.11956
	RPV $\tilde{t} \to \mu b$	displaced vtx + muon	164	$\tilde{t}$ lifetime 0.0015-3.0 m	$m(\tilde{t})$= 1.4 TeV	**2603.01991**
	RPV $\tilde{\chi}_1^0 \to ee/e\mu/\mu\mu$	displaced lepton pair	140	$\tilde{\chi}_1^0$ lifetime 0.001-10.0 m	$m(\tilde{g})$= 2.0 TeV, $m(\tilde{\chi}_1^0)$= 0.1-1.7 TeV	**2601.05664**
	RPV $\tilde{\chi}_1^0 \to qqq$	displaced vtx + jets	139	$\tilde{\chi}_1^0$ lifetime 0.00135-9.0 m	$m(\tilde{\chi}_1^0)$= 1.0 TeV	2301.13866
	GGM $\tilde{\chi}_1^0 \to Z\tilde{G}$	displaced dimuon	32.9	$\tilde{\chi}_1^0$ lifetime 0.029-18.0 m	$m(\tilde{g})$= 1.1 TeV, $m(\tilde{\chi}_1^0)$= 1.0 TeV	1808.03057
	GMSB	non-pointing or delayed γ	139	$\tilde{\chi}_1^0$ lifetime 0.24-2.4 m	$m(\tilde{\chi}_1^0, \tilde{G})$= 60, 20 GeV, $\mathcal{B}_{\mathcal{H}}$= 2%	2209.01029
	GMSB $\tilde{\ell} \to \ell\tilde{G}$	displaced lepton	139	$\tilde{\ell}$ lifetime 6-750 mm	$m(\tilde{\ell})$= 600 GeV	2011.07812
	GMSB $\tilde{\tau} \to \tau\tilde{G}$	displaced lepton	139	$\tilde{\tau}$ lifetime 9-270 mm	$m(\tilde{\tau})$= 200 GeV	2011.07812
	GMSB $\tilde{\tau} \to \tau\tilde{G}$	disappearing track	137	$\tilde{\tau}$ lifetime 0.036-2.4 m	$m(\tilde{\tau})$= 200 GeV	**2603.08315**
	AMSB $pp \to \tilde{\chi}_1^{\pm}\tilde{\chi}_1^0, \tilde{\chi}_1^+\tilde{\chi}_1^-$	disappearing track	137	$\tilde{\chi}_1^{\pm}$ lifetime 0.063-3.0 m	$m(\tilde{\chi}_1^{\pm})$= 700 GeV	**2603.08315**
	AMSB $pp \to \tilde{\chi}_1^{\pm}\tilde{\chi}_1^0, \tilde{\chi}_1^+\tilde{\chi}_1^-$	large pixel dE/dx	139	$\tilde{\chi}_1^{\pm}$ lifetime 0.3-30.0 m	$m(\tilde{\chi}_1^{\pm})$= 600 GeV	2205.06013
	Stealth SUSY	2 MS vertices	36.1	$\tilde{S}$ lifetime 0.1-519 m	$\mathcal{B}(\tilde{g} \to \tilde{S}g)$= 0.1, $m(\tilde{g})$= 500 GeV	1811.07370
	Split SUSY	large pixel dE/dx	139	$\tilde{g}$ lifetime > 0.45 m	$m(\tilde{g})$= 1.8 TeV, $m(\tilde{\chi}_1^0)$= 100 GeV	2205.06013
	Split SUSY	displaced vtx + E_T^{miss}	137	$\tilde{g}$ lifetime 0.003-8.1 m	$m(\tilde{g})$= 1.8 TeV, $m(\tilde{\chi}_1^0)$= 100 GeV	**2603.12051**
	Split SUSY	0 ℓ, 2 – 6 jets + E_T^{miss}	36.1	$\tilde{g}$ lifetime 0.0-2.1 m	$m(\tilde{g})$= 1.8 TeV, $m(\tilde{\chi}_1^0)$= 100 GeV	ATLAS-CONF-2018-003
Higgs BR = 10%	$H \to S\,S$	1,2 MS vertices	140	S lifetime 0.14-362 m	$m(S)$= 35 GeV	**2503.20445**
	$H \to S\,S$	0 – 2ℓ, ≥1 low-EMF trackless jets	140	S lifetime 0.095-11.0 m	$m(S)$= 35 GeV	**2407.09183**
	$H \to S\,S$	0 – 2ℓ + ≥1 displaced vertices	140	S lifetime 1-474 mm	$m(S)$= 40 GeV	**2403.15332**
	FRVZ $H \to 2\gamma_d + X$	2 μ–jets	139	γ_d lifetime 0.654-939 mm	$m(\gamma_d)$= 400 MeV	2206.12181
	FRVZ $H \to 4\gamma_d + X$	2 μ–jets	139	γ_d lifetime 2.7-534 mm	$m(\gamma_d)$= 400 MeV	2206.12181
	$H \to Z_d Z_d$	displaced dimuon	32.9	Z_d lifetime 0.009-24.0 m	$m(Z_d)$= 40 GeV	1808.03057
	$H \to ZZ_d$	2 e,μ + low-EMF trackless jet	36.1	Z_d lifetime 0.21-5.2 m	$m(Z_d)$= 10 GeV	1811.02542
Scalar	Φ(200 GeV) $\to S\,S$	0 – 2ℓ, ≥1 low-EMF trackless jets	140	S lifetime 0.151-13.0 m	$\sigma \times \mathcal{B}$= 1 pb, $m(S)$= 50 GeV	**2407.09183**
	Φ(200 GeV) $\to S\,S$	1,2 MS vertices	140	S lifetime 0.165-325 m	$\sigma \times \mathcal{B}$= 1 pb, $m(S)$= 50 GeV	**2503.20445**
	Φ(600 GeV) $\to S\,S$	0 – 2ℓ, ≥1 low-EMF trackless jets	140	S lifetime 0.12-52.1 m	$\sigma \times \mathcal{B}$= 1 pb, $m(S)$= 150 GeV	**2407.09183**
	Φ(600 GeV) $\to S\,S$	1,2 MS vertices	140	S lifetime 0.21-1000 m	$\sigma \times \mathcal{B}$= 1 pb, $m(S)$= 150 GeV	**2503.20445**
	Φ(1 TeV) $\to S\,S$	0 – 2ℓ, ≥1 low-EMF trackless jets	140	S lifetime 0.123-131 m	$\sigma \times \mathcal{B}$= 1 pb, $m(S)$= 275 GeV	**2407.09183**
	Φ(1 TeV) $\to S\,S$	1,2 MS vertices	140	S lifetime 0.308-1000 m	$\sigma \times \mathcal{B}$= 1 pb, $m(S)$= 275 GeV	**2503.20445**
HNL	$W \to N\ell, N \to \ell\ell\nu$	displaced vtx ($\mu\mu$,μe, ee) + μ	139	N lifetime 0.74-42 mm	$m(N)$= 6 GeV, Dirac	2204.11988
	$W \to N\ell, N \to \ell\ell\nu$	displaced vtx ($\mu\mu$,μe, ee) + μ	139	N lifetime 3.1-33 mm	$m(N)$= 6 GeV, Majorana	2204.11988
	$W \to N\ell, N \to \ell\ell\nu$	displaced vtx ($\mu\mu$,μe, ee) + e	139	N lifetime 0.49-81 mm	$m(N)$= 6 GeV, Dirac	2204.11988
	$W \to N\ell, N \to \ell\ell\nu$	displaced vtx ($\mu\mu$,μe, ee) + e	139	N lifetime 0.39-51 mm	$m(N)$= 6 GeV, Majorana	2204.11988
	$W \to N\ell, N \to \ell\ell\nu$	displaced vtx ($\mu\mu$,μe, ee, lhad) + μ	140	N lifetime 0.17-1640 mm	$m(N)$= 1 GeV, Dirac	**2503.16213**
	$W \to N\ell, N \to \ell\ell\nu$	displaced vtx ($\mu\mu$,μe, ee, lhad) + μ	140	N lifetime 0.17-1760 mm	$m(N)$= 1 GeV, Majorana	**2503.16213**
	$W \to N\ell, N \to \ell\ell\nu$	displaced vtx ($\mu\mu$,μe, ee, lhad) + e	140	N lifetime 0.17-1520 mm	$m(N)$= 1 GeV, Dirac	**2503.16213**
	$W \to N\ell, N \to \ell\ell\nu$	displaced vtx ($\mu\mu$,μe, ee, lhad) + e	140	N lifetime 0.17-1590 mm	$m(N)$= 1 GeV, Majorana	**2503.16213**

*Only a selection of the available lifetime limits is shown.

†Expressed as the speed of light (c) times lifetime in the particle's rest frame (τ).

EFT and New Physics

- **Effective Field Theory (EFT),** SM (Wilson coefficients $f_{\text{I}} = 0$) + BSM operators

$$\mathcal{L}_{\text{eff}} = \mathcal{L}_{\text{SM}} + \sum_i \frac{f_i^{(6)}}{\Lambda_i^2} O_i^{(6)} + \sum_j \frac{f_i^{(8)}}{\Lambda_i^4} O_j^{(8)} + \ldots$$

f: Wilson coefficients
Λ: Scale of new physics (~TeV)
$O^{(6)}$: Dimension-6 operators
$O^{(8)}$: Dimension-8 operators

- Constrain BSM operators via anomalous TGC or QGC.
  - Dim-6 operators affect Triple-Gauge-Couplings (TGCs) at low energy
  - Dim-8 operators control Quartic-Gauge-Couplings (QGCs) at high energy
    Eboli-Gouzevitch basis: Tensor (T-) / Scalar (S-) / Mixed (M-) operators
- SM predicts QGCs that contain at least two charged W: WWWW, WWZZ, WWγγ, WWZγ
- QGCs with pure neutral bosons (ZZZZ, ZZZγ, ZZγγ, Zγγγ, γγγγ) are SM-forbidden

Anomalous QGCs serve as a powerful probe for new physics BSM.

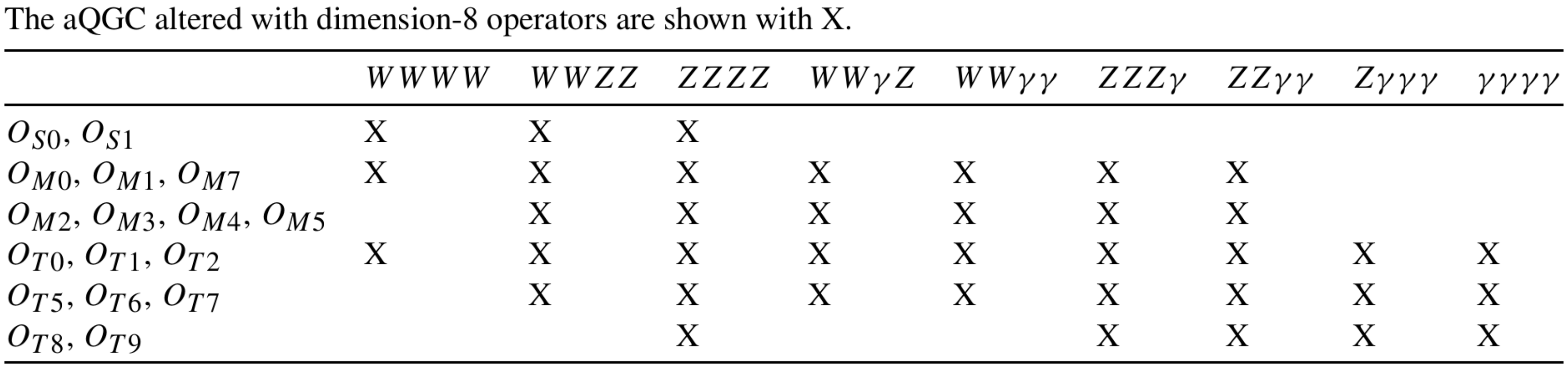

The aQGC altered with dimension-8 operators are shown with X.

	$WWWW$	$WWZZ$	$ZZZZ$	$WW\gamma Z$	$WW\gamma\gamma$	$ZZZ\gamma$	$ZZ\gamma\gamma$	$Z\gamma\gamma\gamma$	$\gamma\gamma\gamma\gamma$
O_{S0}, O_{S1}	X	X	X						
O_{M0}, O_{M1}, O_{M7}	X	X	X	X	X	X	X		
O_{M2}, O_{M3}, O_{M4}, O_{M5}		X	X	X	X	X	X		
O_{T0}, O_{T1}, O_{T2}	X	X	X	X	X	X	X	X	X
O_{T5}, O_{T6}, O_{T7}		X	X	X	X	X	X	X	X
O_{T8}, O_{T9}			X			X	X	X	X

SMEFT Dim-8 Operators

$$\mathcal{L}_{eff} = \mathcal{L}_{SM} + \sum_{k=0}^{1} \frac{f_{S,k}}{\Lambda^4} O_{S,k} + \sum_{i=0}^{7} \frac{f_{M,i}}{\Lambda^4} O_{M,i} + \sum_{j=0,1,2,5,6,7,8,9} \frac{f_{T,j}}{\Lambda^4} O_{T,j}$$

- Contribution of operators with Gauge boson field

$$O_{T,0} = Tr[W_{\mu\nu} W^{\mu\nu}] \times Tr[W_{\alpha\beta} W^{\alpha\beta}],$$
$$O_{T,1} = Tr[W_{\alpha\nu} W^{\mu\beta}] \times Tr[W_{\mu\beta} W^{\alpha\nu}],$$
$$O_{T,2} = Tr[W_{\alpha\mu} W^{\mu\beta}] \times Tr[W_{\beta\nu} W^{\nu\alpha}],$$
$$O_{T,5} = Tr[W_{\mu\nu} W^{\mu\nu}] \times B_{\alpha\beta} B^{\alpha\beta},$$
$$O_{T,6} = Tr[W_{\alpha\nu} W^{\mu\beta}] \times B_{\mu\beta} B^{\alpha\nu},$$
$$O_{T,7} = Tr[W_{\alpha\mu} W^{\mu\beta}] \times B_{\beta\nu} B^{\nu\alpha},$$
$$O_{T,8} = B_{\mu\nu} B^{\mu\nu} B_{\alpha\beta} B^{\alpha\beta},$$
$$O_{T,9} = B_{\alpha\mu} B^{\mu\beta} B_{\beta\nu} B^{\nu\alpha}.$$

V. Ari et.al. NPB 989 (2023) 116133

- Contribution of operators with covariant derivatives only (Scalar field):

$$O_{S,0} = [(D_\mu \Phi)^\dagger (D_\nu \Phi)] \times [(D^\mu \Phi)^\dagger (D^\nu \Phi)],$$
$$O_{S,1} = [(D_\mu \Phi)^\dagger (D^\mu \Phi)] \times [(D_\nu \Phi)^\dagger (D^\nu \Phi)],$$
$$O_{S,2} = [(D_\mu \Phi)^\dagger (D_\nu \Phi)] \times [(D^\nu \Phi)^\dagger (D^\mu \Phi)].$$

- Contribution of both operators with covariant derivatives and field strength tensors field):

$$O_{M,0} = Tr[W_{\mu\nu} W^{\mu\nu}] \times [(D_\beta \Phi)^\dagger (D^\beta \Phi)],$$
$$O_{M,1} = Tr[W_{\mu\nu} W^{\nu\beta}] \times [(D_\beta \Phi)^\dagger (D^\mu \Phi)],$$
$$O_{M,2} = [B_{\mu\nu} B^{\mu\nu}] \times [(D_\beta \Phi)^\dagger (D^\beta \Phi)],$$
$$O_{M,3} = [B_{\mu\nu} B^{\nu\beta}] \times [(D_\beta \Phi)^\dagger (D^\mu \Phi)],$$
$$O_{M,4} = [(D_\mu \Phi)^\dagger W_{\beta\nu} (D^\mu \Phi)] \times B^{\beta\nu},$$
$$O_{M,5} = [(D_\mu \Phi)^\dagger W_{\beta\nu} (D^\nu \Phi)] \times B^{\beta\mu} + h.c.,$$
$$O_{M,7} = [(D_\mu \Phi)^\dagger W_{\beta\nu} W^{\beta\mu} (D^\nu \Phi)].$$

SM Productions at LHC

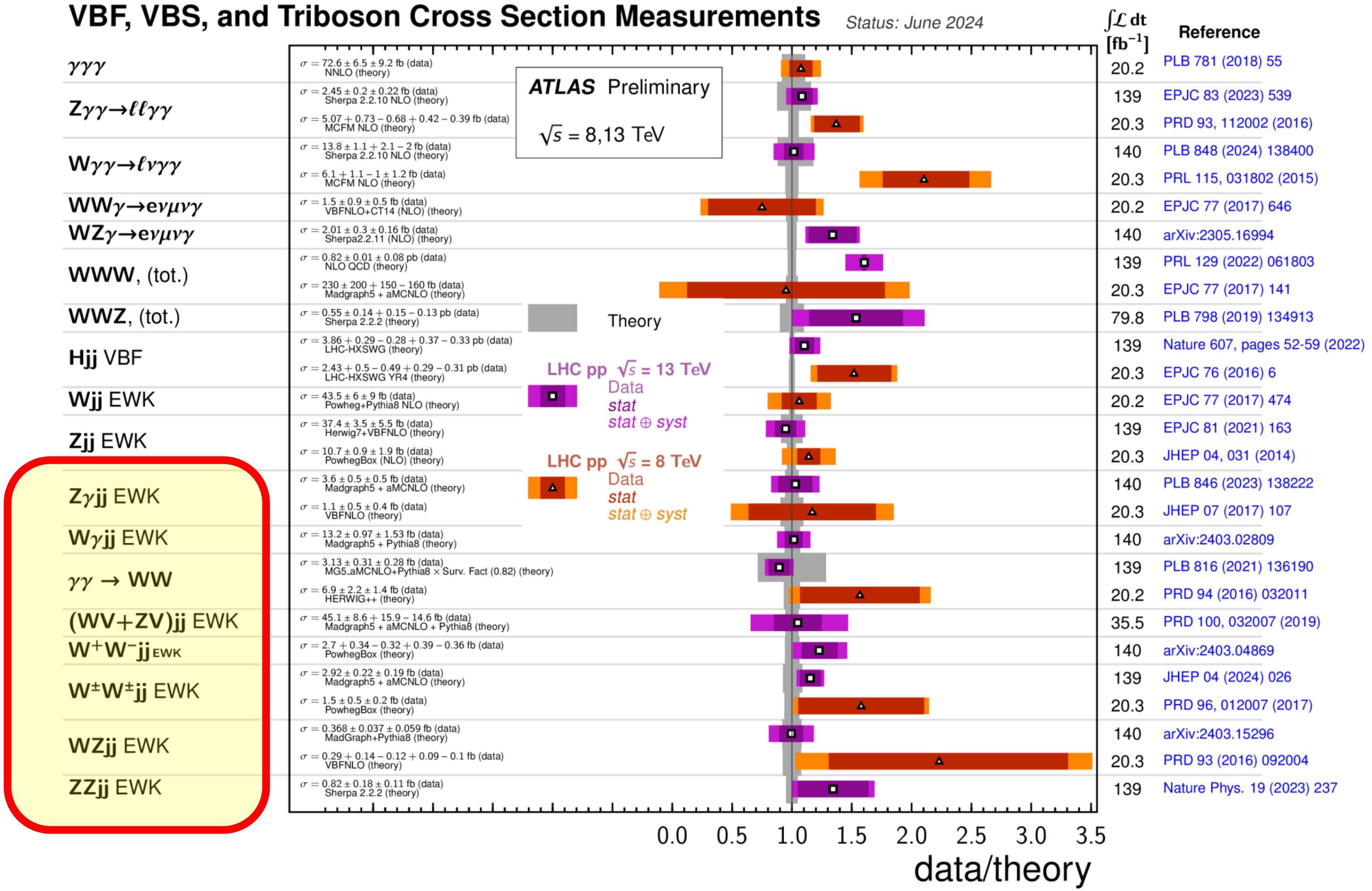

ATLAS Detector

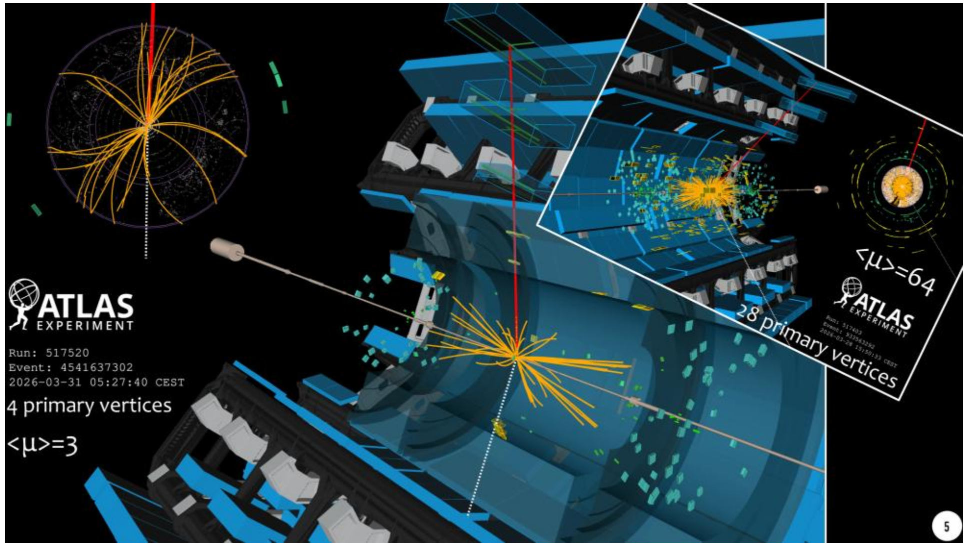

Why light ions?

- Bridge between large (Pb+Pb) and small (pp, *p*+Pb) systems
  - Is QGP production and evolution smooth with transverse size down a proton?
  - Increasing role of viscosity & fluctuations as size shrinks
- Direct probe of nuclear structure
  - α-clustering structure of ^{16}O
  - Elongated ("bowling-pin") deformation of ^{20}Ne
- New testing ground for jet quenching
  - Path-length dependence of energy loss
  - Central O+O ≈ cleaner geometry than peripheral Pb+Pb

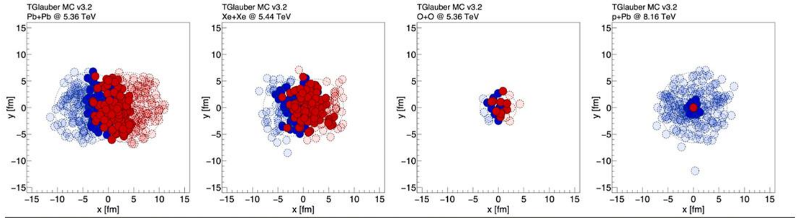

2